UNIVERSIDADE FEDERAL DE PERNAMBUCO
CENTRO DE CIÊNCIAS EXATAS E DA NATUREZA
PROGRAMA DE PÓS-GRADUAÇÃO EM FÍSICA

DIEGO CAVALCANTE CIRNE

IMPACT OF ENVIRONMENTAL CHANGE ON EVOLUTIONARY PROCESSES

Recife
2024

DIEGO CAVALCANTE CIRNE

IMPACT OF ENVIRONMENTAL CHANGE ON EVOLUTIONARY PROCESSES

Thesis presented to Programa de Pós-Graduação em Física of Universidade Federal de Pernambuco, as a partial requirement for obtaining the title of PhD in Physics.

Area of Concentration: Theoretical and Computational Physics

Advisor: Prof. Paulo Roberto de Araújo Campos

Recife

2024

.Catalogação de Publicação na Fonte. UFPE - Biblioteca Central

Cirne, Diego Cavalcante.
Impact of environmental change on evolutionary processes / Diego Cavalcante Cirne. - Recife, 2025.
129f.: il.

Tese (Doutorado) - Universidade Federal de Pernambuco, Centro de Ciências Exatas e da Natureza, Programa de Pós-Graduação em Física, 2024.
Orientação: Paulo Roberto de Araújo Campos.
Inclui referências.

1. Environmental change; 2. Fitness landscape; 3. Adaptive walk; 4. Predictability; 5. Phenotypic plasticity. I. Campos, Paulo Roberto de Araújo. II. Título.

UFPE-Biblioteca Central

DIEGO CAVALCANTE CIRNE

IMPACT OF ENVIRONMENTAL CHANGE ON EVOLUTIONARY PROCESSES

Thesis presented to Programa de Pós-Graduação em Física of Universidade Federal de Pernambuco, as a partial requirement for obtaining the title of PhD in Physics.

Approved on: 16/12/2024.

EXAMINING BOARD

Prof. Paulo Roberto de Araújo Campos
Advisor
Universidade Federal de Pernambuco

Prof. Azadeh Mohammadi
Internal Examiner
Universidade Federal de Pernambuco

Prof. José Fernando Fontanari
External Examiner
Universidade de São Paulo

Prof. Fernando Fagundes Ferreira
External Examiner
Universidade de São Paulo

Prof. Flávia Maria Dirce Marquitti
External Examiner
Universidade Estadual de Campinas

A meus pais, Marcelo e Sayonara.

ACKNOWLEDGEMENTS

Primeiramente, agradeço a CNPq e CAPES pelo fomento indespensável a esta pesquisa.
Agradeço também a Ivana Carneiro, pelo símbolo da alma gêmea;
A Samuel Gualberto, pelo símbolo da convicção;
A José Carlos, pelo símbolo do amigo;
A Bruno Carneiro, pelo símbolo do físico;
E, por fim, a Terezinha Cavalcante, pelo símbolo da tradição.

"Fracassei em tudo o que tentei na vida.
Tentei alfabetizar as crianças brasileiras, não consegui.
Tentei salvar os índios, não consegui.
Tentei fazer uma universidade séria e fracassei.
Tentei fazer o Brasil desenvolver-se autonomamente e fracassei.
Mas os fracassos são minhas vitórias.
Eu detestaria estar no lugar de quem me venceu."
(Darcy Ribeiro)

RESUMO

O presente trabalho aborda o problema da adaptação a ambientes em mudança. No contexto da teoria dos relevos de adaptação, o impacto de uma mudança ambiental sazonal e unidirecional finita sobre os níveis de adaptação e, mais importante, sobre a repetibilidade do processo evolutivo são explorados. A implementação de relevos de adaptação que variam ao longo do tempo, por vezes denominados *seascapes*, permite investigar concomitantemente as duas principais contingências do efeito de uma mutação: as condições ambientais e a interação entre loci, mais conhecida como *epistasia* nas ciências biológicas. Os relevos de adaptação e a dinâmica populacional aplicados correspondem tanto a processos estocásticos, como é comum no paradigma evolucionário, quanto a sistemas complexos, de modo que os resultados são obtidos a partir de simulações de Monte Carlo. As trajetórias evolutivas são registradas como séries temporais de genótipos, a partir das quais é realizada uma análise estatística. Alternativamente, um cenário de mudança ambiental sustentada é estudado analiticamente. Partindo da hipótese padrão de seleção e mutação Gaussianas, o estado estacionário da evolução fenotípica de uma população muito grande é encontrado, e o paradigma da população em declínio é explorado em termos da taxa crítica de mudança ambiental. Neste modelo de genética quantitativa, a presença de plasticidade linear manifesta uma propriedade interessante: apesar dos benefícios inegáveis para a aptidão média da população, a plasticidade também acarreta um custo em termos de tempo de recuperação de perturbações.

Palavras-chave: Mudança ambiental. Relevo de adaptação. Caminhada adaptativa. Previsibilidade. Plasticidade fenotípica.

ABSTRACT

The present work addresses the problem of adaptation to changing environments. Under the fitness landscape theory, the impact of a seasonal as well as a finite unidirectional environmental change on the levels of adaptation and, most importantly, on the repeatability of the evolutionary process are explored. The implementation of time-varying fitness landscapes, sometimes dubbed *seascapes*, allows a concomitantly investigation of the two major contingencies of the effect of a mutation: environmental conditions and interaction among loci, better known as *epistasis* in biological sciences. Fitness landscapes and the population dynamics applied correspond both to stochastic processes, as it is common in the evolutionary paradigm, as well as to complex systems, so that results are obtained from Monte Carlo simulations. Evolutionary trajectories are recorded as temporal series of genotypes, from which a statistical analysis is performed. Alternatively, a scenario of sustained environmental change is studied analytically. Departing from the standard hypothesis of Gaussian selection and mutation, the stationary state of the phenotypic evolution of a very large population is found, and the declining population paradigm is explored in terms of the critical rate of environmental change. In this quantitative genetics model, the presence of linear plasticity manifests an interesting property. Despite the undeniable benefits to the mean population fitness, development also incurs a cost in terms of the recovery time from disturbances.

Keywords: Environmental change. Fitness landscape. Adaptive walk. Predictability. Phenotypic plasticity.

LIST OF FIGURES

CONTENTS

1 INTRODUCTION

The Theory of Evolution and Natural Selection is one of the greatest achievements of modern science. In fact, its formulation played a fundamental role in the consolidation of the scientific method itself. However, the evolution of species is far from being a complete and closed theory. Its structure has been continually reformulated through the elucidation of several of the inherent mechanisms due to the wide range of variables involved (MORRIS, 2009). Among these variables, there is one that always stands out whatever the biological system in focus: time.

Current estimates confidently indicate that our planet was born almost 4.5 billion years ago, embedded in a Universe of roughly three times its age (CHABOYER, 1998; DALRYMPLE, 2001; VALCIN et al., 2020). A primary triumph of geology is precisely the corroboration that during all this time, change has ruled on Earth, which is itself the historical proof of events of extremely diverse spatial and temporal scales (HIDE; DICKEY, 1991; GRADSTEIN et al., 2012; STERN, 2018). The findings of paleontology strongly confirm the fundamental and irreversible role of life in this process and, conversely, geological events of significant intensity and range have triggered equally important evolutionary responses (PARSONS, 1987; MCELWAIN; PUNYASENA, 2007; DOBRETSOV; KOLCHANOV; SUSLOV, 2008; SESSIONS et al., 2009; WILLIAMS et al., 2015). These must belong to three non-exclusive types: migration, adaptation, and development (CRONIN; SCHNEIDER, 1990; HOLT, 1990; CARLSON; CUNNINGHAM; WESTLEY, 2014).

It is common knowledge among ecologists that the gravity of environmental changes resides precisely in the endless chain of side effects. Given the intricate relationship between species through the food web as well as with the environment, variations in a single biotic or abiotic factor always have the potential to unveil several disruptions in the entire community (TYLIANAKIS et al., 2008). A typical scenario of changing environment is related to the phenomenon of coevolution, such as that found in the victim-exploiter relationship and its well-known variants predator–prey and host-parasite systems. In those systems, each species determines most of the other's selective constraints through an intricate balance between attack and defense traits (GILMAN; NUISMER; JHWUENG, 2012).

Environmental changes are not just one more ingredient in adaptation but commonly delineate the onset of events that spur any evolutionary process and innovation. Moreover, there is clear evidence that the achievement of optimal biological solutions takes exponential time and adaptation can only operate locally, targeting sufficient rather than perfect responses, so time is of the essence in the evolutionary paradigm (CHATTERJEE et al., 2014). In order to cope with the amplitude and constancy of environmental changes, living organisms have evolved, among other features, the capacity to regulate gene expression in tune with immediate physiological needs, a mechanism that is thought to fuel phenotypic variation and evolutionary innovation (LÓPEZ-MAURY; MARGUERAT; BÄHLER, 2008). Besides, the complexity of biological systems is such that theoretical works have already revealed scenarios where recurrent environ-

mental changes are paramount to survival by preventing excessive adaptation and consequent large loss of fitness under sudden fluctuations (TRUBENOVA et al., 2019). It was also on a simulational basis that an even more impressive finding had arisen: occasionally, the evolution towards temporally varying goals is substantially faster than towards fixed ones, a difference that is amplified with the complexity of the problem. This result is in agreement with the idea that evolution is far more capable of solving a problem once it has already solved a similar one (KASHTAN; NOOR; ALON, 2007). Indeed, environments are substantially correlated through time, specifically when the former best sequences remain at high-rank positions on fitness after an environmental change. Once a significant fraction of mutations are deleterious and give rise to individuals unable to perform the required functions in both initial and final environments, it is unlikely that the wild-type sequence falls into this group after the transition (ORR, 2005).

Along with environmental conditions, the genetic background sets the other major contingency on the properties of a genotype or, alternatively, on the effect of a mutation. Naturally, the interaction between loci, known as *epistasis*, has been one of the most explored phenomena in the evolutionary theory. Both theoretically and experimentally, this task has been substantially carried out through the concept of fitness landscapes (HALL et al., 2019), introduced in the early 30's by WRIGHT (WRIGHT, 1931). Formally, the fitness landscape is a mapping from genotype to reproductive capacity. The fundamental elements are the set of sequences which are the conveyors of information and the attribution of a proxy of performance to them which is ultimately related to their chances of replication. In any case, the space of sequences is discrete and subject to the metrics of the Hamming distance (or its generalizations), while fitness sets the topography, the determinant of the course of evolution: adaptation is depicted as the uphill movement of the distribution of genotypes in the population towards fitness peaks. In physics, the concept is analogous to that of energy landscapes, relating possible states of a system to their corresponding energy levels (SHIRES; PICKARD, 2021). While from a biological perspective, evolution is portrayed as a hill-climbing process toward higher peaks of the fitness landscape, physical systems are driven to states of low energy (NOWAK; KRUG, 2015).

The fitness landscape theory successfully harbors crucial evolutionary constraints and the potential for adaptation and speciation, allowing direct links between evolution, molecular biology, and systems biology (FRAGATA et al., 2019). The typical experimental approach consists of characterizing the topography of empirical fitness landscapes by analyzing the interactions among a small subset of mutations and re-constructing all possible genotypes from the wild-type to the evolved one (VISSER et al., 2018). In turn, genotypic fitness landscape models have been widely used to explain experimental data (SZENDRO et al., 2013b; ROWE et al., 2010). Obviously, the genotype-fitness relationship describes a particular environment. Under frequently changing environments, multiple fitness landscapes should be measured (LI; ZHANG, 2018). The investigation of temporally varying fitness landscapes targets thus the fundamental bridge where ecology meets evolution (VOS; SCHOUSTRA; VISSER, 2018). In this thesis, such investigation is performed theoretically in the first two chapters resorting to different fitness

landscape models.

In Section 3, Fisher's Geometric Model (FGM) is explored. The genotypic landscape under Fisher's Geometric Model provides a genotype $\rightarrow$ phenotype $\rightarrow$ fitness map, in which an additional layer is considered relative to genotypic landscape models. These landscapes are an important and useful extension of the original Fisher's formulation in which mutation effects on the phenotypes are assumed to be additive. So deviations from additivity on the genotype-fitness map are a direct consequence of the nonlinear mapping from phenotype to fitness (HWANG; PARK; KRUG, 2017). Epistasis emerges due to this nonlinearity of the phenotype to the fitness map and is particularly important around the optimum phenotype, where the curvature is larger. The levels of epistasis and ruggedness of the fitness landscape are fundamental features of the process of adaptation (WEINREICH; WATSON; CHAO, 2005; POELWIJK et al., 2011; BLANQUART et al., 2014), influencing its degree of repeatability and predictability (COLEGRAVE; BUCKLING, 2005; SALVERDA et al., 2011; CHEVIN; DECORZENT; LENORMAND, 2014).

The FGM has been a valuable tool in the study of the impact of environmental variations on many processes found in both evolutionary and ecological contexts (BÜRGER; LYNCH, 1995; GORDO; CAMPOS, 2013; MATUSZEWSKI; HERMISSON; KOPP, 2014), including those leading to ecological diversification and speciation events (AMICONE; GORDO, 2021; FREITAS; ARAUJO; CAMPOS, 2022). A common approach for the FGM in the study of environmental variation is to assume that the population or community adapts to a dynamic optimum phenotype (BÜRGER; LYNCH, 1995; GORDO; CAMPOS, 2013). The effect of the environment on reshaping the landscape is analogous to physical systems, such as the effect of temperature in changing the energy landscape associated with protein folding, RNA macromolecules and amorphous solids (GUO; LAMPOUDI; SHEA, 2004; SHAH; GILCHRIST, 2010; LIU; FAN, 2021). The influence of the rate of environmental variation is quite a controversial issue, especially in the face of the debate about the role of climatic and ecological changes in shaping biodiversity (BOTTA et al., 2019).

In Section 4 we concentrate on a scenario similar to that of TRUBENOVA et al.. A basic premise of the modeling is the existence of a mechanism of gene regulation, which enables the cells to induce or repress a gene's expression, thus helping the cell organism to respond to environmental changes appropriately and thrive under different external conditions LÓPEZ-MAURY; MARGUERAT; BÄHLER(LÓPEZ-MAURY; MARGUERAT; BÄHLER, 2008). We simulate the changing environment by assuming that different sets of genes can be expressed according to environmental conditions that change seasonally. The contribution of Section 4 to the framework of TRUBENOVA et al. concerns the introduction of a crucial element. In the mentioned work, the absence of epistasis TRUBENOVA et al. creates a modular structure in the genome, where different parts evolve independently, either subject to strong selection when gene expression is induced, or to neutral selection when gene expression is suppressed. Epistasis, however, prevents modular structures.

To mimic the existence of interactions among genes, we consider a class of fitness land-

scapes known as the NK landscape model KAUFFMAN et al.; MACKEN; PERELSON. An essential feature of the NK landscape model is that the degree of ruggedness is tunable through the number of epistatic interactions among the genome elements. The choice of the NK model resides in two aspects. First, its ability to control the level of epistasis is essential since predictability is intimately related to this phenomenon (VISSER; KRUG, 2014). Second, the NK model has undeniable historical importance in the realm of fitness landscapes. Its properties and results for the static situation are well known, allowing a clear understanding of the new features associated with the time changing kind.

The formulation of time-dependent fitness landscapes is not new, and the NK fitness landscape model has also been explored within such a context. It is worth mentioning the contributions by WANG; DAI and WILKE; MARTINETZ, in which a dynamic fitness landscape is generated by periodically changing the individual contribution of each site to the organism's adaptation. Contrarily, here we follow a similar approach to that of TRUBENOVA et al.'s combined with the convenience of the NK landscape model, thereby avoiding the modular genotype structure of their approach. The resulting fitness landscape is time-dependent not because locus contributions are changed but because different sets of genes are expressed as a consequence of environmental variation. Thus, it is crucial to understand how epistasis can restrain the adaptive responses to environmental changes.

While understanding in what conditions the population presents adaptability, i.e., the ability to endure abrupt changes of selective forces, sets an exclusive objective of Section 4, clarifying the consequences to the predictability of evolutionary trajectories sets a common problem to both initial chapters. The issue of repeatability in evolution arises from the conflict between the deterministic factor, promoted by selection, and the stochastic factor, intrinsic to mutation and sampling (SZENDRO et al., 2013b). Evolutionist Stephen Jay Gould summed up the problem in a simple question: if the movie of life could be replayed, would we end up with beings and structures similar to those we have today, or completely different systems (GOULD, 1989)? In Section 4, a measure of entropy, as previously defined by SZENDRO et al., is used as a proxy for the level of repeatability of the resulting genoypes at the end of each evolutionary phase. Other measurements of predictability and path divergence are used in Section 3 to quantify the degree of repeatability of the evolutionary endpoints as well as trajectories upon environmental variation.

The third and last chapter is concerned with quite a different framework. In Section 5, a discrete-time model is developed on the phenotypic evolution of a metric character under a sustained environmental change, as well as Gaussian selection and mutation. Unlike previous chapters, this work is completely analytical. A varied handful of works has been performed in this manner, covering many scenarios of population dynamics, yet all concerned with the chances of persistence and, therefore, invariably leading to critical values, especially the critical rate of environmental change (LYNCH; GABRIEL; WOOD, 1991; LYNCH; LANDE, 1993; GOMULKIEWICZ; HOULE, 2009; CHEVIN; LANDE; MACE, 2010). While several parameters asso-

ciated with demography and environment influence this quantity, emphasis on the role played by the genetic variance needs to be improved.

The dynamics of the genetic variance is, indeed, a key feature of long-term selection. Gradual evolution requires genetic variation, and despite the feasibility of significant phenotypic changes based only on the genetic variance of the original population (EISEN, 1980; KEIGHTLEY; HILL, 1990; WEBER; DIGGINS, 1990; BARRETT; SCHLUTER, 2008), polygenic mutation is indispensable to the maintenance of variation when it comes to sustained environmental change (LYNCH, 1988; NOTTER, 1999; CABALLERO; TORO; LOPEZ-FANJUL, 1991). Incorporating such elements in a model is defying, and hence a theme of historical debate (BARTON; TURELLI, 1989). Nonetheless, even in the realm of populations of infinite size under stabilizing selection, which notably has received more attention than any other domain (LANDE, 1976a; TURELLI, 1984; SLATKIN, 1987; BARTON; TURELLI, 1989; LYNCH; LANDE, 1993), it remains an uncomfortable conceptual vacancy among the models: dynamics of the mean phenotype and phenotypic variance subject to natural selection are not directly related in any case, i.e., they result from completely distinct assumptions.

Here, we address this conceptual problem by extending the reasonings developed by LANDE for populations of infinite size with constant phenotypic fitnesses and discrete generations. Rather than independently focusing on the evolution of the mean phenotype or phenotypic variance, each evolutionary force operates over the entire distribution of phenotypes. Under Gaussian stabilizing selection and normally distributed mutation effects, the stationary distribution of phenotypes must also be normal, and the dynamics comes down to that of the mean phenotype and the phenotypic variance. Such dynamics constitute a two-dimensional map that fruitfully allows analysis based on the theory of Dynamical Systems (OTT, 2002) and evinces two fundamental aspects of long-term adaptation. First, an optimal value of mutation rate naturally emerges since the phenotypic load is opposed by the approximation to the phenotypic optimum as variance increases, as first observed by MATHER. The second and main finding concerns the role of development.

Development is here explored through phenotypic plasticity. The mathematical description of plasticity for continuous traits involves the concept of reaction norm, the function associating phenotype to an environmental variable for each genotype (SCHEINER, 1993; CHEVIN; LANDE; MACE, 2010). For simplicity, one constrains the discussion to linear reaction norms. More precisely, it is linear when measured relative to the phenotypic distance to the optimum phenotype, which is a more appropriate assumption, since in the context of sustained environmental change, linearity on the environmental variable clearly induces a monotonically increasing magnitude of plasticity, accumulated over generations and unfeasible due to physiological constraints (ROCHA; MEDEIROS; KLACZKO, 2009). Remarkably, departing from no a priori assumption on constitutional or inherent costs of plasticity (DEWITT; SIH; WILSON, 1998; CROZIER; HUTCHINGS, 2014), the present modeling presents a clear trade-off between viability and stability as a function of the magnitude of development.

2 THEORETICAL FOUNDATION

The Theory of Evolution is a landmark of science. The recognition of its stochastic nature was decisive in the consolidation of probabilistic systems as an essential discipline, at a time dominated by the deterministic school of thought. The dynamic character of the species highlighted, in turn, the relevance and generality of phenomena out of thermodynamic equilibrium. The collective aspect opened the doors to a newly born scientific vision, emergentism, while reinforcing the importance of interdisciplinarity in understanding the natural world.

2.1 EVOLUTION

The evolutionary process is based on three pillars: reproduction, mutation and selection. All living organisms have been and are continually shaped by these factors, at the most diverse scales of organization, space and time. In a favorable environment, a living being must reproduce. When two types of individuals compete for resources and reproduce at different rates, selection occurs, favoring the one with the higher rate (NOWAK, 2006). It turns out that at the level of DNA and RNA, reproduction means replication, i.e., copying information, a process usually prone to errors (DOMINGO; SCHUSTER, 2015). These occasional errors in the transmission of genetic material produce new types of individuals and, with them, diversity, which will be subject to selection, perpetuating the cycle. It is important to emphasize that the ability to evolve does not belong to genes, cells or organisms, but rather to populations. Only populations can maintain and transmit the information generated in the process (NOWAK, 2006).

There are two basic postulates. First, mutations are random with respect to their effectiveness or functionality (SMITH, 1970). It should be clear that nothing is said, however, about randomness concerning their generation, in terms of their chemical and physical origins. In fact, the process can be very biased in this regard, resulting, for example, in the existence of certain regions in genetic sequences that are strongly affected by mutations (SMITH, 1970; EIGEN; MCCASKILL; SCHUSTER, 1989). The second hypothesis states the natural selection of favorable mutations. In the case of neutral mutations, fixation occur by chance. These hypotheses are strong, no plausible alternative has ever been suggested and no evidence to invalidate them has been found so far (SMITH, 1970). However, an apparent incompatibility in the structure of this system is the subject of intense discussion and is worth mentioning.

First of all, it is necessary to have an idea of the magnitudes involved in the number of possibilities of genomic and protein sequences. Consider proteins constituted of 100 amino acids, for instance, which is quite a modest length. Once there are 20 distinct amino acids, it results in a diversity of 20^{100} possible proteins, or about 10^{130}. Comparatively, it is estimated that there are about 10^{80} protons in the Universe (NOWAK, 2006). These numbers reveal

that evolution has not been and will not be able to explore more than a small subset of all possibilities.

Aware of this fact, SALISBURY noted an inconsistency: the astronomical number of possibilities associated with genomes and proteins seems to make adaptation via random mutations unsustainable, that is, favorable mutations would be too rare to be found by chance. In this scenario, natural selection would have nothing to act on. However, this conflict is only apparent and the result of an incorrect way of interpreting the probabilities in question. In fact, the probability of any given sequence being functional is not the relevant quantity in the evolutionary process. The probability that plays a central role is that of a mutant being better or equally efficient than its predecessor, that is, the one from which it was generated, within the particular set of all mutants accessible to this ancestor (SMITH, 1970). To understand how this conditional probability is sufficient to sustain adaptation, it is necessary to go deeper into what is meant by *accessible mutants*. From this need arises the concept of sequence space.

2.2 SEQUENCE SPACE

One can distinguish between two classes of mutations: (i) those that cause small changes, as a replacement, addition or deletion of a single informational basis, and (ii) those related to major changes. In many respects, it is plausible to assume that mutations involving more than one locus are not evolutionarily determinant, considering that the probability that they result in an efficient product must be very low (SMITH, 1970).

Figure 1 – Space of binary sequences of length $L = 3$. For a binary alphabet of arbitrary length, the space of sequences constitutes a hypercube.

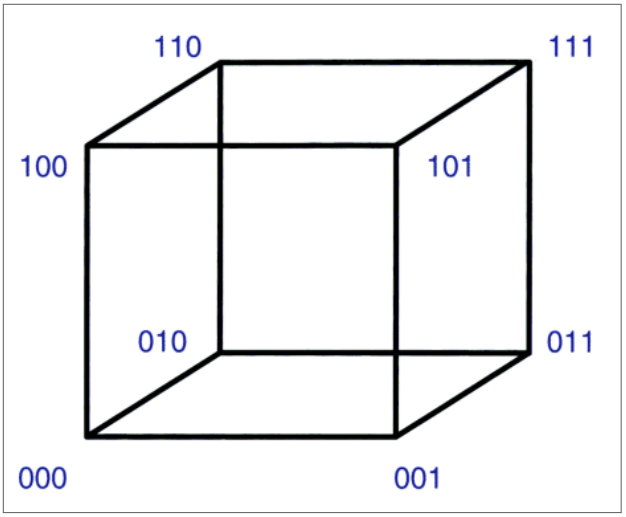

Source: NOWAK (2006)

Under this assumption, the archetype of the evolutionary dynamics that leads from a wild-type sequence to a favorable mutant sequence becomes that of a process that occurs by unitary mutational steps, via intermediate sequences that are also favorable. Such a process

must therefore involve a continuous network of functional sequences immersed in the space of all possible sequences. Continuity here refers to the passage exclusively through neighboring sequences, and neighborhood, in turn, refers to sequences that differ from each other by the mutation of a single locus (SMITH, 1970). We thus have the sequence space as the abstraction of the complete set of possible sequences of the same length endowed with the concept of neighborhood defined by the Hamming distance, measured by the number of sites by which two objects differ (NOWAK, 2006). Fig. 1 illustrates the concept for binary sequences, where vertices represent genomes and edges connect first neighbors.

It is now clear that the term *accessible mutant* refers to the set of first neighbors of a given sequence and we are now able to clarify the problem raised in the last section. The evolutionary process follows an algorithm based on already existing sequences, and therefore, functional sequences. It turns out that there is a strong correlation between the efficiency of a sequence and its neighbors, resulting in a greater probability of finding an efficient mutant in the neighborhood of an also efficient sequence than of selecting an efficient sequence from all sequences by pure chance. Illustratively, it is easier to find a peak in the Andes than to choose any place on the surface of the Earth (SMITH, 1970).

While pictures like the one above are quite useful, they do have their limitations and should be considered with caution. Sequence spaces are peculiar places characterized by high dimensionality and a huge number of close neighbors, as well as routes between two points. In particular, there are $d!$ direct routes between any two sequences that differ by d sites (NOWAK, 1992; EIGEN; MCCASKILL; SCHUSTER, 1989). Taking the estimate of protons in the Universe as a reference, a space with 10^{80} points would have a diameter of 133 units, and clearly a small number of mutations would lead to totally different regions. From this it can be inferred that any walk in spaces of this nature requires a very effective guide. In evolution, natural selection plays this role (NOWAK, 1992).

2.3 FITNESS LANDSCAPE

The concepts of fitness and evolutionary walk motivated the formulation of the sequence space. The attribution of reproductive capacity into the picture, known as the *fitness*, gives rise to another entity known as fitness landscape. The fitness landscape was introduced by Sewall Wright in 1932 (NOWAK, 2006; NOWAK, 1992). WRIGHT proposed the concept through the following question: if all possible combinations of genes were graded in some way with respect to their adaptive value, what would be the nature of this entity?

In order to imagine such a space, let us start with the combination with the greatest adaptive value. In relation to that, the fitness of the other sequences must decline more or less regularly according to the number of substitutions by which they differ. A distribution of individuals concentrated in one of these intermediate sequences would then be able to "feel" the adaptive gradient and "climb" until it stabilizes at the top, that is, those sequences close

Figure 2 – Two-dimensional representation of a fictitious fitness landscape. + and - signs represent fitness maxima and minima, respectively.

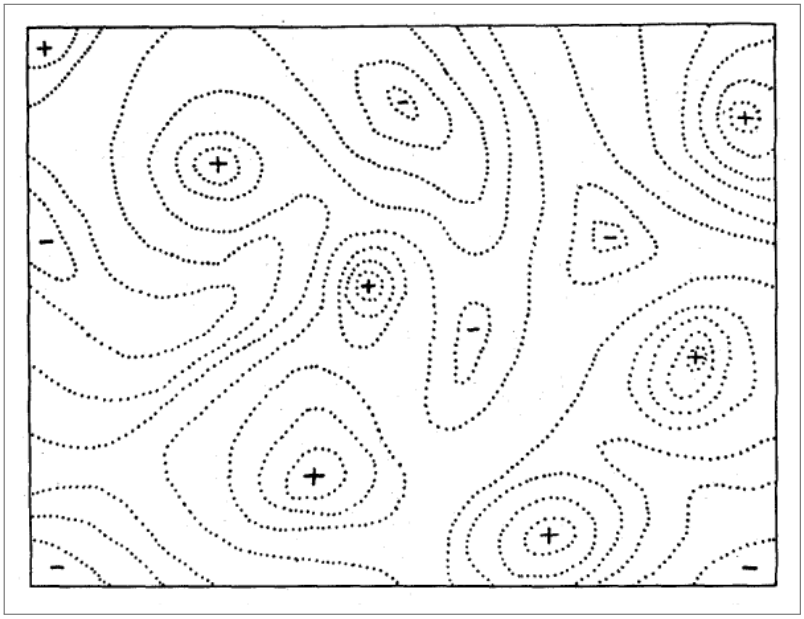

Source: WRIGHT (1932)

to the fittest tend to dominate in the population and mutations directed at them become fixed more frequently. (WRIGHT, 1932). Due to the difficulty of graphically representing these hyperdimensional spaces, 2D or 3D illustrations are inappropriate caricatures and often resemble representations of contour lines as in Fig. 2, presented by WRIGHT under the term "field of gene combinations".

Actually, these landscapes usually have more than one peak. Given an arbitrary initial condition, the selective force drives the population towards the nearest peak. Since adaptive peaks are separated by valleys of fitness, the gradient can no longer guide the optimization process once a peak has been reached. The evolutionary problem abstracted onto a rugged terrain like this is then characterized by the need for a search engine that allows the population to explore the surroundings of the small region it occupies waiting to experience a gradient belonging to another peak, thus having the chance to be continually taken from lower to higher peaks. The mechanism in question is trial and error, fueled by the occurrence of *de novo* mutations (WRIGHT, 1932).

2.4 THEORETICAL MODELS

Parallel to the slow progress of experimental studies, the theoretical area was extensively explored through various models. Such models were built on a wide variety of hypotheses, some even contradictory to each other (SZENDRO et al., 2013b). They have an important complementary role to experimental advances, being useful, for example, to quantify deviations associated with the inference of large-scale experimental landscapes from small samples

(VISSER; KRUG, 2014).

A widely explored class of models concerns the random field models. In these landscapes, fitness is attributed directly to each genotype through some probabilistic algorithm. They are especially useful in assessing how landscapes vary with dimensionality. The simplest model of this class is known as *House of Cards*, in which fitness is independently assigned to each sequence from a fixed probability distribution (VISSER; KRUG, 2014). Another example is the *Rough Monti Fuji*. Departing from an additive model, i.e., one in which each locus additively contributes to fitness, and then a noise is applied to that individual contribution. Through the intensity of the noise it is possible to adjust the deviation of the additivity and, therefore, the roughness of the landscape (VISSER; KRUG, 2014).

Following this adjustment capacity of the *Rough Monti Fuji*, there is also the *NK model*. It is characterized by the length L of the genomes and the number K of epistatic interactions. A given gene forms a set of $K+1$ interacting genes, and the fitness of the 2^{K+1} possible combinations of this set is randomly assigned (VISSER; KRUG, 2014). For $K = 0$, the contribution of each gene is independent of the others and the sequence with the highest adaptive value is obtained by optimizing all genes simultaneously and individually, giving rise to the only maximum of the landscape. With $K = N - 1$, however, each gene depends on all the others and, therefore, it is not possible to optimize even a single pair of them simultaneously, characterizing the phenomenon of frustration and resulting in a completely uneven landscape. Between these two extremes, intermediate levels of roughness can be obtained. The NK Model incorporates the ability to simulate the statistics associated with genetic interactions that lead to different roughness in the landscape without the need to formulate the biochemical mechanisms involved (SZENDRO et al., 2013b).

All the landscapes mentioned so far share one similarity. In these models the formulation of the structural origins of properties such as roughness is avoided in favor of the direct application of their immediate effects. A priori constructs, based on the chemical and physical underpinnings of proteins and genetic sequences, such as binding affinity, stability, and interactions, provide an alternative class of models made from first principles. Due to their larger complexity, they usually require great simulation and analysis capacity, which can represent an unnecessary difficulty depending on the object of study (SZENDRO et al., 2013b; VISSER; KRUG, 2014).

2.5 EVOLUTIONARY PREDICTABILITY

Considering the undeniable component of randomness involved in the directions and results of evolution, a list of pertinent questions arise (MORRIS, 2009):

- Would evolution be predictable in some way?
- Is it possible to identify and quantify the viability of alternative forms of biological

organization?

- How fortuitous are major transitions in the history of life?
- How bound by the past is evolutionary diversification?
- Do evolutionary solutions come closer to a merely sufficient answer or a highly efficient one?

Figure 3 – Differentiation of populations (shaded and patterned circles) subject to different environmental conditions (lines) since their origin from an unknown ancestor. Repeatable evolution can be referred to as the attainment of the same final character state, or the undergoing of the same evolutionary processes by different independent lineages. In terms of process, C and D are equivalent (repeatable), although the pattern is different: C represents parallel evolution, while D shows convergent evolution. Divergent evolution, represented by A and B, will exacerbate initial phenotypic and genetic differences between populations, either under different (A) or similar (B) environmental conditions. With parallel evolution, those same differences will be maintained.

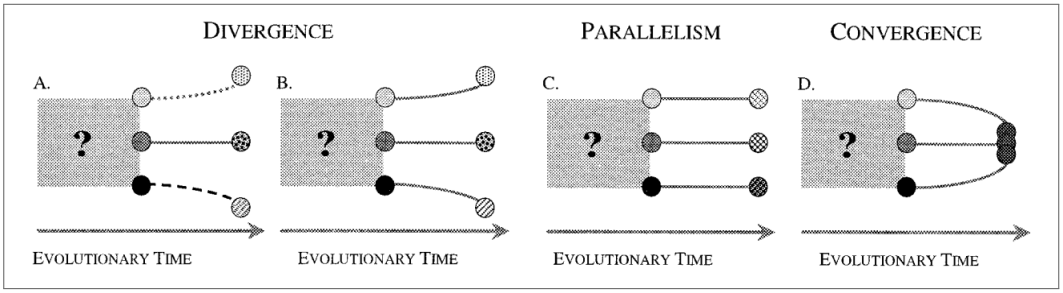

Source: TEOTÓNIO; ROSE (2001)

These questions, far from representing an objection to the existence of evolution and the consistency of the selection mechanism, only bring to light the fact that we most likely do not have a complete explanation of the phenomenon yet (MORRIS, 2009). There is no doubt that nature flaunts a great divergence of populations and species, and even under the assumption that divergence is inherently adaptive, we are still left with another question: is such divergence an adaptive response to different environments or a different adaptation to the same environment? In other words, does the diversity of solutions represent the diversity of the problem or the contingency of the process (DYKHUIZEN, 1992)? In practice, two lines can be directly explored: (i) identical populations evolving in parallel or (ii) different populations converging to the same solution (COLEGRAVE; BUCKLING, 2005). Parallelism, convergence, and divergence are illustrated in Fig. 3.

The adaptive process is ruled by essentially two types of factors, deterministic selective forces and fortuitous events of reproduction and mutation, whose influence on the evolutionary outcome is the cause of intense discussion and the reason behind great experimental and theoretical efforts. Experimentally, the study of predictability has been approached at the micro evolutionary scale through the repeatability of adaptive changes in replicated populations of microbes. In one of these studies, for example, strong evidence was observed of parallelism in the acquisition of antibiotic resistance by certain pathogens, a highly relevant result in the

context of pharmaceutical development (SZENDRO et al., 2013a). While the first experimental studies of predictability were limited to inference from their final result, currently the use of microorganisms offers a much richer procedure. Due to the short time between generations, microorganisms can be used to monitor adaptation in real time and under controlled environmental conditions. Furthermore, such beings can be maintained in an inanimate state, which allows direct comparison between ancestors and descendants (DYKHUIZEN, 1992; COLEGRAVE; BUCKLING, 2005).

One of the oldest studies in microbial evolution involves the bacteria *Escherichia coli*, investigated since 1988, and leads to some interesting results. In one of the experiments, LENSKI et al., twelve identical populations were subjected to a glucose-limited environment and their fitness was measured through direct competition with the ancestor. The experiment indicates that similar phenotypes can be obtained in different ways, through mutations in different genes. In this same study, the role of initial conditions was also explored. Although different populations showed divergences in fitness, this divergence did not depend on the starting point (COLEGRAVE; BUCKLING, 2005).

Figure 4 – Two possible adaptive landscapes for a simple two-gene organism. The circles represent the four possible genotypes and the size of the circle indicates the fitness of that genotype. To consider how evolution occurs on such landscapes, we will make a number of simplifying assumptions: (1) mutations only occur one at a time (so for example an ab individual cannot mutate to an AB individual in a single step), (2) genetic change is very rapid compared to the rate at which mutations occur, so that populations are effectively genetically uniform and, if a mutation arises that increases fitness, it will immediately spread through the population, whilst a deleterious mutation is immediately lost. Evolutionary changes that will be favored by selection are shown by arrows. Left panel: A smooth landscape, all trajectories lead to the AB genotype, and so selection will inevitably get to the same point wherever it begins. Right panel: A rugged landscape with two adaptive peaks (AB and ab) separated from each other by lower fitness genotypes. Now whether a population that starts at Ab evolves to the AB peak or the ab peak will depend on which mutations occur first, and a population that starts at the ab peak has no way of reaching the fitter AB peak.

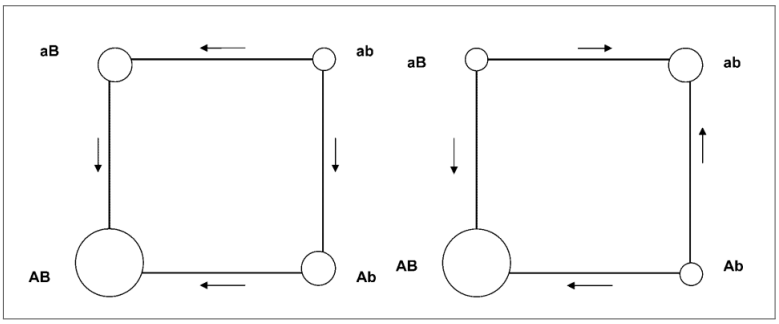

Source: COLEGRAVE; BUCKLING (2005)

Many factors can influence the repeatability of adaptive trajectories, the main ones being population size, mutation rate and landscape topography, the latter closely related to epistatic interactions (SZENDRO et al., 2013a). Regarding the relationship between topography and predictability, a notably important aspect is the roughness of the landscape. In a landscape with a single peak, for example, it is expected that regardless of the initial genotype and the order in which mutations occur, at the end of any walk the population will have reached the

global maximum. In rugged terrain, however, even when the initial condition is fixed, each step can be decisive in leading toward the basin of attraction of one of the several local maxima. Thus, the distinction between smooth and rough landscapes characterizes one of the most general and common ways of approaching the problem of evolutionary predictability. Roughness and abundance of local maxima have another immediate effect: often the population will not achieve the best possible result (COLEGRAVE; BUCKLING, 2005; KORONA et al., 1994). The great variability of the landscapes is so striking that even the smallest possible landscape, one of dimension two with only one type of mutation in each gene (see Fig. 4), is not a trivial case in terms of roughness and number of peaks and, consequently, possible walks. Such a landscape is capable of presenting two notably different situations that, ultimately, are decisive in the adaptive biases (COLEGRAVE; BUCKLING, 2005).

According to the intuition of stochastic processes, the dependence of evolutionary predictability on population size is expected to be quite simple: the larger the population, the more deterministic the system. A more detailed analysis of the problem, however, reveals a much richer relationship. Population and mutation rate together determine mutant breeding regimes whose effect on trajectory repeatability is nontrivial, for instance the SSWM (*strong selection weak mutation*), clonal interference, and stochastic tunneling (SZENDRO et al., 2013a). The first and simplest regime, SSWM, is characterized by a mutation rate low enough that the emergence and fixation of a given mutant occurs in isolation, that is, rarely there is the presence of two or more different mutations. In this way, the population behaves as a homogeneous entity, a walker forced to perform unitary mutation steps of ascending fitness. In general, such monotonically increasing paths are not abundant in the landscapes, which implies considerable predictability in the SSWM (SZENDRO et al., 2013a).

Despite its solidity, Darwinian theory should not be considered a complete theory. There is still a great lack of understanding of fundamental aspects, such as the way in which organisms take on increasingly complex forms and why evolutionary convergence is so recurrent. Underlying these doubts is growing evidence that these processes are predictable to some extent (MORRIS, 2010).

3 ADAPTIVE WALKS ON TIME-VARYING FISHER'S LANDSCAPES

The results displayed in this chapter correspond to the article published by CIRNE; CAMPOS.

DOI: 10.1103/PhysRevE.106.064408

3.1 PROLOGUE

Most evolutionary biologists are familiar to the concept of fitness landscapes and the general problem of combinatorial optimization. A stand-out class of fitness landscapes are the phenotypic fitness landscapes, those which map phenotype to fitness. Since the Neo-Darwinian paradigm of evolution, the set of possible phenotypes has been usually modeled into Euclidean vector spaces (STADLER; STADLER, 2006). Such mappings typically involve multiple nonlinearities that are paramount to the actual effect of mutations (SRIVASTAVA; PAYNE, 2022). Under biologically realistic genotype-phenotype maps, fitness landscapes become quite navigable even under random fitness assignment, presenting pervasive neutral networks and fitness maxima that can be reached from almost any other phenotype (GREENBURY; LOUIS; AHNERT, 2022).

The most important theoretical instance of a phenotype-fitness map is probably the Fisher Geometric Model (FGM) (FISHER, 1958). The FGM assumes a continuous multidimensional phenotypic landscape originally built to investigate the properties of individual mutation effects (TENAILLON, 2014), and successfully demonstrates the experimentally observed tendency of accumulation for small deleterious mutations (KIBOTA; LYNCH, 1996). Despite slightly detrimental mutations being somewhat less likely to become fixed than favorable ones, the former kind is far more abundant (HARTL; TAUBES, 1996). Under the FGM, this property emerges from geometrical properties associated with pleiotropy, i.e., the capacity of a mutation to affect multiple traits.

If supplemented with the assumption of additivity of mutational effects on phenotypic traits, the FGM provides a class of fitness landscapes where epistasis emerges from the nonlinear phenotype-fitness map (HWANG; PARK; KRUG, 2017). In the region where the curvature of the map is maximized, in particular, the associated fitness landscape presents reciprocal sign epistasis, i.e., pairs of genes that are separately unfavorable but jointly advantageous and known as a necessary condition for the existence of multiple fitness peaks (POELWIJK et al., 2011). Epistasis, the conditional effect of a mutation on the genetic background, is widely observed and is thought to play a fundamental role in evolution by natural selection (WEINREICH; WATSON; CHAO, 2005), and the FGM has been proven to be very useful in the understanding of the theme (BLANQUART et al., 2014).

As a framework targeted to multidimensional phenotypes, the FGM has been equally important in the investigation of the constraints imposed by multiple trait combinations in a species response to environmental changes (LAUGHLIN; MESSIER, 2015). Under distinct envi-

ronments, mutation effects usually vary significantly, affecting the patterns of evolution. More precisely, stressful conditions are thought to cause an increased variance of mutations' fitness effects, average value, and a number of expressed mutations (MARTIN; LENORMAND, 2006). Once again, the FGM can account for the observed patterns of fitness change (PERFEITO et al., 2014). In this context, here we propose a model of genotypic evolution in a changing environment based on Fisher landscapes.

3.2 MODEL

Here we propose a model for the genotypic evolution of isogenic populations under a period of stabilizing and directional selection. The adaptation process is depicted in a fitness landscape, which is built in two steps: (i) a genotype-phenotype map is produced by associating fixed phenotypic changes to a set of mutations that occur upon the ancestral phenotype to determine the resultant phenotype of each possible mutant; (ii) a phenotype-fitness map is provided by the Fisher Geometric Model (FGM). The environmental change is implemented in this last mapping, where the phenotypic global optimum, which originally coincides with the ancestral phenotype, is gradually moved to match the phenotype of the antipode sequence, the genotype that accumulates all mutations under investigation. The strong-selection weak-mutation regime (SSWM) is assumed, so that the population is isogenic most of the time and thus may be described as a single adaptive walker on the fitness landscape.

3.2.1 Fisher's landscapes

The usual design of experimental setups of adaptation is focused on a particular set of mutations that confer some advantage to the population relative to the ancestral genotype. Generally, this reasoning applies not only to the genome with its four genetic basis but to any level of biologic codification, such as proteins with amino acids. In any case, the actual alphabet concerned is irrelevant as it is only necessary to identify the absence or presence of each of the L mutations of interest, which occur in distinct loci, so that the material basis of information may be treated as a binary sequence $G = (G^{(1)}, G^{(2)}, \ldots, G^{(L)})$, where $G^{(l)} \in \{0, 1\}$. Hence, the genotypic space contains 2^L possible configurations which are subject to the metrics of the Hamming distance.

To each sequence G corresponds a phenotype $\vec{z}(G) = (z^{(1)}(G), z^{(2)}(G), \ldots, z^{(N)}(G))$ with N continuous-valued traits. Once the phenotype $\vec{z}(G_0)$ of the ancestral genotype $G_0 = (0, 0, \ldots, 0)$ is ascribed, then defining a particular displacement vector $\vec{\eta}_l = (\eta_l^{(1)}, \eta_l^{(2)}, \ldots, \eta_l^{(N)})$ in the phenotypic space to the mutation in the l-th locus is enough to uniquely determine the

phenotype of any combination. The phenotype of an arbitrary sequence is given by

$$\vec{z}(G) = \sum_{l=1}^{L} G^{(l)} \vec{\eta}_l \quad . \tag{3.1}$$

In particular, the antipode of the ancestral genotype, the sequence $\overline{G}_0 = (1, 1, \ldots, 1)$ that accumulates all mutations, has the following phenotype,

$$\vec{z}(\overline{G}_0) = \vec{z}(G_0) + \vec{\eta_1} + \vec{\eta_2} + \ldots + \vec{\eta_L} \quad . \tag{3.2}$$

At this point it is fundamental to highlight that, in nature, the phenotypic effect of a mutation usually depends on the genetic background, .i.e., the state of the other loci. Here, the mutational displacement vectors are constant, however, and according to Eq. 3.2, mutations are combined additively in this model, at least in phenotypic terms. Furthermore, mutations are assumed to be isotropic, so that each component of each mutational displacement vector is assumed to be an independent normal variable of null mean and standard deviation δ,

$$\eta_l^{(i)} \sim \mathcal{N}(0, \delta) \quad \forall \quad l, i \quad . \tag{3.3}$$

The genotype-phenotype map is settled and the next step is to assign the phenotype-fitness map. For this purpose, we resort to the FGM. Under this framework, the fitness of a given phenotype is a monotonically decreasing function of the phenotypic distance to the optimum phenotype, denoted by $\vec{\theta}$. The most common estimation of fitness for this model is known as Gaussian selection,

$$W(\vec{z}) = W_{opt} \exp\left[-\frac{1}{2}\left(\frac{\vec{z} - \vec{\theta}_t}{\omega}\right)^2\right] \quad , \tag{3.4}$$

where W_{opt} is the optimum fitness, and ω is the selection width (with $1/\omega$ as the strength of stabilizing selection). By setting $\omega = 1$, the phenotypic distances to the optimum $z^{(i)} - \theta_t^{(i)}$, the rate of environmental change $B^{(i)}$, and the mutation effect δ, are measured in units of the width of selection.

We have formally defined the fitness landscapes in which the adaptation process is depicted. These particular genotype-fitness maps under investigation are equipped with an intermediate phenotypic layer given by the FGM. Its main property is the presence of pleiotropy, i.e., the capacity of a mutation to affect multiple traits.

3.2.2 Moving optimum

The environmental change proposed is implemented in phenotypic terms. In the scenario of interest, it is assumed that the ancestral genotype G_0 used to be the fittest one in the original environment. Thus, the phenotype associated with G_0 is taken as the closest one to the optimum phenotype in the original environment. In order to avoid one more parameter,

Figure 5 – Top: The distinct phenotype-fitness maps experienced by two consecutive generations $t = 0$ and $t = 1$ are shown from left to right along with the optimum phenotype (blue) and each mutant phenotype (red). Bottom: The respective fitness landscapes $\mathcal{F}_0$ and $\mathcal{F}_1$ are shown with the gradients of fitness indicated by arrows, and maxima and minima symbolized by up and down triangles, respectively, and circles otherwise. The transient time interval, sequence size and number of traits are set at $\tau = 3$, $L = 2$, and $N = 2$, respectively.

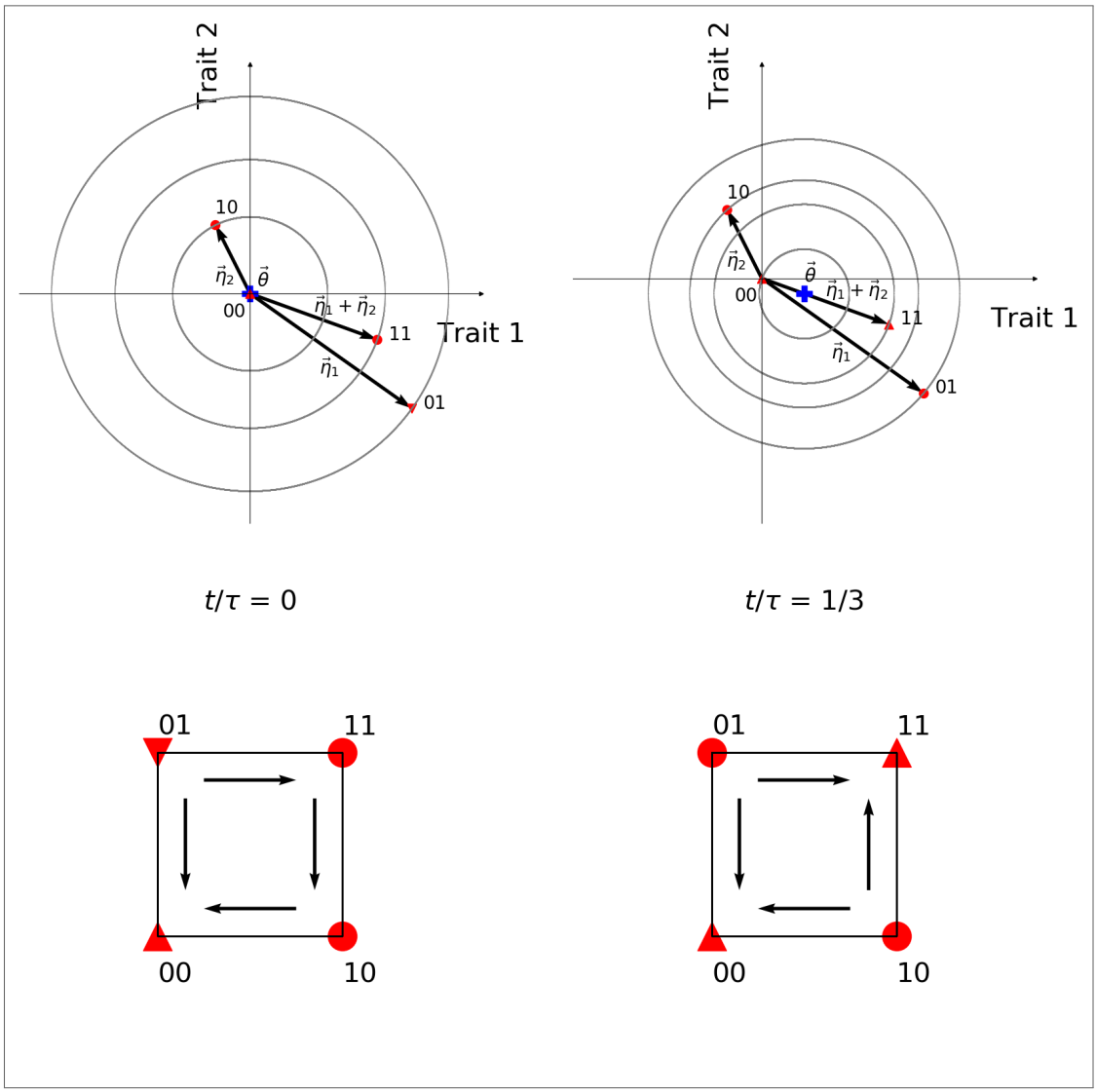

Source: Prepared by the author (2024)

we further assume that they coincide initially. Similarly, the optimum phenotype ends up at the phenotype of the ancestral genotype's antipode, in accordance with the experimental bias that the mutations addressed are precisely those which lead to the greatest adaptation in the new environment. Such change occurs uniformly along the straight line that connects these two phenotypes and during τ discrete time steps, so that the rate of environmental change is given by

$$\vec{B} = \frac{\vec{z}(\overline{G}_0) - \vec{z}(G_0)}{\tau} \quad . \tag{3.5}$$

Since the total change is finite, the parameter τ is called the transient time interval. It

Pseudocode
1: time $= 0$
2: $\vec{\theta} = \vec{z}(G_0)$
3: walker $= G_0$
4: **repeat**
5: $\vec{\theta} \rightarrow \vec{\theta} + \vec{B}$
6: **if** (walker $\neq$ local maximum)
7: adaptive step
8: time $\rightarrow$ time $+ 1$
9: **until** (time $= \tau$)
10: **repeat**
11: adaptive step
12: **until** (walker $=$ local maximum)

Table 1 – Pseudocode for the evolutionary dynamics concurrent to the ecological dynamics.

should be noted that neither $\vec{z}(G_0)$ nor $\vec{z}(\overline{G}_0)$ have an influence on the environmental dynamics, but only the phenotypic displacement $\vec{z}(\overline{G}_0) - \vec{z}(G_0)$ between them. Thus, $\vec{z}(G_0)$ is initially placed at the origin without loss of generality. After each time step, the fitness landscape is reshaped, and the t-th step is denoted by $\mathcal{F}_t$. A complete illustration is provided in Fig. 5.

3.2.3 Adaptive walk

Figure 6 – Illustration of the strong-selection weak-mutation regime. The y-axis represents the frequency of genotypes that carry a specific mutation. Most of the time the population is composed of a single genotype, as new mutations (represented by different colors) are quickly either fixed (green, blue, cyan) or lost (red).

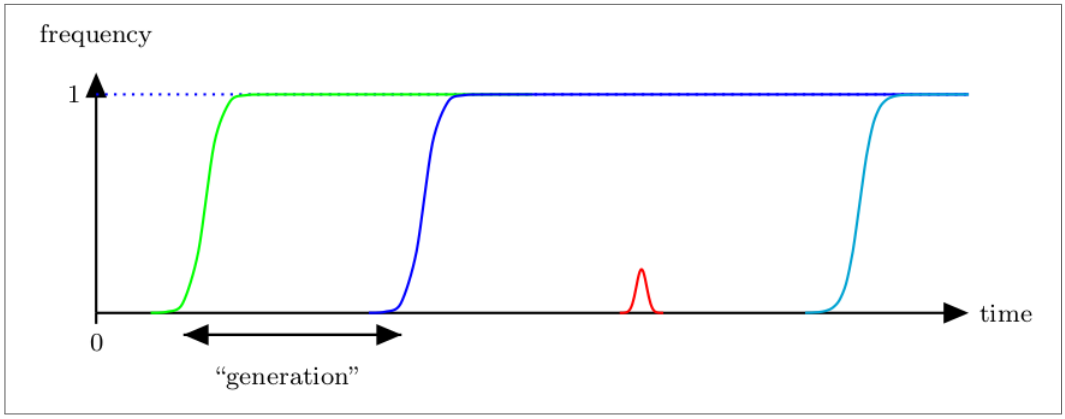

Source: PAIXÃO et al.(2017)

Here we consider a particular pattern of adaptation known as the strong-selection weak-mutation (SSWM) regime. As suggested by its designation, this regime is characterized by two

hypotheses. Under low mutation rates or small population sizes, the consecutive emergence and establishment of two mutants are separated by several generations (see Fig. 6). As a result, the adaptive process of the whole population may be depicted as the random walk of a single genotype on the fitness landscape. In this context, the temporal steps correspond to mutational events rather than biological generations.

The population in the isogenic state G has L first neighbors but can only move to those that are fitter. When allowed, the passage to the first neighbor G_l that differs from G in locus l occurs with a chance that is proportional to the gain of fitness $s_l = W(\vec{z}(G_l)) - W(\vec{z}(G))$ conferred, a quantity known as selective advantage, so that the associated transition probability is given by

$$p(G,l) = \frac{s_l H(s_l)}{\sum_{l'=1}^{L} s_{l'} H(s_{l'})} \quad , \tag{3.6}$$

where H denotes the Heaviside step function. The version of the walk described above is known as a natural adaptive walk. Note that the optimum fitness is canceled out in the transition probabilities so that one is dealing with relative fitness.

The connection between evolutionary and ecological dynamics is simple. During the transient time interval, the adaptive walker is allowed to execute a unique mutational step at each new landscape it faces in the series $\mathcal{F}_1 \to \mathcal{F}_2 \to \ldots \to \mathcal{F}_\tau$. Once $\mathcal{F}_\tau$ is attained, the environmental change ceases and the adaptive walker keeps following the positive gradients of fitness until it reaches a local maximum. At this point, the adaptive dynamics is also concluded.

Actually, the population may also stall at fitness peaks even during the transient period. These states, however, may be metastable, as subsequent environmental change may modify the distribution of local maximums and allow the re-establishment of the adaptive dynamics. Moreover, since the landscape $\mathcal{F}_0$ plays no role (the first step is taken at $\mathcal{F}_1$), $\tau = 1$ corresponds to a standard adaptive walk study on the static fitness landscape $\mathcal{F}_\tau$. Naturally, the initial condition of this evolutionary process is the ancestral genotype G_0, so that the population is adapted to the original environment $\mathcal{F}_0$. A pseudocode (basic algorithm) of the complete dynamics is provided in Tab. 1.

3.2.4 Simulation protocol

The realization of the above model is subject to chance twice: (i) the mutational displacement basis $\{\vec{\eta}_l\}$ and (ii) the adaptive step (Eq. 3.6). For a given mutational basis, the family $\{\mathcal{F}_1, \mathcal{F}_2, \ldots \mathcal{F}_\tau\}$ of fitness landscapes is completely determined. Monte Carlo simulations are performed over 10^3 samples of families, and 10^3 initially identical populations are left to evolve independently in each family. All simulations were implemented in the C++ language.

3.3 LANDSCAPE CHARACTERIZATION

The investigation begins with determining the signature of the FGM in the fitness landscapes. First, departing from the ancestral genotype, the probability P_b of the last mutation acquired by the ancestral strain being beneficial is computed and shown in Fig. 7-A as a function of the sequence size and the number of traits. Since the ancestral strain has the optimum phenotype initially, the first mutation is harmful in any circumstance. With each new mutation, P_b increases along with the average distance to the optimum phenotype. The slope, however, is monotonically decreasing with L, saturating at 0.5 as the distance diverges. The phenotypic complexity also plays a role as its increment causes a decrease in the chances of beneficial mutations. These are the main properties of the FGM and they have been thoroughly examined so far (TENAILLON, 2014; ORR, 2006; RAM; HADANY, 2015).

In Figs. 7-B and 7-C, the dependences of the number and density of local maxima with the number of traits and sequence size are also addressed. As a function of N, both quantities are monotonically decreasing, a trend that follows the diminishing of the probability of beneficial mutations. The stronger the bias on the mutation effect, the more correlated the fitness of the first neighbors and the smoother the landscape (STADLER, 2002). Moreover, the decrease of the density with L is expected since even in the uncorrelated landscapes the increment in the number of maxima is below the exponential increment of the total number of sequences (KAUFFMAN; LEVIN, 1987; WEINBERGER, 1991).

Figure 7 – Panel A: Probability P_b of the L-th mutation acquired by the ancestral strain being beneficial for different numbers of traits N. The magnitude of the mutation effect is set at $\delta = 1$ and the error bars are the standard deviation of the mean over 10^5 independent realizations of the mutational displacement basis $\{\vec{\eta}_i\}$. Panel B: Number of local maxima versus number of traits N for different values of sequence size L. The magnitude of the mutation effect is set at $\delta = 0.05\omega$ and the measures are averages over 10^3 independent realizations of the mutational displacement basis $\{\vec{\eta}_i\}$. Panel C: Density of local maxima versus number of traits N for different values of sequence size L. The magnitude of the mutation effect is set at $\delta = 0.05\omega$ and the measures are averages over 10^3 independent realizations of the mutational displacement basis $\{\vec{\eta}_i\}$.

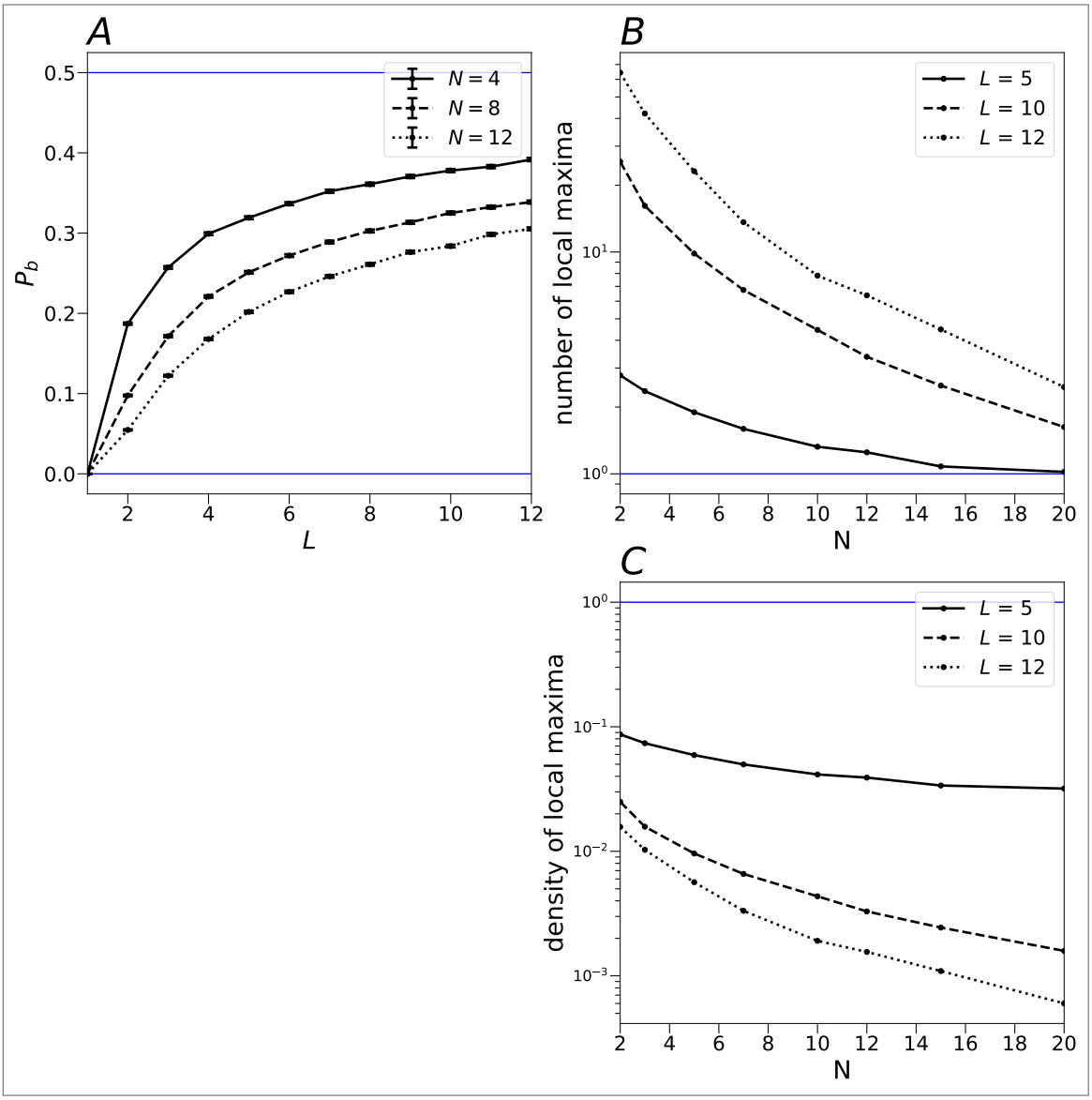

Source: Prepared by the author (2024)

3.4 WALK LENGTH

A measure invariably present in static adaptive walk studies is the mean walk length, i.e., the average number of substitutions in the genome up to reaching a fitness peak. As previously discussed, such fitness peak must belong to the final landscape $\mathcal{F}_\tau$ in our model. This quantity is strongly influenced by the density of local maxima or, alternatively, by the level of correlation

of the fitness landscape (FILHO et al., 2012).

Figure 8 – Panel A: Mean walk length versus transient time interval τ for different values of sequence size L and number of traits set at $N = 12$. Panel B: Mean walk length versus transient time interval τ for different values of number of traits N and sequence size set at $L = 12$. Panel C: Mean walk length of the subset of trajectories which ends up at the antipode $\overline{G}_0$ versus transient time interval τ for different values of number of traits N and sequence size set at $L = 12$. In all panels the magnitude of the mutation effect is set at $\delta = 0.05\omega$ and the error bars are the standard deviation of the mean over 10^3 independent populations and 10^3 realizations of the mutational displacement basis $\{\vec{\eta}_i\}$.

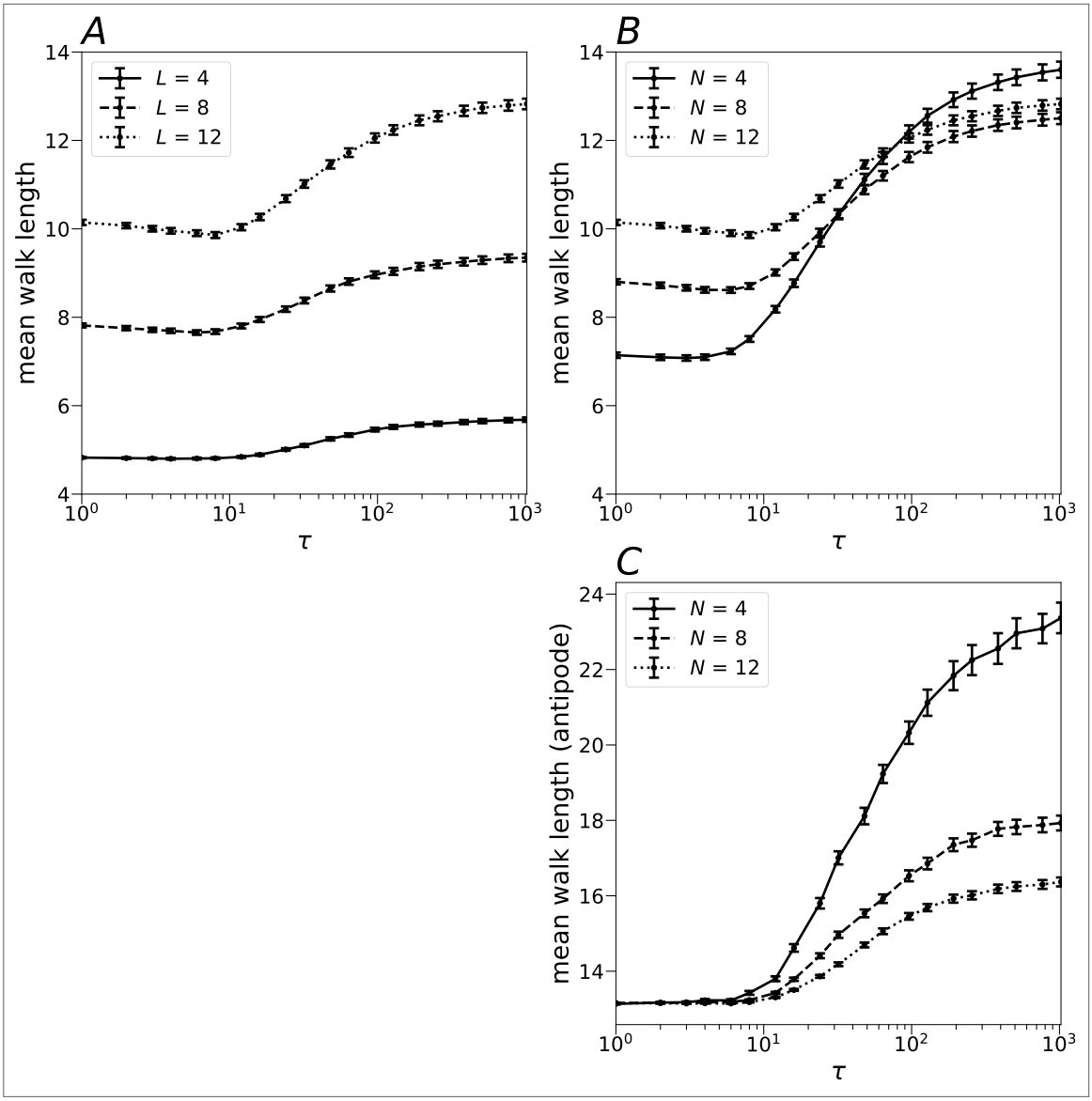

Source: Prepared by the author (2024)

In Fig. 8 the dependence of the mean walk length on the transient time interval, sequence size and number of traits are shown. A general observation across the panels concerns the time scale of adaptation to steady environments, inferred from the values displayed for $\tau = 1$, which are of the order of 10 mutational events, and seems to mark the threshold of influence of the ecological dynamics on the adaptive dynamics. While τ is below this value, corresponding to abrupt changes, it has little effect on the number of gene substitutions. Above this value,

however, there is noticeable increase with τ.

According to Fig. 8-A, increased genome size results in longer adaptive walks, a feature not seen in uncorrelated fitness (CAMPOS; MOREIRA, 2005; ORR, 2003). Under the FGM and Gaussian selection, sign epistasis is prevalent among the genotypes whose phenotypes are closer to the phenotypic optimum as a consequence of the enhanced curvature of the fitness function in this region (BLANQUART et al., 2014; HWANG; PARK; KRUG, 2017). As the optimum phenotype moves, the local maxima follow it through the genotypic space and are expected to finish the transient period clustered around the domain of $\overline{G}_0$. Thus, the walker is compelled to accumulate mutations towards this domain, a number that increases with the genome size.

The effect of the number of traits, shown in Fig. 8-B, is contingent on the magnitude of the transient time. Below the time scale of adaptation to steady landscapes, increasing N enlarges the trajectories as a consequence of the decreasing number of local maxima. Above this threshold, a conflict takes place. An increment of N also makes the routes less erratic through the intensification of the bias in the mutation effect, leading to an opposite effect in the mean walk length. This feature becomes more clear among the paths ending up in $\overline{G}_0$ as they are the longer ones, analyzed separately in Fig. 8-C. Under this condition, a larger number of traits is certainly associated to shorter walks.

3.5 ENDPOINT PREDICTABILITY

In this section the degree of determinism of the evolutionary trajectories is investigated. The measures defined below are designed to quantify how repeatable is the adaptive process and are key to distinguishing between possible evolutionary patterns such as parallelism, convergence and speciation (MORRIS, 2009; MORRIS, 2010; DYKHUIZEN, 1992; COLEGRAVE; BUCKLING, 2005; TEOTÓNIO; ROSE, 2001). Stochasticity manifests itself in many forms so there is no unique way to make this evaluation.

Let G^i_{end} denote the endpoint of the i-th independent adaptive walk for a fixed mutational displacement basis. Then, the probability distribution of the random variable G_{end} associated with the endpoints is given by

$$p_{end}(G_{end} = G) = \frac{\sum_i \delta(G^{(i)}_{end}, G)}{\sum_i 1} \quad , \tag{3.7}$$

where $\delta(G^{(i)}_{end}, G)$ is the Kronecker delta between sequences $G^{(i)}_{end}$ and G, whose application may be more simply visualized in terms of the one-to-one correspondence of the genotypic space $\{G\}$ with the natural subset $\{1, 2, \ldots, 2^L\}$, and $\sum_i 1$ accounts for all independent realizations of the adaptive walk. Then, the first measure, named endpoint predictability and denoted by $p_{2,end}$, stands for the probability that two arbitrary independent trajectories result in the same

genotype,

$$p_{2,end} = \sum_{\{G\}} [p_{end}(G_{end} = G)]^2 \quad , \tag{3.8}$$

where the sum runs over the whole the genotypic space (WEINREICH et al., 2006).

Figure 9 – Panel A: Endpoint predictability $p_{2,end}$ versus transient time interval τ for different values of sequence size L and numbers of traits set at $N = 12$. Panel B: Endpoint predictability $p_{2,end}$ versus transient time interval τ for different values of numbers of traits N and sequence size set at $L = 12$. In all panels the magnitude of the mutation effect is set at $\delta = 0.05\omega$, the probabilities $p_{end}(G_{end} = G)$ are estimated from 10^3 independent populations and the error bars are the standard deviation of the mean over 10^3 realizations of the mutational displacement basis $\{\vec{\eta}_i\}$.

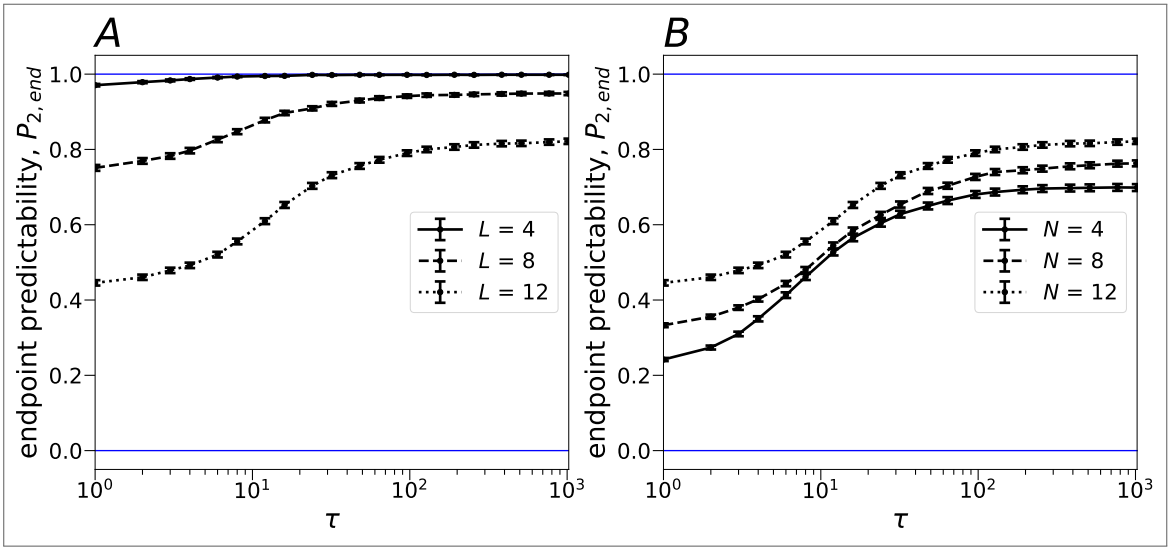

Source: Prepared by the author (2024)

According to Fig. 9, the dependence of the endpoint predictability on the sequence size and number of traits simply reflects the influence of these quantities on the total number of local maxima. There is increasing availability of fitness peaks both with increasing L and decreasing N thus making the outcome less predictable. Actually, the strengthening of the bias to detrimental mutations also intensifies this effect concerning the number of traits. Further, unlike the mean walk length, the endpoint predictability is strongly affected by the rate of environmental change under the time scale of adaptation to steady environments. As expected, smoother environmental variations always lead to more predictable outcomes. This feature is portrayed in more detail in Fig. 10 in terms of the accessibility of the endpoints in two sample landscapes, i.e., the fraction of the adaptive walks ending up in a given local maximum. Both landscapes allow access to all of their fitness peaks when $\tau = 2$ but have this number severely diminished as the transient time increases. The ecological dynamics has been shown to be crucial in the evolutionary trajectories by reshaping the attraction basin of endpoints.

Figure 10 – Accessibility of endpoints for different values of the transient time. Each row corresponds to an independent sample landscape of size $L = 12$, number of traits $N = 12$, mutation effect $\delta = 0.05\omega$, and 10^4 independent populations. The global optimum is highlighted in red. Local maxima are in ascending order of fitness from left to right.

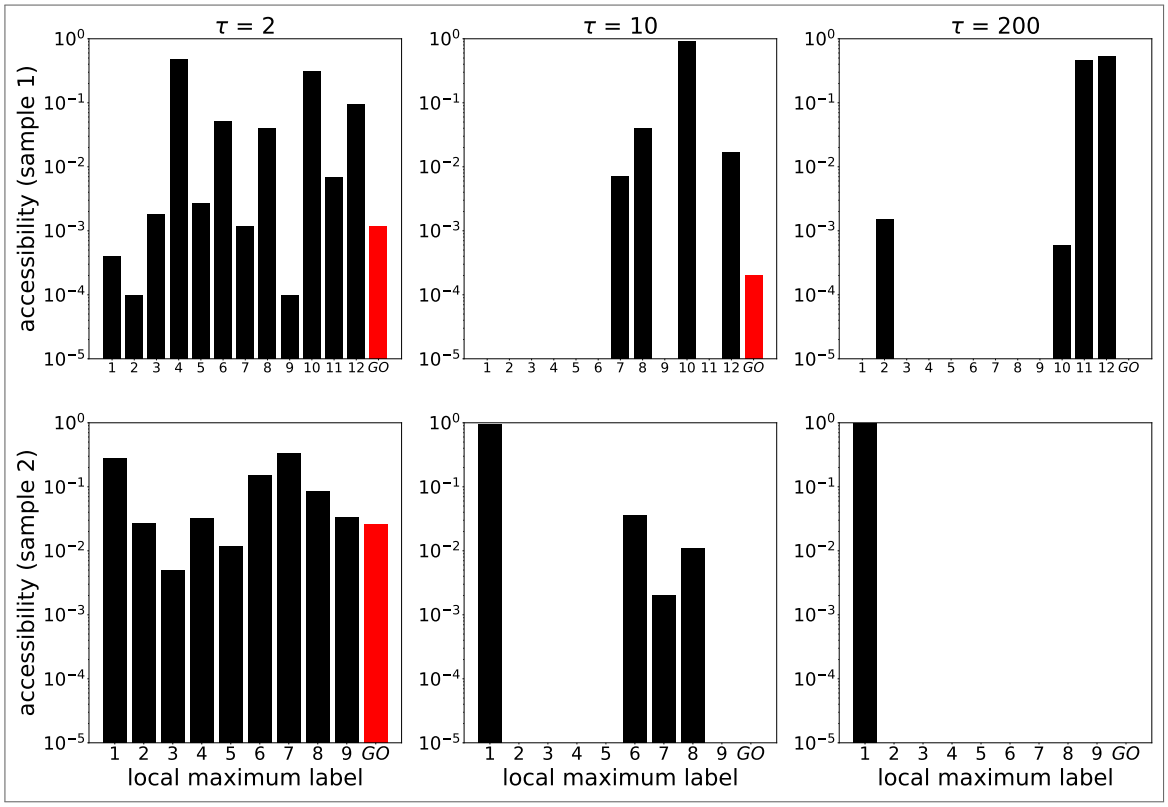

Source: Prepared by the author (2024)

3.6 PATH PREDICTABILITY

Alternatively, one can consider the repeatability of evolutionary pathways. Following a similar procedure, the ensemble of simulated paths gives rise to the probabilities $p_{path}(T_{evo} = T)$ that the evolutionary trajectory T_{evo} corresponds to the trajectory T among all possible series of sequences $\{T\}$ in the genotypic sequence,

$$p_{path}(T_{evo} = T) = \frac{\sum_i \delta(T_{evo}^{(i)}, T)}{\sum_i 1} \quad , \tag{3.9}$$

where $\sum_i 1$ accounts for all independent realizations of the adaptive walk. Then the quantity known as path predictability and denoted by $p_{2,path}$ is built by the same principle,

$$p_{2,path} = \sum_{\{T\}} [p_{path}(T_{evo} = T)]^2 \quad , \tag{3.10}$$

as the probability that an arbitrary and fixed path is drawn twice in a row by chance.

Its dependence on the magnitude of the transient time and the number of traits is plotted in Fig. 11 for the complete ensemble as well as for the set of paths ending up at the antipode. Except for small N, the path predictability is a monotonically increasing function of τ. As

Figure 11 – Panel A: Path predictability $p_{2,path}$ versus transient time interval τ for different numbers of traits N. Panel B: Path predictability of the subset of trajectories which ends up at the antipode $p_{2,end}(\overline{G}_0)$ versus transient time interval τ for different numbers of traits N. In all panels the sequence size and the magnitude of the mutation effect are set at $L = 12$ and $\delta = 0.05\omega$, respectively, the probabilities $p_{end}(G_{end} = G)$ are estimated from 10^3 independent populations and the error bars are the standard deviation of the mean over 10^3 realizations of the mutational displacement basis $\{\vec{\eta}_i\}$.

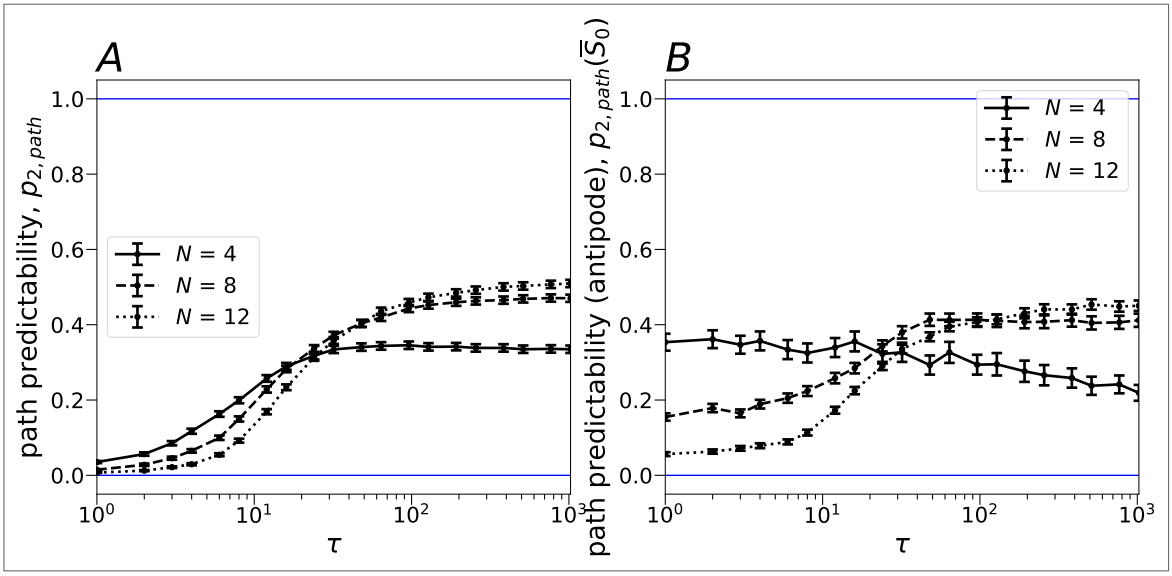

Source: Prepared by the author (2024)

observed for the endpoints, smother changes lead to more predictable paths too. When it comes to the number of traits, the outcome depends on the regime of environmental change. Under low rates of change, path predictability decreases with N as the trajectories become less erratic and towards less endpoints. Under high rates, on the other hand, the effect on the mean walk length is more determinant in the path predictability, making it decrease with the phenotypic complexity. Naturally, this trend is clearer among the paths ending up in the antipode.

3.7 DIVERGENCE

One more measure of evolutionary repeatability is provided in order to overcome an important limitation present in the path predictability: similarity between trajectories is not taken into account. In other words, pairs of trajectories that slightly differ contribute to $p_{2,path}$ in the same way as completely divergent paths. First we define the pairwise divergence $d(T, T')$ between two paths T and T' as the sum of the minimum distance $h_{min}(G, T')$ from each sequence $G \in T$ to T' added to the same sum in the opposite direction, then pondered by the sum of the total lengths,

$$d(T, T') = \frac{1}{n + n'} \left(\sum_{G \in T} h_{min}(G, T') + \sum_{G' \in T'} h_{min}(G', T) \right) \quad , \tag{3.11}$$

where n denotes the number of genotypes composing trajectory T. Note that the pairwise divergence is symmetric with respect to the paths. Next, the mean path divergence is estimated from the ensemble of simulated trajectories,

$$\overline{d} = \sum_{\{T\}} p_{path}(T_{evo} = T) \sum_{\{T'\}} p_{path}(T'_{evo} = T')\, d(T_{evo}, T'_{evo}) \quad . \tag{3.12}$$

In addition to the conceptual differences, predictability and divergence also differ on an important operational aspect. While the former considers any set of paths, the latter is meaningful only when applied to paths that share the same initial and final genotypes. In this context, for such a given set, $\overline{d}$ is calculated separately, weighted by the accessibility of endpoints (the initial sequence is always the ancestral strain) and then summed to generate the average value $\overline{D}$ (LOBKOVSKY; WOLF; KOONIN, 2011; MANHART; MOROZOV, 2014; LOBKOVSKY; KOONIN, 2012).

Figure 12 – Panel A: Mean path divergence $\overline{D}$ versus transient time interval τ for different numbers of traits N. Panel B: Mean path divergence $\overline{D}(\overline{G}_0)$ versus transient time interval τ for different numbers of traits N. In all panels the sequence size and the magnitude of the mutation effect are set at $L = 12$ and $\delta = 0.05\omega$, respectively, the probabilities $p_{path}(T_{evo} = T)$ are estimated from 10^3 independent populations and the error bars are the standard deviation of the mean over 10^3 realizations of the mutational displacement basis $\{\vec{\eta}_i\}$.

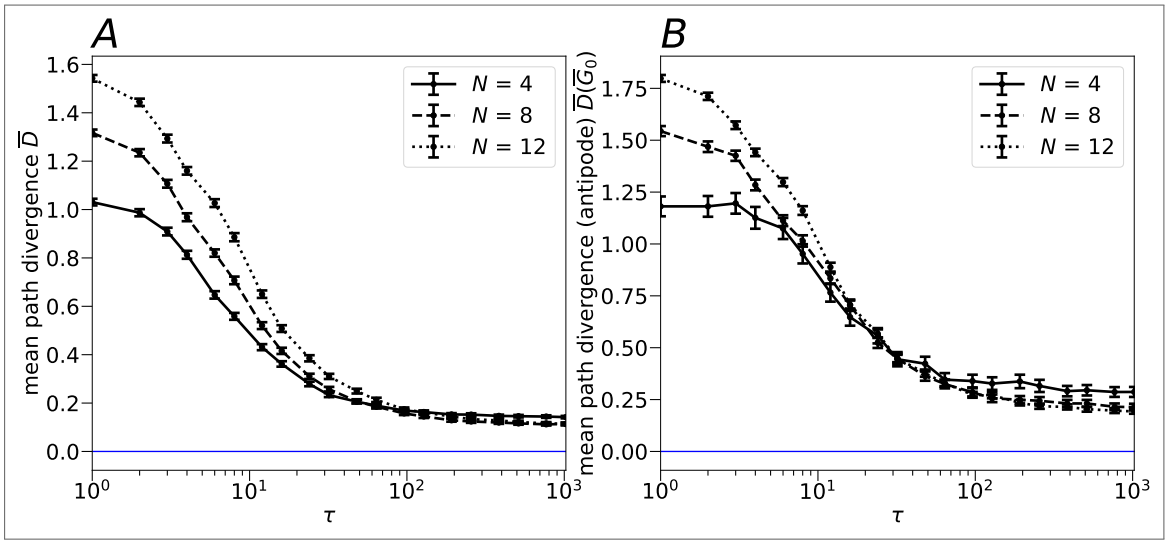

Source: Prepared by the author (2024)

In Fig. 12 the mean path divergence is plotted as a function of the transient time for the complete ensemble as well as for the set of paths ending up at the antipode. In all scenarios, $\overline{D}$ is a monotonically decreasing function of τ so smoother changes must be associated with less diffuse paths. Besides, the rate of environmental change regulates the effect of the number of traits on this measure too. Below the threshold of adaptation to steady environments, $\overline{D}$ grows with N. For large τ, the influence of the number of traits on $\overline{D}$ is mitigated. Concerning the relation with predictability, mean path divergence is negatively correlated except for small N (REIA; CAMPOS, 2020). The discrepancy observed under a small number of traits indicates the

existence of a considerably diverse collection of evolutionary paths yet very similar, differing only by a few sequences.

3.8 QUASI-STATIC APPROXIMATION

Lastly, an alternative dynamics is proposed in which the ecological timescale of environmental change is much slower than the timescale of adaptation. Operationally, this is implemented by allowing an environmental change only after the walker has attained a local maximum. In other words, variations in the fitness landscape occur as in the original formulation while the population is allowed to achieve complete adaptation to the current environment, at least locally. In this context, the parameter τ is no longer the transient but the exact number of moves performed by the optimum phenotype before reaching the antipode's phenotype. The pseudo-code associated with the quasi-static approximation is provided in Tab. 2. Some results for the quasi-static approximation are compared to those of the original formulation in Fig. 13. For $\tau = 1$, both approaches are formally equivalent, while an effective equivalence also occurs for very large τ. For the mean walk length, the quasi-static approximation establishes an upper bound, obviously. Probably for this reason both types of predictability are also higher under the quasi-static approximation.

Pseudo-code
1: time $= 0$
2: $\vec{\theta} = \vec{z}(G_0)$
3: walker $= G_0$
4: **repeat**
5: $\quad \vec{\theta} \rightarrow \vec{\theta} + \vec{B}$
6: $\quad$ **repeat**
7: $\quad\quad$ adaptive step
8: $\quad$ **until** (walker $=$ local maximum)
9: $\quad$ time $\rightarrow$ time $+ 1$
10: **until** (time $= \tau$)
11: **repeat**
12: $\quad$ adaptive step
123: **until** (walker $=$ local maximum)

Table 2 – Pseudo-code for the quasi-static approximation.

Figure 13 – Panel A: Endpoint predictability $p_{2,end}$ under the original formulation (filled) and under the quasi-static approximation (empty) versus transient time interval τ for different numbers of traits N. Panel B: Path predictability $p_{2,path}$ under the original formulation (filled) and under the quasi-static approximation (empty) versus transient time interval τ for different numbers of traits N. Panel C: Mean walk length under the original formulation (filled) and under the quasi-static approximation (empty) versus transient time interval τ for different numbers of traits N. In all panels the sequence size and the magnitude of the mutation effect are set at $L = 12$ and $\delta = 0.05\omega$, respectively. The probabilities $p_{end}(G_{end} = G)$ and $p_{path}(T_{evo} = T)$ are estimated from 10^3 independent populations and 10^3 realizations of the mutational displacement basis $\{\vec{\eta}_i\}$. Error bars are omitted for better visualization.

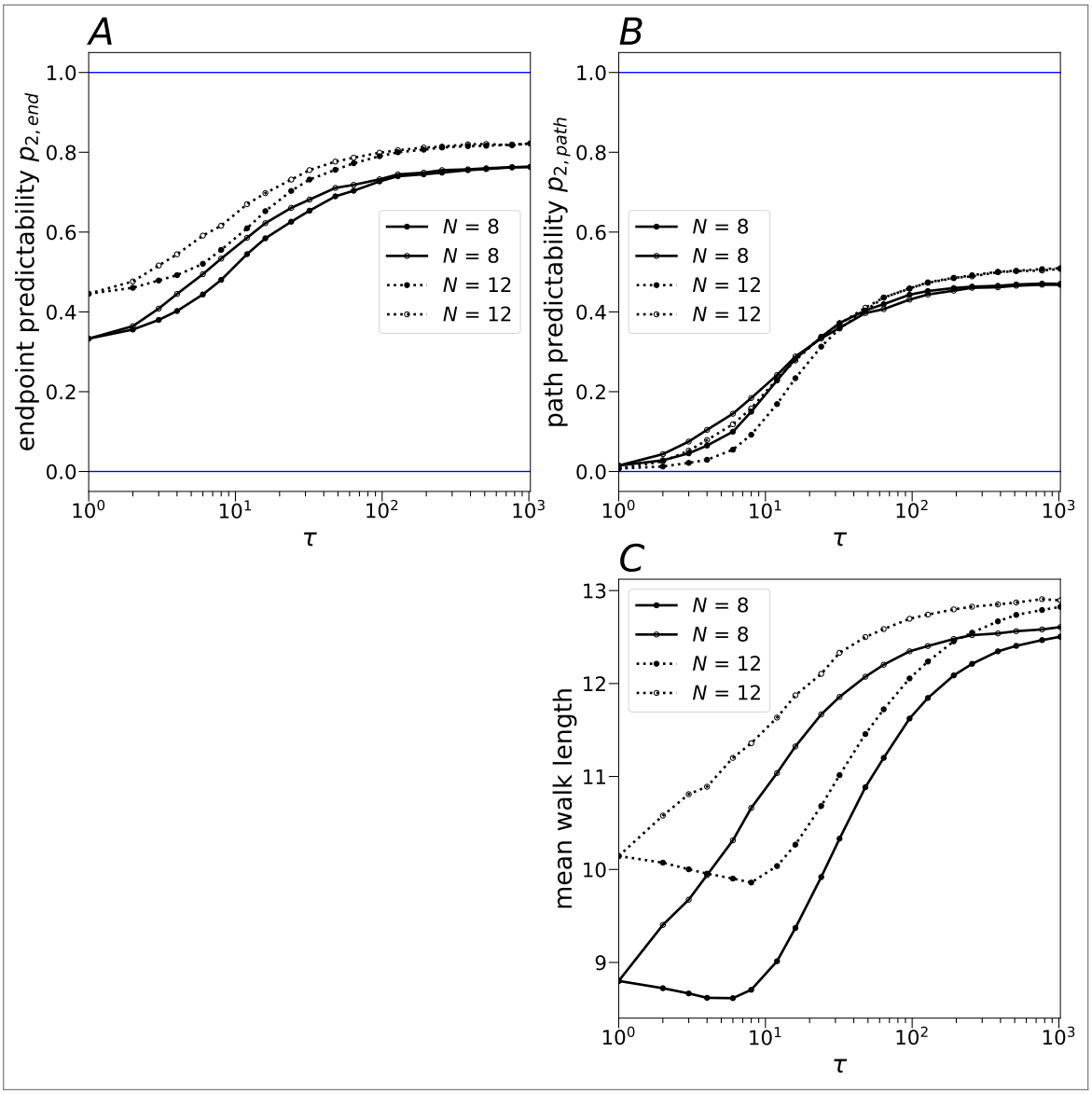

Source: Prepared by the author (2024)

3.9 SYNTHESIS AND PERSPECTIVES

Using an adaptive walk approximation, expected to hold in the strong-selection weak-mutation regime, the evolutionary patterns and outcomes induced by an ecological change occurring over a series of temporary intermediate states have been investigated. Under this

scenario, our simulations evince that the timescale of adaptation to static environments sets a threshold that delimits distinct regimes of influence of the rate of environmental change in the number of substitutions. While transient times below 10 units have very little influence on the walk length, slowly changing environments (several time steps) are associated with a greater number of substitutions. Concerning repeatability, on the other hand, the same threshold coincides with a steeper growth of the endpoint predictability. While abrupt environmental changes are proven to lead to more unpredictable outcomes, increasing τ causes the rise of $p_{2,end}$ through a drastic reduction of accessibility of most locally optimal genotypes. Concomitantly, the measures of path predictability and mean path divergence point to an increased constraint of the paths as the magnitude of transient time grows. Lastly, the quasi-static approximation evinces that temporary maladaptation is the major cause of the unpredictability of outcomes and trajectories. At this point, the immediate direction of extension for this work seems to reside in the relaxation of the strong-selection weak mutation regime, so that finite population dynamics should be explicitly simulated.

4 EPISTASIS AND SEASONAL GENE EXPRESSION

The results displayed in this chapter correspond to the article published by CIRNE; CAMPOS.

DOI: 10.1016/j.physa.2021.126453

4.1 PROLOGUE

All species are subject to seasonally changing selective pressures. Thus, the coordination of seasonal activities through adaptive physiological and behavioral changes according to the circannual timing is paramount to persistence (SCHWARTZ; ANDREWS, 2013). In trees, conserved periodic gene expression patterns arise from the response to day length or temperature, which determines their adaptive evolution (CHU et al., 2024). The investigation of the eco-physiological shifts of harmful cyanobacteria *Microcystis* from rapid growth in early summer to bloom maintenance in late summer and autumn may be decisive to the maintenance of freshwater resources globally (TANG et al., 2018). The extreme photoperiodic conditions experienced by the Antarctic krill *Euphausia superba* demand a flexible behavior and physiology provided by seasonal gene expression (HÖRING et al., 2021). Similarly, the annual migration of a bird requires accurately timed seasonal changes, where the differential expression of genes associated with cell adhesion, proliferation and motility indicates regulation by seasonal neural plasticity (JOHNSTON et al., 2016). In a study with two *Junco hyemalis* subspecies exposed to identical seasonal environmental cues, 547 genes differentially expressed were identified along with pronounced differences when comparing migrant juncos and resident breeders (FUDICKAR et al., 2016).

The theme is equally pertinent to human health as several diseases and physiological processes display annual periodicities. Indeed, multiple cell counts demonstrate significant association with a 12-month seasonal cycle, especially those linked to immune function, which is expected to vary throughout the year in healthy individuals, a behavior that stems mainly from red blood cells and blood platelets. During winter, for example, the blood is marked by a profound pro-inflammatory transcriptomic profile and increased levels of risk biomarkers for cardiovascular, psychiatric and autoimmune diseases characteristic of the season, a response that unveils even cytoarchitectural changes in brain regions. The elucidation of an atlas of how transcriptomes from human tissues adapt to major cycling environmental conditions is therefore an invaluable endeavor (GOLDINGER et al., 2015; JONG et al., 2014; DOPICO et al., 2015; WUCHER et al., 2023).

At the same time, the phenomenon of the maturation of the immune response was precisely the subject of a remarkable application within the fitness landscape theory carried by KAUFFMAN; WEINBERGER. In this work, a simple fitness landscape model originally introduced by KAUFFMAN; LEVIN to evaluate the role of epistasis in the adaptive process had been used

to build a general picture of the microevolutionary process sustained by hypermutation and clonal selection on the antibody V region mutant variants towards a higher affinity for the immunizing antigen. Notwithstanding, the same model also implies that complex biological systems, such as genetic regulatory systems, have evolved so as to be close to the mean properties of the ensemble of alternatives explored by evolution. Most importantly, all these results are open to detailed testing by in vitro mutagenesis experiments on the "affinity" landscape for the immunizing antigen.

More than evolutionary frameworks, fitness landscapes are fundamentally linked to the broad problem of complex combinatorial optimization processes. Mathematically, the concept stands for a mapping of the vertices of a finite graph to the real numbers. In this context, the NK model has been used to address the NP-completeness of the traveling salesman problem, for instance (WEINBERGER et al., 1996), while physically it corresponds to a dilute K-ary spin glass, i.e., one in which the state of each site is affected by that site and K of its neighbors, useful for approximating unconventional landscapes beyond the quadratically coupled spin glasses (WEINBERGER, 1991), and whose properties have been extensively investigated by simulation as well as analytically (DURRETT; LIMIC, 2003). In general, the NK model has been proven to be impressively suitable for modeling the process of innovation as an iterative, trial-and-error search (GANCO, 2017).

Concerning selection under seasonal gene expression, it has been recognized by (TRUBENOVA et al., 2019) that modularity, i.e., the independent adaptation of traits associated to the selective pressures of distinct seasons, is structurally maintained as long as epistasis is not present. Although modular behavior is common among regulatory networks without structural modularity (VERD; MONK; JAEGER, 2019), a model is presented here where even a low number of epistatic interactions leads to loss of functional modularity.

4.2 MODEL

Here we propose a model for the genotypic evolution of finite-size populations under seasonal environmental changes. The adaptation process is depicted in a fitness landscape, which is reshaped between seasons as a consequence of the alternation of selective pressures, a mechanism known as gene regulation. Special attention is paid to the role of epistasis as it prevents modularity, i.e., the independent adaptation of the distinct sets of traits. The degree of frustration may be tuned among a discrete set by using the NK model. The Wright-Fisher algorithm of reproduction is considered. Results are obtained from Monte Carlo simulations over two sources of stochasticity: (i) the NK model realization and (ii) the Wright-Fisher process.

4.2.1 NK model

In the original NK model, the genotype of an individual is represented by a binary string $G = (G^{(1)}, G^{(2)}, \ldots, G^{(L)})$ of size L, where $G^{(l)} \in \{0, 1\}$. The fitness of such genetic sequence,

$$W(G) = \frac{1}{L} \sum_{l=1}^{L} w_l(G^{(l)}, G^{(l_1)}, G^{(l_2)}, \ldots, G^{(l_K)}) \quad , \tag{4.1}$$

is the average value over the individual fitness contribution of each locus, which depends not only on its state but on the states of a set $\Omega(l) = \{l_1, l_2, \ldots, l_K\}$ of K other loci called epistatic neighbors. The set of epistatic neighbors is particular to each locus and assigned randomly from a discrete uniform distribution among the remaining $L - 1$ loci. Thus, w_l can assume 2^{K+1} distinct values across genotypic space. These are obtained from independent continuous uniform distributions,

$$w_l \sim \mathcal{U}(0, 1) \quad . \tag{4.2}$$

4.2.2 Gene regulation

Species respond to the seasonal dynamics of the environment through gene regulation. Gene regulation implies that each temporal phase $P \in \{1, 2, \ldots, N_P\}$, from a total of N_P phases supposed equally spaced of period τ, inflicts selective pressures on different traits. Each of these traits, in turn, is encoded by a particular set of genes $\Gamma(P)$, which are assumed to have no overlapping among different phases and a constant size L_R, so that $L = N_P L_R$. Since the epistatic interactions are randomly allocated, there is no loss of generality in ascribing the sets $\Gamma(P)$ sequentially, i.e., $\Gamma(P) = \{(P-1)L_R + 1, (P-1)L_R + 2, \ldots, PL_R\}$. In this context, each phase is associated with its own fitness landscape,

$$W_R(G, P) = \frac{1}{L_R} \sum_{l \in \Gamma(P)} w_l(G^{(l)}, G^{(l_1)}, G^{(l_2)}, \ldots, G^{(l_K)}) \quad . \tag{4.3}$$

Due to epistasis, in addition to the directly selected genes of a given phase, there is also an indirect selection of genes belonging to other phases, in general. Nonetheless, the fitness of an arbitrary sequence under phase P does not depend on all L loci necessarily, but only on a number that depends on the superposition among the set $\Gamma(P)$ and the sets $\Omega(l)$ of the epistatic neighbors of each locus $l \in \Gamma(P)$. Consequently, the concept of global optimum can be subject to degenerescence, in the physical sense. We denote by $\{G_{GO}(P)\}$ the set (or network) of all sequences that share the highest value in the fitness landscape but differ in any of the loci that do not contribute to fitness, when available. Further, it is useful to define the optimal subconfiguration $G_{GO,\Gamma}(P)$ of phase P as the state of the portion of $G_{GO}(P)$ located at $\Gamma(P)$.

4.2.3 Wright-Fisher process

We consider haploid organisms that reproduce asexually through the Wright-Fisher model. This model describes a population with discrete, non-overlapping generations of constant size M. Reproduction is abstracted as the replacement of every individual of the parental generation by a new one, whose parent is chosen by random sampling with a probability $p_{WF}(G)$ that is proportional to the fitness $W(G)$ of the genotype G it carries. Let $f(G,t)$ denote the fraction of individuals with this genotype in generation t, then

$$p_{WF}(G,t) = \frac{f(G,t)W_R(G,P(t))}{\sum_{\{G'\}} f(G',t)W_R(G',P(t))} \quad , \tag{4.4}$$

where the sum runs all over the 2^L sequences of the genotypic space $\{G\}$. The genotypic structure of the whole offspring is a random variable of multinomial distribution, consequently.

Actually, it is more precise to say that Eq. 4.4 describes the gametic distribution. The ensemble of gametes, in turn, is subject to mutations that act in the following form: there is a chance $0 < \delta < 1$ that a newborn individual inherits a genotype that differs from its parent's genotype by a unique locus. The locus by which parent and prole differ is a random variable ruled by a discrete uniform distribution among the loci. Therefore, the probability $p_{mut}(G,G')$ that sequence G mutates into sequence G' can be formally written as

$$p_{mut}(G,G') = \begin{cases} 1-\delta, & \text{if} \quad G = G' \\ \delta/L, & \text{if} \quad h(G,G') = 1 \\ 0, & \text{if} \quad h(G,G') > 1 \end{cases} \quad , \tag{4.5}$$

where $h(G,G')$ is the Hamming distance between sequences G and G'. Taking mutations into account, the Wright-Fisher probabilities (Eq. 4.5) give place to the reproductive probabilities $p_{rep}(G,t)$:

$$p_{rep}(G,t) = \sum_{\{G'\}} p_{mut}(G',G)p_{WF}(G',t) \tag{4.6}$$

$$= \frac{\sum_{\{G'\}} p_{mut}(G,G')f(G,t)W_R(G,P(t))}{\sum_{\{G''\}} f(H'',t)W_R(G'',P(t))} \quad . \tag{4.7}$$

4.2.4 Simulation protocol

The realization of the above model is subject to chance twice: (i) the NK model landscape realization and (ii) the Wright-Fisher process (selection and mutation). Monte Carlo simulations are performed on 10^2 samples of landscapes and 10^4 initially identical populations are left to evolve independently in each landscape. For fixed sequence size L and epistatic parameter K, the ensemble of landscapes is the same. All simulations were implemented in the C++ language.

4.3 FITNESS CORRELATION

A key measure in characterizing the topography of a fitness landscape is the fitness correlation $\rho(h(G,G'))$ of two sequences G and G' as a function of their Hamming distance $h(G,G')$. Originally, the correlation between first neighbors is estimated as the chance that a single mutation does not affect the individual fitness contribution of a fixed and arbitrary locus. In the NK model, such mutation should neither hit the focal locus nor any of its K epistatic neighbors, so that $\rho(1) = (L-K-1)/L$. Following similar reasoning, w_l will pass unharmed by two mutations in distinct loci with a chance $\rho(2) = (L-K-1)(L-K-2)/[L(L-1)]$. By induction, it is possible to achieve the general formula (CAMPOS; ADAMI; WILKE, 2002)

$$\rho(h) = \frac{(L-K-1)!(L-h)!}{(L-K-1-h)!L!} \quad . \tag{4.8}$$

Obviously, the correlation is a monotonically decreasing function of the number of epistatic interactions. For $K = 0$, the mean fitness variation caused by one mutation is $1/L$ and the similarity of first neighbors approaches unity, $\rho(1) = (L-1)/L$. When $K = L-1$, on the other hand, any two genotypes present no correlation since the fitness of a sequence is randomly assigned, or more precisely, assigned by independent and identical distributions that tend to normal distributions as L increases, in accordance with the Central Limit Theorem. In this case, any mutation certainly affects a given locus contribution, and the correlation is null for any Hamming distance.

Under gene regulation, however, a subtle modification arises once the chance that a unitary mutation does not alter w_l gains one more type of event in its favor. For a given phase P, the focal locus l can simply be out of the region $\Gamma(P)$, which occurs with a probability of $1 - L_R/L$. Otherwise, Eq. 4.8 still holds, so that the modified correlation function is given by

$$\rho_R(h) = \left(1 - \frac{L_R}{L}\right) + \frac{L_R}{L}\rho(h) \tag{4.9}$$

$$= \left(1 - \frac{1}{N_P}\right) + \frac{1}{N_P}\rho(h) \quad . \tag{4.10}$$

The main difference relative to the original formula concerns the presence of an inferior bound for the correlation (see Fig. 14), therefore, resulting in smoother fitness landscapes. This effect is associated to the existence of neutral networks percolating the genotype space when the genome is fragmented into regions that alternate periods of selective pressure (AGUIRRE et al., 2018).

Figure 14 – Fitness correlation ρ_R versus Hamming distance h for different numbers of phases N_P, different numbers of epistatic neighbors K and sequence size set at $L = 16$. In the limit case $N_P = 1$ (black curves), the modified correlation ρ_R equals the original one ρ.

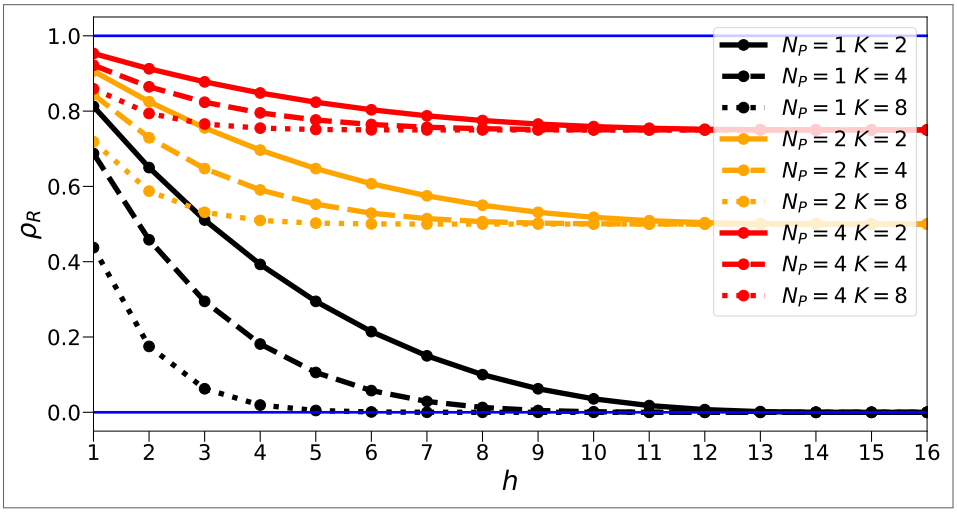

Source: Prepared by the author (2024)

4.4 ADAPTATION LEVELS

The average response of a population to seasonal environmental change is portrayed in Fig. 15 in terms of the time series of the mean population fitness $\overline{W}(t)$ (measured relative to the global optimal set) as well as the Hamming distance $h(G_{MA}(t), G_{GO}(P(t)))$ of the most adapted sequence $G_{MA}(t)$ in the population to the global optimum of the respective phase $G_{GO}(P(t))$ (usually the dominant one). The stationary state is an oscillatory dynamics of period τ, as expected. Discontinuous changes in both quantities reflect the instantaneous reshaping of the fitness landscape, while continuous ones manifest the gradual action of selection supplied by mutation.

The enlargement of the amplitude of oscillations in fitness with the phase's length is noticeable. The larger the period the closer the population gets to the global optimum set, a distancing which is still high so that the evolutionary solution attained is considered intermediate. The gap to G_{GO} immediately after a phase change is also smaller as τ increases, even though the initial level of adaptation becomes poorer under the same circumstance.

Naturally, one can also track the approximation of the phase subset state $G_{MA,\Gamma}(P)$ (the portion of genotype G_{MA} located at $\Gamma(P)$) to the corresponding optimal subconfiguration $G_{GO,\Gamma}(P)$. Note that the upper limit is L_R. The general picture of the temporal evolution of the Hamming distance $h(G_{MA,\Gamma}(P), G_{GO,\Gamma}(P))$ of the distinct phases is depicted in Fig. 16.

The abrupt fall at the beginning of a phase indicates that considerable part of the adaptation is preserved during a complete cycle. Notwithstanding, the continuous decrease for the target phase is accompanied by a symmetrical increase for the other phase when $N_P = 2$, excluding the hypothesis of neutral evolution for the unexpressed genes and evincing the considerable indirect selective pressure on them even at a low number of epistatic neighbors. For

Figure 15 – Panel A: mean population fitness $\overline{W}$ of a single population versus time (number of generations) t for different values of period τ. Panel B: Hamming distance of the most adapted sequence in the population to the global optimum $h(G_{MA}, G_{GO}(P))$ versus time (number of generations) t for different values of period τ. In both panels the population size, mutation rate, sequence size, number of epistatic neighbors and number of phases are set at $M = 10^4$, $\delta = 10^{-4}$, $L = 16$, $K = 2$ and $N_P = 2$ ($L_R = 8$), respectively, and the measures are averages over 10^4 independent populations in a single fitness landscape.

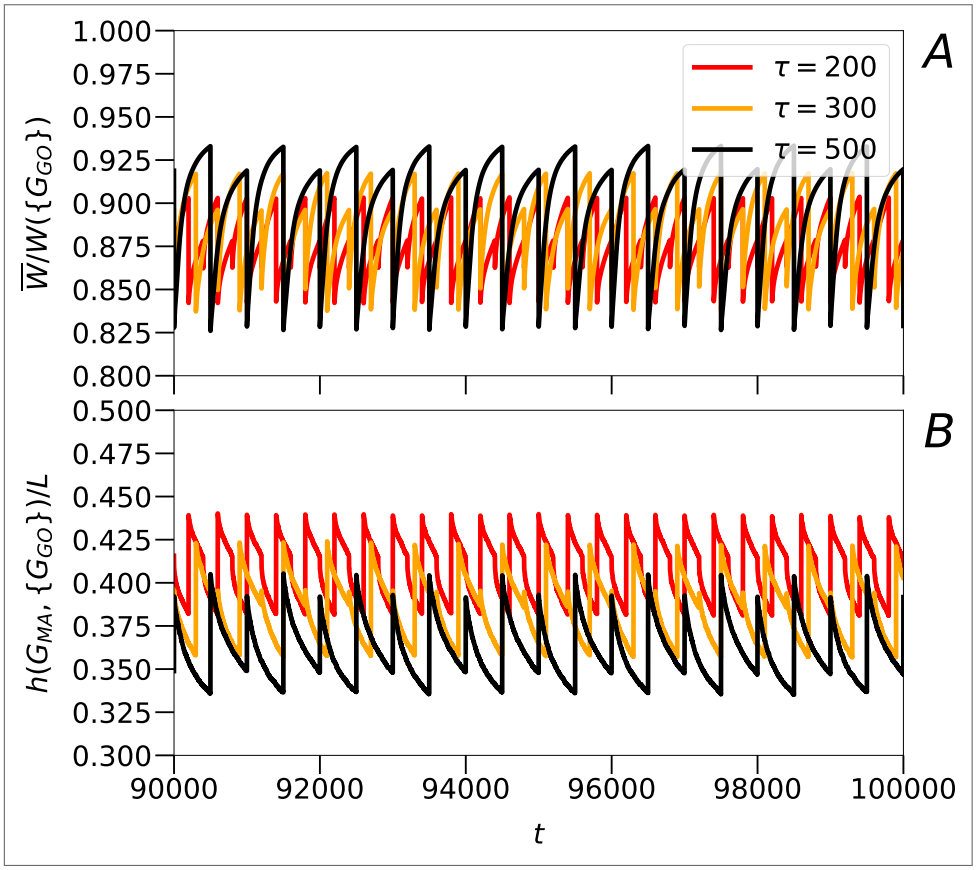

Source: Prepared by the author (2024)

$N_P = 4$, this is observed in the reinforced rises under phase switches that keep the focal phase out of selection.

A more detailed analysis of the mean population fitness is brought in Fig. 17. Maximum and minimum values, denoted by W_{max} and W_{min}, respectively, as well as the amplitude of the oscillations $W_{amp} = W_{max} - W_{min}$ are plotted. The tendency previously pointed out in Fig. 15 is decidedly corroborated now: the longer the phases the larger the amplitude of oscillations. Such behavior has already been observed in additive fitness landscapes (TRUBENOVA et al., 2019), and is also achieved by an increasing number of phases. As a matter of fact, N_P has no effect on W_{max}, and the variation in W_{amp} comes entirely from the diminishing of W_{min}. The reason is simple. As the number of phases increases so does the time during which a subset $\Gamma(P)$ is not targeted, which enables greater misalignment of this portion relative to the optimal subconfiguration of the phase owing to accumulation of mutations. On top of that, the effect is enhanced by epistasis as genetic drift gives place to selection against the optimal subconfiguration. In fact, when any other phase P' in under direct selection, each

Figure 16 – Hamming distance of the phase subset state of the most adapted sequence in the population to the corresponding optimal subconfiguration $h(G_{MA}(P), G_{GO}(P))$ versus time (number of generations) t for all phases, with number of phases set at $N_P = 2$ in panel A and $N_P = 4$ in panel B. In both panels the population size, mutation rate, sequence size, number of epistatic, neighbors and period are set at $M = 10^4$, $\delta = 10^{-4}$, $L = 16$, $K = 2$ and $\tau = 200$ respectively, and the measures are averages over 10^4 independent populations in a single fitness landscapes.

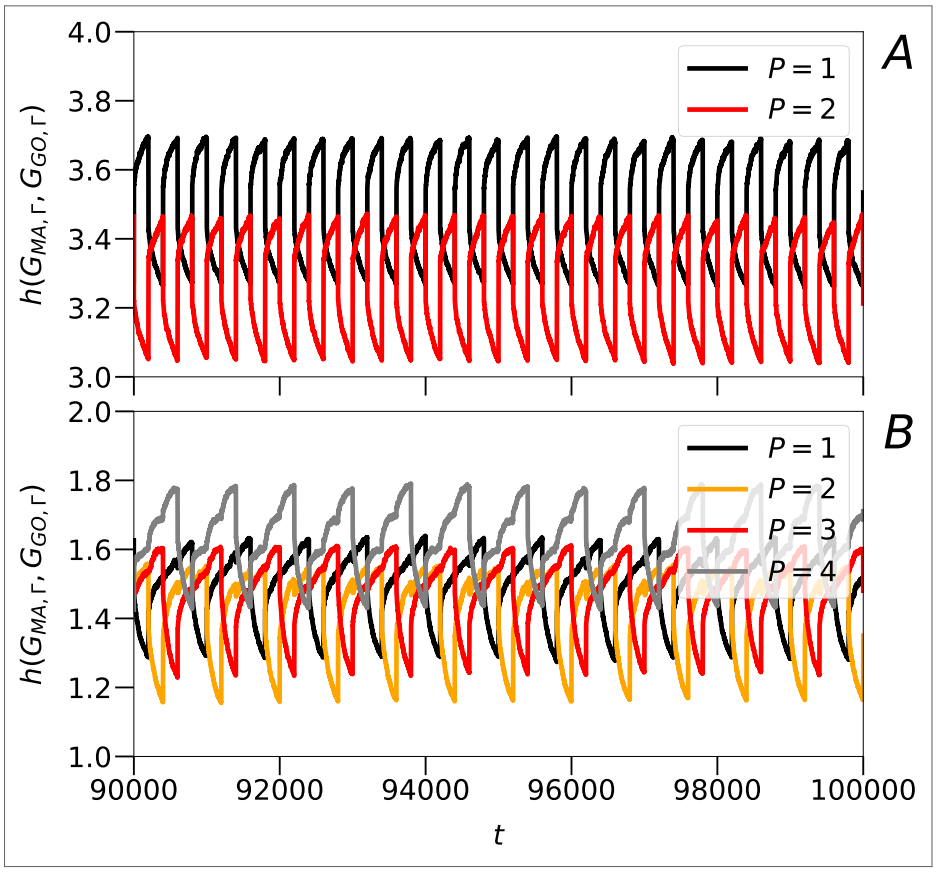

Source: Prepared by the author (2024)

locus $l \in \Gamma(P)$ of a given phase P which is the epistatic neighbor of a locus $l' \in \Gamma(P')$ will be selected in favor of $G_{GO,\Gamma}(P')$ instead of drifting. Furthermore, larger K also leads to poorer adaptation. The lower values of both minimum and maximum mean population fitness are caused by the greater accessibility of lower peaks observed in more rugged landscapes. Indeed, for $N_P = 4$ and $K = 8$, the average minimum approaches $0.5W(\{G_{GO}\})$, which is exactly the mean fitness value all over the ensemble of landscapes.

As another option, the role of epistasis is endorsed by measures of the Hamming distance from the phase subset state of the most adapted genotype in the population to the optimal subconfiguration. Minimum and maximum values attained $h_{min}(G_{MA}\Gamma, G_{GO,\Gamma})$ and $h_{max}(G_\Gamma, G_{GO,\Gamma})$, respectively, as well as the amplitude of oscillation $h_{amp} = h_{max} - h_{min}$ are plotted in Fig. 18. Additionally, the case $K = 0$ is also shown, for which a perfect adaptation is feasible even for small periods. The maximum value of about 1 confirms that the distancing from $G_{GO,\Gamma}$ under genetic drift is very small.

Last but not least, the effect of the population size on the level of adaptation is addressed

Figure 17 – Panel A: minimum mean population fitness $\overline{W}_{inf}$ (dashed line) and maximum population fitness $\overline{W}_{sup}$ (solid line) versus period τ for different values of number of phases N_P and number of epistatic neighbors K. Panel B: amplitude of oscillation in the mean population fitness $\overline{W}_{amp}$ versus period τ for different values of number of phases N_P and number of epistatic neighbors K. In both panels the population size, mutation rate and sequence size are set at $M = 10^4$, $\delta = 10^{-4}$ and $L = 16$, respectively, and the measures are averages over N_P phases, 10^4 independent populations and 10^2 distinct fitness landscapes.

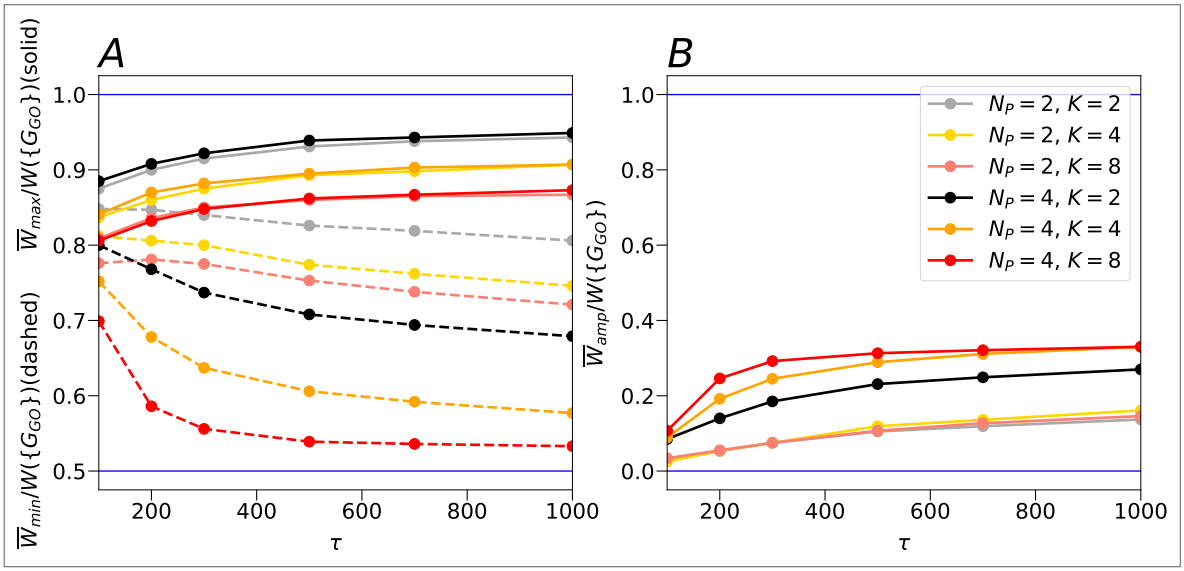

Source: Prepared by the author (2024)

in Fig. 19. The role played by the population size is very similar to that of the period. Increasing number of individuals also allows higher levels of adaptation at the end of the phase but leads, in turn, to lower minimum levels at the beginning of the following phase as well as the greater amplitude of oscillation. Unlike τ, however, M is not associated with a saturating behavior. Moreover, the dependence with N_P is not affected by the population size.

Figure 18 – Panel A: minimum Hamming distance of the phase subset state of the most adapted genotype in the population to the optimal subconfiguration $h_{min}(G_{MA,\Gamma}(P), G_{GO,\Gamma}(P))$ (dashed line) and maximum Hamming distance of the phase subset state of the most adapted genotype in the population to the optimal subconfiguration $h_{max}(G_{MA,\Gamma}(P), G_{GO,\Gamma}(P))$ (solid line) versus period τ for different values of number of epistatic neighbors K. Panel A: amplitude of oscillation in the minimum Hamming distance of the phase subset state of the most adapted genotype in the population to the optimal subconfiguration $h_{amp} = h_{max} - h_{min}$ versus period τ for different values of number of epistatic neighbors K. In both panels the population size, mutation rate, sequence size and number of phases are set at $M = 10^4$, $\delta = 10^{-4}$, $L = 16$ and $N_P = 2$, respectively, and the measures are averages over N_P phases, 10^4 independent populations and 10^2 distinct fitness landscapes.

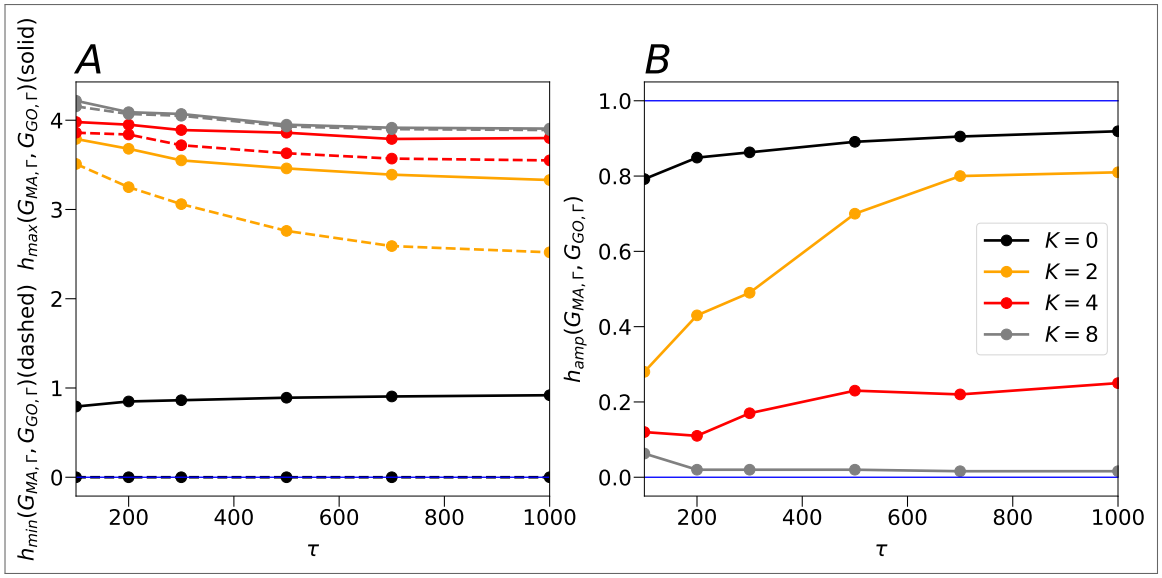

Source: Prepared by the author (2024)

Figure 19 – Panel A: minimum mean population fitness $\overline{W}_{min}$ (dashed line) and maximum mean population fitness $\overline{W}_{max}$ (solid line) versus population size M for different values of number of phases N_P and number of epistatic neighbors K. Panel B: amplitude of oscillation in the mean population fitness $\overline{W}_{amp}$ versus population size M for different values of number of phases N_P and number of epistatic neighbors K. In both panels the mutation rate, sequence size, number of epistatic neighbors and period are set at $\delta = 10^{-4}$, $L = 16$, $K = 2$ and $\tau = 200$, respectively, and the measures are averages over N_P phase, 10^4 independent populations and 10^2 independent fitness landscapes.

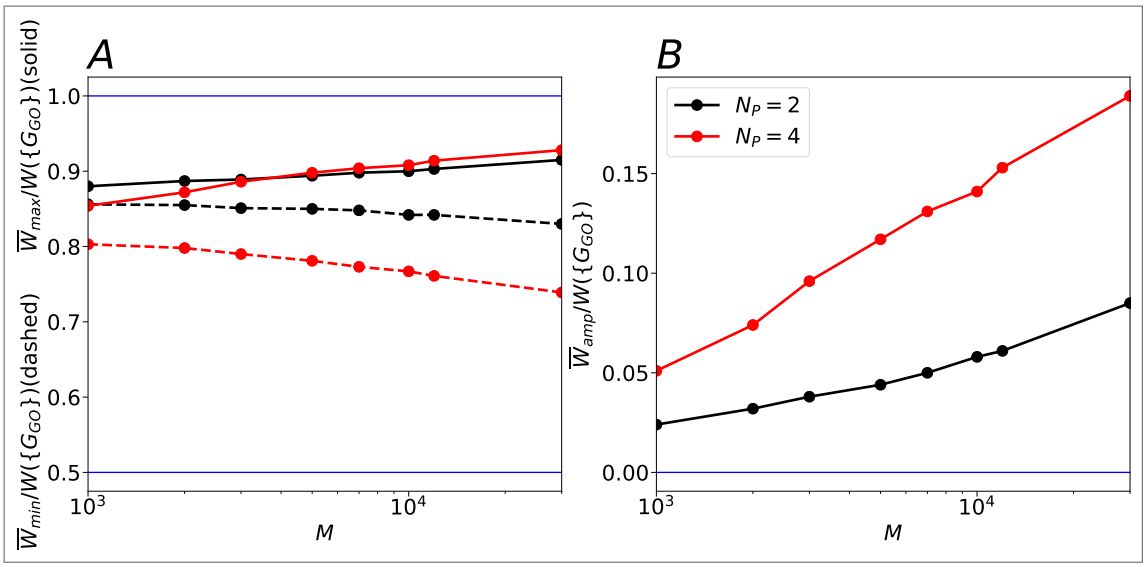

Source: Prepared by the author (2024)

4.5 REPEATABILITY

A more complete investigation of the evolutionary process may be achieved through the analysis of the degree of determinism in the trajectories, which is intimately associated with the establishment of the evolutionary pattern of the species. For this purpose we record the time series of the most adapted genotype present in the population at the end of a given phase, which is invariably a fitness peak. Let $G_{end}^{(ij)}(P)$ denote the sequence recorded in the i-th occurrence of phase P of the j-th population dynamics for a fixed and arbitrary fitness landscape. According to this definition, the indexes i and j correspond to the intra- and inter-trajectory sources of stochasticity, respectively. Each source has its own biological meaning and is dealt with separately. In both cases, however, the unpredictability of the endpoint is measured by means of the Shannon entropy.

First, the probability distribution of the random variable $G_{end}^{(j)}(P)$ associated with the temporal series of the j-th path is given by

$$p_{temp}^{(j)}(G_{end}^{(j)}(P) = G) = \frac{\sum_i \delta(G_{end}^{(ij)}, G)}{\sum_i 1} \quad , \tag{4.11}$$

where $\delta(G_{end}^{(ij)}, G)$ is the Kronecker delta between sequences $G_{end}^{(ij)}$ and G, whose application may be more simply visualized in terms of the one-to-one correspondence of the genotypic space $\{G\}$ with the natural subset $\{1, 2, \ldots, 2^L\}$, and $\sum_i 1$ accounts for all realizations of the phase in the j-th trajectory. This gives rise to the temporal entropy of the j-th path

$$S_{temp}^{(j)}(P) = \sum_{\{G\}} p_{temp}^{(j)}(G_{end}^{(j)}(P) = G) \quad . \tag{4.12}$$

Finally, an average over the ensemble of paths is taken

$$S_{temp}(P) = \frac{\sum_j S_{temp}^{(j)}(P)}{\sum_j 1} \quad . \tag{4.13}$$

Alternatively, the probability distribution associated to the endpoint $G_{end}^{(i)}(P)$ of the i-th occurrence of phase P in the ensemble of paths reads

$$p_{path}^{(i)}(G_{end}^{(i)}(P) = G) = \frac{\sum_j \delta(G_{end}^{(ij)}, G)}{\sum_j 1} \quad , \tag{4.14}$$

where $\sum_j 1$ accounts for all i-th occurrences of phase P among the trajectories, and for which the path entropy is calculated as

$$S_{path}^{(i)}(P) = \sum_{\{G\}} p_{path}^{(i)}(G_{end}^{(i)}(P) = G) \quad , \tag{4.15}$$

whose average over the repetitions of the phase results in

$$S_{path}(P) = \frac{\sum_i S_{path}^{(i)}(P)}{\sum_i 1} \quad . \tag{4.16}$$

Figure 20 – Panel A: temporal entropy S_{temp} versus period τ for different values of number of phases N_P and number of epistatic neighbors K. Panel B: path entropy S_{path} versus period τ for different values of number of phases N_P and number of epistatic neighbors K. In both panels the population size, mutation rate and sequence size are set at $M = 10^4$, $\delta = 10^{-4}$ and $L = 16$, respectively, and the measures are averages over the N_P phases and 10^2 distinct fitness landscapes.

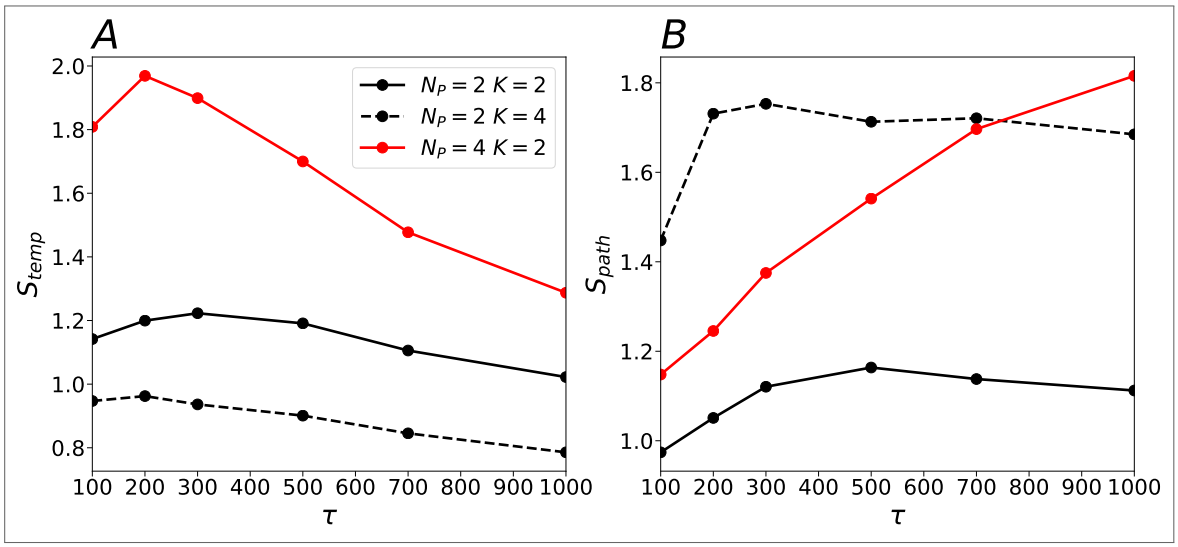

Source: Prepared by the author (2024)

Numerical results are shown in Fig. 20. Due to practical reasons, however, the measure of path entropy was taken in a slightly different way of the one defined above. Instead of the data for S_{path}, we have calculated the overall entropy,

$$S(P) = \sum_{\{G\}} p^{(ij)}(G^{(ij)}_{end}(P) = G) \quad , \tag{4.17}$$

associated to the joint distribution,

$$p^{(ij)}(G^{(ij)}_{end}(P) = G) = \frac{\sum_{ij} \delta(G^{(ij)}_{end}, G)}{\sum_{ij} 1} \quad , \tag{4.18}$$

of the random variable $G^{(ij)}_{end}$ of both the ensemble of paths and occurrences of the phase, and then obtained the temporal entropy as the difference

$$S_{path}(P) = S(P) - S_{temp}(P) \quad , \tag{4.19}$$

relying on the additive property of entropy. In fact, averages were also taken over the N_P phases and ensemble of landscapes before this operation, as usual, so the approach is certainly not numerically equivalent. We expect, however, that it conveys a reasonable proxy of $S_{path}(P)$.

Curiously, the minimum values of the temporal entropy are obtained under large periods, despite the population having a longer time to explore a larger domain of the fitness landscape. There is an opposite situation for the path entropy, which is minimized at low values of τ. In sum, the increased degree of repeatability of the evolutionary response in a given population as the phases are extended is not accompanied by an increased evolutionary convergence among

independent populations. A similar antagonism is seen in the dependence on the number of epistatic neighbors. In this case, the increase of path entropy with K is associated with the increase in the number of local maxima of the fitness landscape. As the fitness landscape becomes more rugged, experiments of parallel evolution tend to display divergent adaptive solutions. The frustration of the adaptive topography, however, seems to severely constrain the domain explored by a given population. Concerning the number of phases, the effect is the same in both measures. As previously discussed in terms of the fitness correlation, the growth of N_P leads to the formation of larger neutral networks, which enhances drift in the genotypic space and, therefore, diminishes temporal as well path predictability.

Figure 21 – Panel A: temporal entropy S_{temp} versus population size M for different values of number of phases N_P. Panel B: path entropy S_{path} versus population size M for different values of number of phases N_P In both panels the mutation rate, sequence size, number of epistatic neighbors and period are set at $\delta = 10^{-4}$, $L = 16$, $K = 2$ and $\tau = 200$, respectively, and the measures are averages over the N_P phases and 10^2 distinct fitness landscapes.

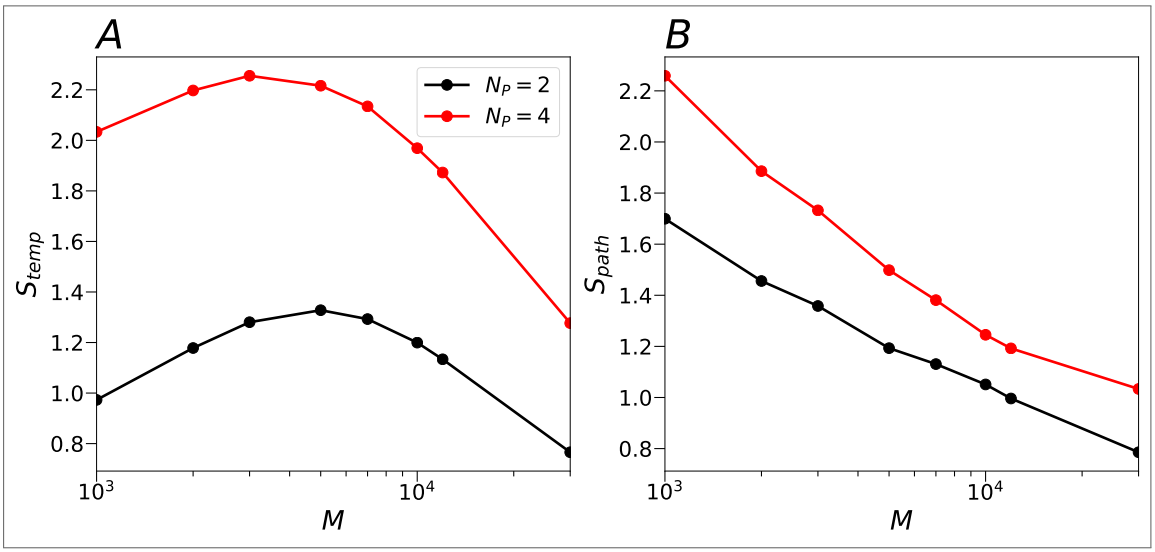

Source: Prepared by the author (2024)

Lastly, the effect of the population size on the predictability of the endpoints is examined in Fig. 21. The minimum levels of both kinds of entropy are achieved at higher M, as expected.

5 NON-STOCHASTIC DISCRETE-TIME PHENOTYPIC EVOLUTION

The results displayed in this chapter correspond to the article published by CIRNE; CAMPOS.

DOI: 10.1016/j.amc.2024.128781

5.1 PROLOGUE

A model is proposed for the phenotypic evolution of a very large population under sustained environmental change and non-overlapping generations, with a single trait considered. Due to an extension of the standard law of quantitative inheritance, each evolutionary mechanism corresponds to a function between random variables associated with distinct stages of the life cycle. Such an approach leads to a two-dimensional map where the dynamics of the phenotypic mean and variance are directly connected. Then, the declining population paradigm is explored in terms of the critical rate of environmental change and use of techniques of the dynamical systems theory. Our results first reveal the opposing pressures on the phenotypic variance due to the conflict between phenotypic load and the ability to pursue the optimum, translated into an optimal value for maximizing the critical rate. Secondly, the introduction of development, through the particular case of linear plasticity, leads to a decreasing degree of stability with the magnitude of plasticity, which means that the recovery time from disturbances is increased as the plastic effect intensifies, even though no constitutive costs have been assumed, a feature almost as important as the mean fitness to the viability of populations subject to persistent changes. Notwithstanding, the system is stable, and the growth rate benefits from increased plasticity, as expected.

5.2 MODEL

Here we propose a model for the phenotypic evolution of effectively infinite populations under sustained environmental change. Only one metric character is considered. This trait subject to Gaussian selection to a steadily moving optimum which means there is directional and stabilizing selection at the same time. The population is under Gaussian mutation as well. Furthermore, heritability and plasticity are also introduced as evolutionary mechanisms. Each of these mechanisms is associated to a transformation between random variables that describe distinct stages of the life cycle. After a complete life cycle one obtains the phenotypic distribution of the prole, which occurs in discrete generations. A stationary solution is possible and fully analyzed.

5.2.1 Selection

Selection is assumed to be density-independent and determined by a single continuous-valued trait. The fitness of the phenotype z is given by

$$W_t(z) = W_{max} \exp\left[-\frac{1}{2}\left(\frac{z-\theta_t}{\omega}\right)^2\right] \quad , \tag{5.1}$$

where W_{max} is the optimum fitness, ω is the selection function width (with $1/\omega^2$ as the strength of stabilizing selection), and θ_t is the optimum phenotype at generation t. The sustained environmental change hypothesis resides in a constant pace displacement of the optimum phenotype,

$$\theta_{t+1} = \theta_t + B \quad , \tag{5.2}$$

with B being the rate of environmental change. Admitting an effectively infinite population size and non-overlapping generations, the resulting distribution of the selected phenotypes follows from

$$p_{S,t}(z) = \frac{p_{0,t}(z)\, W_t(z)}{\overline{W}_t} \quad , \tag{5.3}$$

where $p_{0,t}(z)$ is the distribution of phenotypes in the zygotic stage, and $\overline{W}_t$ is the corresponding mean fitness,

$$\overline{W}_t = \int_{-\infty}^{\infty} dz\, p_{0,t}(z) W_t(z) \quad . \tag{5.4}$$

For later purposes, it is worth mentioning that Eq. 5.3 induces a map,

$$Z_{S,t} = S_t(Z_{0,t}) \quad , \tag{5.5}$$

which is denoted by S_t, between random variables $Z_{0,t}$ and $Z_{S,t}$, associated to the zygotic and selection stage, respectively.

Eq. 5.1 establishes what is known as Gaussian stabilizing selection. The main evidence for stabilizing selection is probably the identification of low variability, as it suggests functional optimization for a very specific form of the structures involved. This is frequently observed in reproductive characters, given their intimate relation to fitness. The attributes associated with pollination performance in flowers convey a paradigmatic example of the stabilizing role of selection. Flowers seem to be precisely formed for pollen transfer or, more precisely, for accurate mechanical fit with the pollinators, presenting very low inter and intraspecific levels of variability for this trait (CRESSWELL, 1998). Further, the assumption made in Eq. 5.2 also makes the selection to be directional.

By assuming a deterministic dynamics for the moving optimum, we have eliminated stochastic effects of the environment. The actual importance of such effects essentially depends on

the system in focus. Whilst stochasticity is proven to have a special role in many facets of the evolutionary process, including selection (LENORMAND; ROZE; ROUSSET, 2009), an impressive degree of determinism has been found in the episodes of glacial fluctuation in the Pleistocene epoch, which are predicted by the Milankovitch theory (HAYS; IMBRIE; SHACKLETON, 1976; BERGER, 1980). Actually, evidence of major geological events with a statistically significant periodic component span an even larger interval of about 250 million years (Mesozoic and Cenozoic eras) and are as diverse as increased orogeny, volcanism, global sea level changes, and discontinuities in sea-floor spreading. The Fourier analysis of 89 events grouped into ten clusters displays a spacing of roughly 27 million years at the confidence level of 96% (RAMPINO; CALDEIRA; ZHU, 2021).

Figure 22 – Gaussian smoothing of the ages of the 89 major geologic events from the last 250 million years with a standard deviation of 5 million years centered at every 0.1 million years.

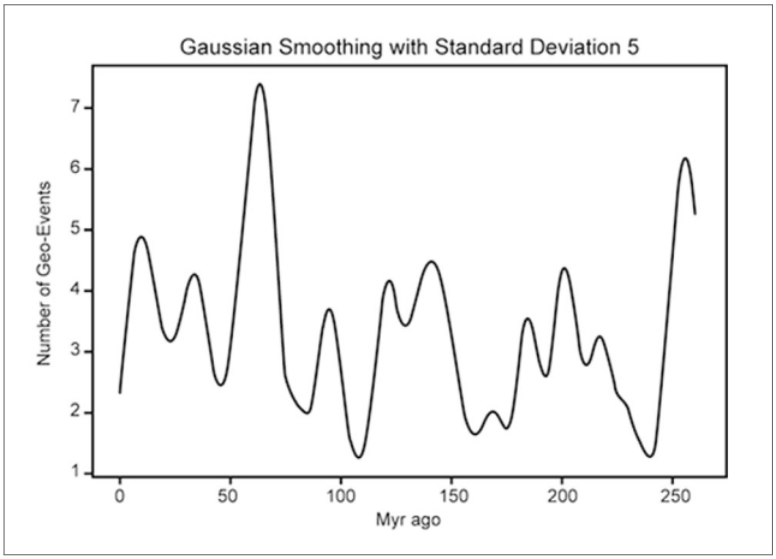

Source: RAMPINO; CALDEIRA; ZHU (2021)

If the causes are not certain, possibly associated with a flux of planetesimals due to the cyclic passage of the Solar System through the central plane of the galaxy, or simply an internal earth-pulsation process, the consequences are unequivocal. These occurrences have seriously impacted the carbon cycle and global climate, and as might be expected, are strongly and positively correlated with mass extinction events (RAMPINO; CALDEIRA, 1992; RAMPINO; CALDEIRA, 1993). Notwithstanding, biostratigraphic studies points the catastrophic incidents as just a portion of the set of periodic occurrences, and while these are associated with extinction, their counterpart have occurred over several stratigraphic stages and have continuously shaped the conditions for the remaining species and ecosystems (RICH et al., 1986; JR, 1989). In this context, the sustained environmental change proposed would be quite adequate for describing, for instance, the selective pressures in half period, from a valley to a peak and vice versa, when the rate of environmental change is nearly constant (see Fig. 22). In general, the interval of the change belongs to one of the four-tier hierarchy of time scales of evolution-

ary processes from which the evolutionary consequences should be contextualized (BENNETT, 1990).

5.2.2 Plasticity

When available, development offers a non-genetic mechanism of adaptation, one that occurs and improves fitness during the lifetime of a single generation. In these circumstances, the actual phenotype Z_t, regardless the life cycle stage (e.g. zygotic, selected), depends on a genetically determined component A_t (or simply genetic component) of the phenotype and on the environment conditions. Here, the reaction norm proposed works adding to the genetic component a fraction $0 \leq b < 1$ of its phenotypic distance to the optimum phenotype,

$$Z_t = A_t + b(\theta_t - A_t) \tag{5.6}$$
$$= (1-b)A_t + b\theta_t \tag{5.7}$$
$$= P_t(A_t) \quad , \tag{5.8}$$

Since some evolutionary mechanisms act directly on the genetic system, it is operationally useful to establish the inverse of P_t,

$$P_t^{-1}(Z_t) = \frac{Z_t - b\theta_t}{1-b} \quad , \tag{5.9}$$

in order to extract the genetic component from a given phenotype.

The proposal of reaction norm in Eq. 5.7 is obviously adaptive. For the interval of the parameter b considered, the plastic effect improves adaptation, by definition. Nonetheless, it is important to highlight that, contrary to expectation, phenotypic plasticity is not necessarily adaptive. If this was the case, then the proximity of a characteristic to fitness and the occurrence of plasticity should be negatively correlated, a hypothesis that has been overturned in a recent analysis of 213 studies. Despite considerable variability of plastic effects among distinct traits, no clear relation with fitness was observed (ACASUSO-RIVERO et al., 2019). If the plastic response results in a harmful or a highly integrated phenotype crucially depends on specific conditions. At this point, however, few theoretical predictions on the issue have been tested (WHITMAN; AGRAWAL et al., 2009). A remarkable example is found in a study of adaptive responses to foliage shade in the Arabidopsis plant. The genotypic selection analysis of the relation between environment and life-history traits revealed that there is no adaptive plasticity to density (crowding) while evidence of both adaptive and maladaptive responses to foliage shade were found. The same study also suggests that active developmental responses usually are more adaptive than passive resource-mediated responses and that costs of plasticity are not common as normally assumed (DORN; PYLE; SCHMITT, 2000).

The debate on the evolution of plasticity, which essentially concerns identification of the underlying genetic mechanisms and selective pressures shaping the reaction norms, is marked

by substantial controversy (VIA et al., 1995). Quantitative genetic models developed in the second half of the last century may be conceptually grouped into one of two kinds: evolution of plasticity is assumed to be either linked or independent from the evolution of the trait involved (NICOGLOU, 2015). According to the first approach, plasticity is not a trait in itself, but rather an outcome of evolution over several loci (a property of the genome as a whole), a view that lacks significant experimental evidence and whose appeal is limited to quantitative genetic models (see (VIA; LANDE, 1985)). The alternative perspective, by the other hand, assumes that plasticity is determined by an specific set of genes exclusively dedicated to the environmentally dependent control of structural gene expression. This view is in line with the observation of an astonishing diversity in the degree of phenotypic sensitivity of closely related species, and is corroborated by a wealth of evidence (SCHLICHTING; PIGLIUCCI, 1993; VIA, 1993). As an example, such single gene region has been found to be in control of the spawning migration timing of the Chinook salmon, a result of paramount importance to the conservation of this threatened species (THOMPSON et al., 2020). Our model presumes this view in which adaptation of the trait does not affect adaptation of the reaction norm and vice versa. While artificial selection experiments have undoubtedly proven the occurrence of selective response of plasticity (SCHEINER; LYMAN, 1991), we further assume that the reaction norm is not under adaptation at all, for simplicity.

5.2.3 Heritability

The standard law of quantitative genetics,

$$\langle A_{H,t}\rangle = h^2\langle A_{S,t}\rangle + (1-h^2)\langle A_{0,t}\rangle \quad , \tag{5.10}$$

states that, due to genetic constraints, the average genetic component of the value inherited by progeny lies between the average genetic component of the zygotic stage and the average genetic component of the selection stage in a proportion assigned by the parameter known as heritability, h^2 (LANDE, 1976b). Here, this principle is extended to the random variables,

$$\begin{aligned} A_{H,t} &= h^2 A_{S,t} + (1-h^2)A_{0,t} && (5.11)\\ &= h^2 A_{S,t} + (1-h^2)P^{-1}(S^{-1}(P(A_{S,t}))) && (5.12)\\ &= H_t(A_{S,t}) \quad , && (5.13) \end{aligned}$$

where H_t designates the corresponding function. The inverse function S_t^{-1}, alike P_t^{-1} in Eq. 5.9, is not associated to a real evolutionary mechanism, but involves the identification of the zygotic phenotypic constitution from the selected one.

5.2.4 Mutation

Once selection has taken place, the genetic component of a portion of the gametes produced by the survivors is subject to change by mutation. In this model, the conditional probability of the mutational effect on the inherited value is normal,

$$p_{M,t}(a) = \int_{-\infty}^{\infty} da'\, p_{H,t}(a') \left\{ \frac{1}{\delta\sqrt{2\pi}} \exp\left[-\frac{1}{2} \left(\frac{a-a'}{\delta} \right)^2 \right] \right\} \quad , \tag{5.14}$$

a hypothesis known as Gaussian mutation, where $p_{M,t}(a)$ is the probability distribution of the genetic component of the mutated stage, $p_{H,t}(a')$ is the probability distribution of the genetic component of the inherited stage, and δ is the magnitude of the mutation effect. Whereas this framework does not address a specific species or trait, no further specification on the magnitude of the mutation effect is made and it is regarded as a fundamental parameter. The underlying function is denoted by M,

$$A_{M,t} = M(A_{H,t}) \quad . \tag{5.15}$$

Unlike the other mechanisms defined so far, mutation does not depend on the optimum phenotype and, consequently, on the generation t.

5.2.5 Progeny

The convention adopted is that a complete life cycle begins and ends at the zygotic stage. In this case, mutation is the last mechanism of genetic change, whereas development to the new environment is the last mechanism of phenotypic change. Then, following Eqs. 5.5, 5.8, 5.9, 5.13 and 5.15, the total phenotypic modification between two consecutive generations is operationally described by

$$\begin{aligned} Z_{0,t+1} &= P_{t+1}(A_{0,t+1}) && (5.16)\\ &= P_{t+1}(A_{M,t}) && (5.17)\\ &= P_{t+1}(M(A_{H,t})) && (5.18)\\ &= P_{t+1}(M(H_t(A_{S,t}))) && (5.19)\\ &= P_{t+1}(M(H_t(P_t^{-1}(Z_{S,t}))\ldots) && (5.20)\\ &= P_{t+1}(M(H_t(P_t^{-1}(S_t(Z_{0,t}))\ldots) \quad . && (5.21) \end{aligned}$$

The operation defined above presents a singular property: if the phenotypic value of the zygotic stage is normally distributed,

$$Z_{0,t} \sim \mathcal{N}(\mu_{0,t}, \sigma_{0,t}) \quad , \tag{5.22}$$

with $\mu_{0,t}$ and $\sigma_{0,t}$ designating mean and standard deviation, respectively, then each mapping composing Eq. 5.21 results in a normal random variable as well. This is proved in the Appendix

(Section 6.1) and is especially valid for the outcome, $Z_{0,t+1}$, making the Gaussian distribution the appropriate *ansatz* for the stationary state. This is a consequence of the Gaussian nature of selection and mutation alongside the linearity of the other mechanisms. Since we are exclusively interested in the long term dynamics, it is reasonable to assume normality for an arbitrary state as well. Actually, most phenotypes do exhibit a normal distribution whatever the circumstances. Due to the polygenic basis of the metric characters, this property is assured by the central limit theorem (FALCONER, 1989). The theory of adaptation of normally distributed characters has been fundamental to development of the theory of quantitative genetics as whole.

5.3 MUTATION-SELECTION BALANCE

Mutation and selection are indispensable forces for any type of long-term directional stress. Accordingly, the mutation-selection balance is explored first. Assuming $b = 0$ and $h^2 = 1$, both operations P_t and H_t become the identity function, and the life cycle reduces to

$$Z_{0,t+1} = M(S_t(Z_{0,t})) \quad . \tag{5.23}$$

From Eqs. 6.44 and 6.47, it follows that the relation between the phenotypic constitutions of the parental and offspring generations is established by the formulas

$$\sigma^2_{0,t+1} = \frac{\omega^2 \sigma^2_{0,t}}{\omega^2 + \sigma^2_{0,t}} + \delta^2 \quad , \tag{5.24}$$

and

$$\mu_{0,t+1} = \frac{\omega^2 \mu_{0,t} + \sigma^2_{0,t}\, \theta_t}{\omega^2 + \sigma^2_{0,t}} \quad . \tag{5.25}$$

Together, these equations constitute a two-dimensional map. Nonetheless, the variance dynamics does not depend on that of the mean dynamics and, therefore, may be handled separately as an unidimensional map.

Expressions for the variance map where the magnitude of the mutation effect is explicitly written in terms of the fundamental properties of the genetic system are provided by LANDE (LANDE, 1976a) for a polygenic character with linked loci in a random mating population, by LANDE (LANDE, 1977) for nonrandom systems of mating, and by (LYNCH; GABRIEL, 1983) for a parthenogenetic species. Since the mean map is the same in any of these circumstances, differences on the phenotypic evolutionary rates are confined to the particularities of the genetic system.

The stationary phenotypic variance is given by,

$$\sigma^2_{0,*} = \frac{\delta^2 + \sqrt{\delta^4 + 4\omega^2\delta^2}}{2} \quad , \tag{5.26}$$

whose value at very small magnitudes of the mutation effect coincides with the equilibrium value of the homologous continuous growth model (LYNCH; GABRIEL; WOOD, 1991),

$$\lim_{\delta \to 0} \sigma^2_{0,*} = \omega\delta \quad . \tag{5.27}$$

The equation above unveils the main role of mutations, that is, maintenance of genetic variability. If the mutational effect is null ($\delta = 0$), the phenotypic variance eventually vanishes as a consequence of the recurrent erosion inflicted by selection (see Eq. 6.4) (FISHER, 1958),

$$\frac{\sigma^2_{S,t}}{\sigma^2_{0,t}} = \frac{\omega^2}{\omega^2 + \sigma^2_{0,t}} \quad , \tag{5.28}$$

where $\sigma^2_{S,t}$ denotes the phenotypic variance of the selection stage. The ubiquity of this ratio makes it worth of a particular designation for the remainder of this chapter: the "coefficient of selection".

The significance of selection is manifested in the mean dynamics. Adapting means getting closer to the optimum phenotype, a task to which mutation is unable to contribute by itself. In the presence of selection, however, the intensity of such approximation is proportional to the phenotypic variance, as evinced by Eq. 5.25. In short, selection produces adaptation, mutation fuels it. These relations enclose the set of interplay determining what is known as the mutation-selection balance. A thorough revision of the set of models on the subject of the maintenance of genetic variability under Gaussian mutation and selection is found in TURELLI. TURELLI concludes that, in spite of reasonable qualitatively agreement across distinct frameworks, there is uncomfortable quantitative divergence. As a consequence, the question of how significant levels of inheritable genetic variance are kept in natural populations remains elusive, at least in terms of mathematical modeling.

Given an environmental change, there are basically two sources of beneficial alleles over which selection may act: pre-existing genetic variation and *de novo* mutations. The outcome of adaptation crucially depends on which of these sources contributes the most and creates a genomic signature that is fundamental for predicting microevolutionary responses to changing environments (BARRETT; SCHLUTER, 2008). Detection of standing genetic variation for a trait in quantitative genetic studies is the rule rather than the exception (LEWONTIN, 1974), and several examples of adaptation fueled by this source have been reported, such as the recent observations of rapid response of the mediterranean mussel *Mytilus galloprovincialis* to reduced seawater pH, a notable stressor from current global changes (BITTER et al., 2019). In another investigation of natural populations of guppies, the higher speed of adaptation of male traits relative to female traits under an artificial scheme of directional selection has been attributed to larger genetic variation (REZNICK et al., 1997). Even among large populations, greater population sizes of *Drosophila melanogaster* are associated to enhanced long term response to selection for ethanol vapor resistance for the same reason (WEBER; DIGGINS, 1990). To provide one more example, the maintenance of large reservoirs of inter and intraspecific diversity has been pointed out as one of the four pillars of the evolutionary success in oaks (KREMER; HIPP, 2020).

In spite of that, it is obvious that the longer the selective pressure the higher the chances of complete utilization of the initial genetic variation being attained. Exhaustion of additive genetic variance has been observed and considered the main cause of stagnation in experiments

of selection for body weight in mice, for instance (EISEN, 1980). While recombination may support further genetic improvement, as observed in livestock population studies, its impact is also finite (NOTTER, 1999). Thus, in the context of sustained environmental change, the only trustable source of variation are de novo mutations. Once de novo mutations are available, a last requirement is that they convey enough adaptive variation, i.e., variation with significant contribution to fitness. Lack of appropriate variability has been shown to curb evolution even in the presence of high levels of protein polymorphism, a condition called *genostasis* (BRADSHAW, 1991). It should be noted that the number of generations that distinguishes short and long term selection, when accessible, depends sensibly on the particular problem. An example is found in the selection for the bristle number in the genus *Drosophila*, where de novo mutations seem to have influence on adaptation in no less than 20 generations (HILL, 1982).

Analysis of adaptation under the stationary state requires measuring the mean phenotype relative to the optimum phenotype. A useful quantity is the phenotypic lag:

$$\Delta_{0,t} = \theta_t - \mu_{0,t} \quad . \tag{5.29}$$

The map for this new quantity reads (see Eq. 6.50),

$$\Delta_{0,t+1} = B + \left(\frac{\omega^2}{\omega^2 + \sigma_{0,t}^2} \right) \Delta_{0,t} \quad , \tag{5.30}$$

while the fixed point is given by

$$\Delta_{0,*} = B \left(\frac{\omega^2 + \sigma_{0,*}^2}{\sigma_{0,*}^2} \right) \quad , \tag{5.31}$$

a result first obtained by CHARLESWORTH (CHARLESWORTH, 1993). The stationary lag is always greater than the rate of environmental change. Despite the distinct essences of the phenotypic variance and the phenotypic lag, the effect of selection on the later is also related to a contraction by the coefficient of selection (see Eq. 6.7),

$$\frac{\Delta_{S,t}}{\Delta_{0,t}} = \frac{\sigma_{S,t}^2}{\sigma_{0,t}^2} \quad . \tag{5.32}$$

Actually, alternative measures of the shrinkage effect of selection had been proposed formerly. For instance, LATTER (LATTER, 1970) defined it as the proportional reduction of the mean phenotype relative to the optimum phenotype,

$$\frac{\Delta_{S,t} - \Delta_{0,t}}{\Delta_{0,t}} = -\frac{\sigma_{0,t}^2}{\omega^2 + \sigma_{0,t}^2} \tag{5.33}$$

$$= -\left(1 - \frac{\sigma_{S,t}^2}{\sigma_{0,t}^2} \right) \quad , \tag{5.34}$$

designated by "coefficient of centripetal selection". Though, the current definition in Eq. 5.28 is much more meaningful in our context.

Although rapid evolution is not considered a standard working hypothesis, its interpretation as an ecological process (evolutionary ecology) potentially sets the most relevant area of applied biological sciences currently (THOMPSON, 1998). One of the latest artificial experiments with *Drosophila melanogaster* have tested this hypothesis under strong and rapidly fluctuating selection, for which it was obtained exceptionally rapid phenotypic adaptation as a result (RUDMAN et al., 2022). A far longer and robust example concerns the changes observed in snail shell form (shape and thickness) of natural populations of the intertidal snail *Littorina obtusata* over more than a century as a response to predation by the intertidal crab *Carcinus maenas* as it expanded its range. These observations are in agreement with the classical paradigm of Darwinian selection and demonstrate that it can lead to rapid morphological transition without speciation (SEELEY, 1986). Nonetheless, some caution is necessary. It is worth mentioning that such reports attributing the phenotypic changes to environmental change usually present at least one of three caveats: (i) difficulty in determining if the changes are genetically based or simply plastic, (ii) assuming rather than testing that the change is adaptive (iii) and climate change is its causal agent (MERILÄ; HENDRY, 2014).

Once the variance map does not depend on the phenotypic lag, the stability analysis of the two-dimensional map becomes significantly easier, the diagonal elements of the Jacobian matrix corresponds to its eigenvalues. Both cumulants are the result of a composite function, likewise the life cycle, so the diagonal elements may also be broken down into the effects of each mechanism by the chain rule, resulting in

$$\frac{d\sigma^2_{0,t+1}}{d\sigma^2_{0,t}} = \frac{d\sigma^2_{M,t}}{d\sigma^2_{0,t}} \tag{5.35}$$

$$= \frac{d\sigma^2_{M,t}}{d\sigma^2_{S,t}} \frac{d\sigma^2_{S,t}}{d\sigma^2_{0,t}} \tag{5.36}$$

$$= \frac{d\sigma^2_{S,t}}{d\sigma^2_{0,t}} \tag{5.37}$$

$$= \left(\frac{\sigma^2_{S,t}}{\sigma^2_{0,t}} \right)^2 \quad , \tag{5.38}$$

and

$$\frac{\partial \Delta_{0,t+1}}{\partial \Delta_{0,t}} = \frac{\partial \Delta_{M,t}}{\partial \Delta_{S,t}} \frac{\partial \Delta_{S,t}}{\partial \Delta_{0,t}} \tag{5.39}$$

$$= \frac{\partial \Delta_{S,t}}{\partial \Delta_{0,t}} \tag{5.40}$$

$$= \frac{\sigma^2_{S,t}}{\sigma^2_{0,t}} \quad , \tag{5.41}$$

where Eqs. 6.4, 6.37, 6.7 and 6.41 have been applied (notice that in the absence of phenotypic plasticity there is no distinction between the phenotype and its genetic component).

Since both stability coefficients correspond to a power of the selection coefficient, the system is stable for any set of physically significant values of the parameters. In both instances

the derivative of the mutational effect equals one. Thereby, it is clear that the degree of stability is determined by the capacity of selection to narrow the distribution. The route to increasing stability is then twofold. The first and most evident is through a greater strength of selection (smaller width of selection). The other is through a greater mutational effect, as it leads to greater stationary variance. In this sense, mutation still plays a role in stability, even if the mechanism itself is not able to mitigate a deviation from the fixed point by any amount.

Lastly, concerning the natural measures of the system, it can be easily verified from each map, as well as from their stationary values, that the variance and the magnitude of the mutation effect may be measured in units of the width of selection, while the lag is measurable in units of the rate of environmental change. These properties establish the eco-evolutionary scale of the system and may be fundamental in locating it as a part of more complex scenarios (LEVIN, 1992).

5.4 CRITICAL RATE OF ENVIRONMENTAL VARIATION

Long term adaptation to sustained environmental change has proven to be dynamically feasible and robust. The other half of the issue concerns examining the circumstances under which the population can maintain a positive growth rate. For discrete generation times, the ratio between the population sizes of two consecutive generations is precisely the mean fitness,

$$N_{t+1} = \int dz\, N_t\, p_{0,t}(z)\, W_t(z) \tag{5.42}$$

$$= N_t\, \overline{W}_t \quad , \tag{5.43}$$

where N denotes the population size. The growth rate is then defined as

$$R_{t+1} = \ln \overline{W}_t \quad . \tag{5.44}$$

Thus the growth rate is also a monotonically increasing function of the fitness so that these quantities are qualitative similar and used interchangeably in this text. For a normally distributed character under Gaussian selection, the mean fitness reads as

$$\overline{W}_t = W_{max} \left(\frac{\omega^2}{\omega^2 + \sigma_{0,t}^2} \right)^{1/2} \exp\left[-\frac{1}{2} \left(\frac{\Delta_{0,t}^2}{\omega^2 + \sigma_{0,t}^2} \right) \right] \quad . \tag{5.45}$$

In the case of perfect adaptation ($\Delta_{0,t} = 0$), the above expression reduces to the first factor, which represents the selective load due to variance on a completely adapted population. As long as the mean phenotype and the optimum phenotype match, any increment in variance will certainly increase the level of maladaptation in the population. This kind of load is usually referred to as mutational or genetic load, as it emerges from the accumulation of mutations through generations in most cases. The mutational load is an important factor determining the extinction risk. The impressive high levels of genetic load among long-lived plants make them a useful case study on the topic (FRANKHAM, 2005; KLEKOWSKI, 1988).

Figure 23 – Mean fitness $\overline{W}_t$ versus phenotypic variance $\sigma^2_{0,t}$ for different values of phenotypic lag $\Delta_{0,t}$. The curves may be distinguished into two types. Below the limiting value of lag ($\Delta_{0,t} = \omega$), the curves decrease monotonically. Above this value, the curves are non-monotonic and present a unique local maximum.

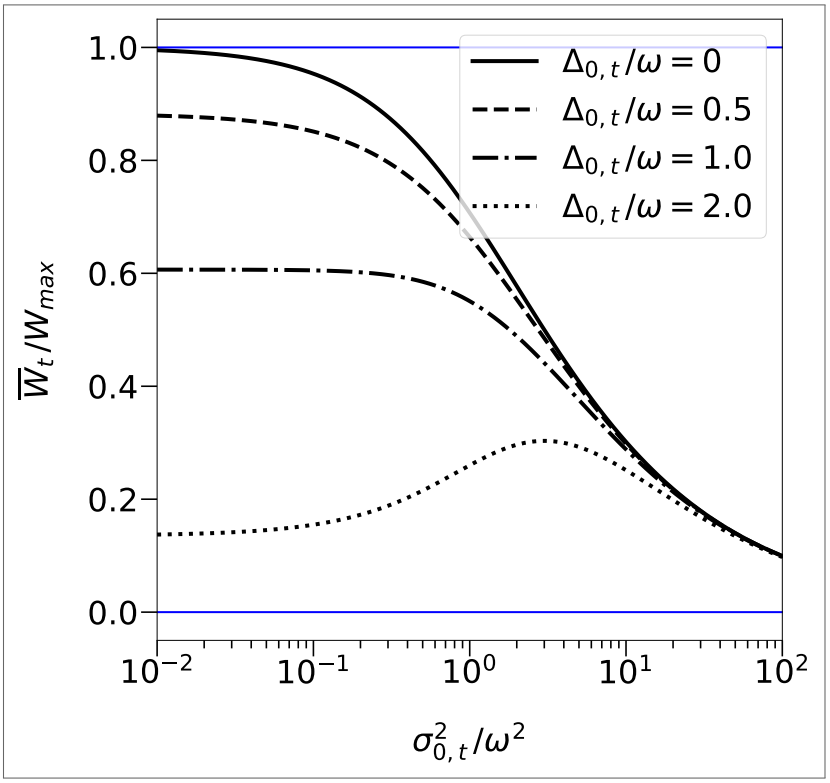

Source: Prepared by the author (2024)

For non-zero lag, the second factor contributes to the mean fitness. It is precisely the relative mean fitness of a population displaced from the optimum by an amount of Δ_t with respect to the perfectly adapted population (LATTER, 1960). An increment of phenotypic variance has an effect on the mean fitness that is contingent on the magnitude of the lag. Note that any increase is made possible through the gain in frequency of the phenotypes between mean and optimum whilst widening the distribution. The net effect depends essentially on the magnitude of the lag, as evinced by the derivative of the mean fitness with respect to the variance,

$$\frac{\partial \overline{W}_t}{\partial \sigma^2_{0,t}} = W_{max} \frac{\omega \left[\Delta^2_{0,t} - \left(\omega^2 + \sigma^2_{0,t}\right)\right]}{2\left(\omega^2 + \sigma^2_{0,t}\right)^{5/2}} \exp\left[-\frac{1}{2}\left(\frac{\Delta^2_{0,t}}{\omega^2 + \sigma^2_{0,t}}\right)\right] \quad . \tag{5.46}$$

If the lag is below the width of the selection function ($\Delta_{0,t} < \omega$), then the smaller the variance the higher the population growth rate. This statement is especially interesting as one visualizes that by compressing the distribution indefinitely, the frequency of the optimum tends to zero. Thus, the absolute concentration of the distribution of phenotypes around the mean phenotype is therefore curiously advantageous for the population (as long as the mean is fixed, obviously). However, when the lag exceeds the selection width ($\omega < \Delta_{0,t}$), the mean fitness is maximized

at an intermediate value of variance of

$$\sigma_{0,t}^2 = \Delta_{0,t}^2 - \omega^2 \quad . \tag{5.47}$$

All reasoning developed so far is portrayed in Fig. 23.

Figure 24 – Mean stationary fitness $\overline{W}_*$ versus stationary variance $\sigma_{0,*}^2$ for different values of rate of environmental change B. Unless the optimum phenotype is static ($B = 0$), the curves are non-monotonic and present a unique local maximum.

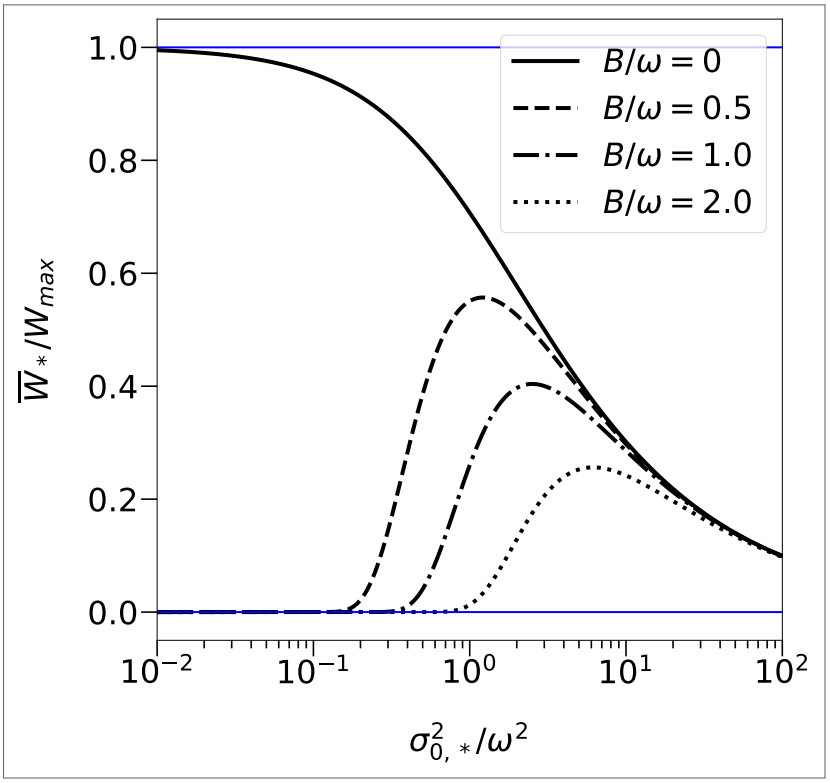

Source: Prepared by the author (2024)

Until now, we have treated the variance and the lag as independent quantities. This is no longer valid in the stationary state, when the lag is constrained by the variance. Due to the dynamics, the stationary mean fitness,

$$\overline{W}_* = W_{max} \left(\frac{\omega^2}{\omega^2 + \sigma_{0,*}^2} \right)^{1/2} \exp\left[-\frac{1}{2} B^2 \left(\frac{\omega^2 + \sigma_{0,*}^2}{\sigma_{0,*}^4} \right) \right] \quad , \tag{5.48}$$

is always a non-monotonic function of the stationary variance, as shown in Fig. 24. While the load prevents expanding the distribution with no bound, as before, excessive concentration is also avoided as long as the approach to the optimum is promoted by the variance. These opposing pressures on the variance of a quantitative character as a consequence of simultaneously directional and stabilizing selection have been recognized by MATHER (MATHER, 1943) long ago, who synthesized the dilemma as the conflict between fitness and flexibility. From the derivative of the stationary mean fitness with respect to the stationary variance,

$$\frac{\partial \overline{W}_*}{\partial \sigma_{0,t}^2} = -W_{max} \frac{\omega \left[\sigma_{0,*}^6 - B^2(\omega^2 + \sigma_{0,*}^2)(2\omega^2 + \sigma_{0,*}^2) \right]}{2\sigma_{0,t}^6 \left(\omega^2 + \sigma_{0,*}^2 \right)^{3/2}} \exp\left[-\frac{1}{2} B^2 \left(\frac{\omega^2 + \sigma_{0,*}^2}{\sigma_{0,*}^4} \right) \right] \quad , \tag{5.49}$$

one obtains a polynomial equation for which the single optimal value of stationary variance observed in Fig. 24 must be one of the roots,

$$0 = \sigma_{0,*}^6 - B^2(\omega^2 + \sigma_{0,*}^2)(2\omega^2 + \sigma_{0,*}^2) \quad . \tag{5.50}$$

This value increases with the rate of environmental change.

In Eq. 5.45, for the mean population fitness, $\Delta_{0,t}$ is no longer measurable in units of B, but rather in units of ω, as is the variance. In the stationary mean fitness (Eq. 5.49), on the other hand, this occurs with B as well. Then, both fundamental parameters of phenotypic nature (B and δ) are scaled by ω regarding the population growth rate in the stationary state.

Figure 25 – Critical rate of environmental change B_c versus stationary variance $\sigma_{0,*}^2$ for different values of maximum fitness W_{max}. All curves are non-monotonic and present a unique local maximum. A limiting value for the variance exists, $\sigma_{0,t}^2 = \omega^2(W_{max}^2 - 1)$, beyond that a progressive decline in population size occurs.

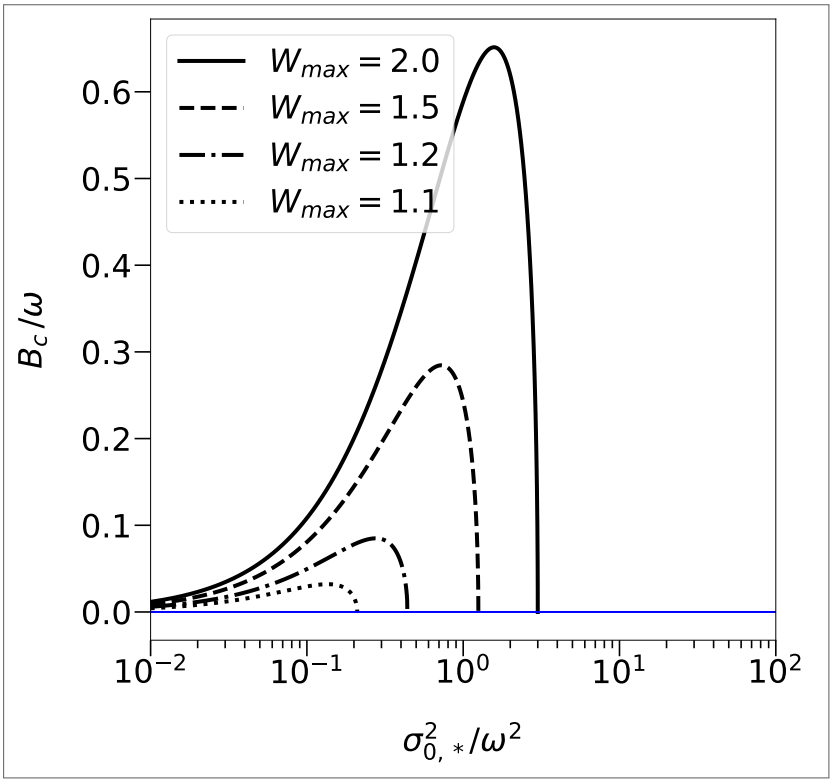

Source: Prepared by the author (2024)

When it comes to conservation issues, it is useful to establish the rate of change below which the growth rate is negative. The quantity designated as the critical rate of environmental change is obtained by equating the stationary mean fitness to one:

$$B_c = \frac{\sigma_{0,*}^2}{\sqrt{\omega^2 + \sigma_{0,*}^2}} \sqrt{\ln\left[W_{max}^2 \left(\frac{\omega^2}{\omega^2 + \sigma_{0,*}^2}\right)\right]} \quad . \tag{5.51}$$

Notice that, for a fixed value of the rate of environmental change, the same procedure may be applied to provide the critical value of any other parameter (e.g. heritability and maximum

fitness). As might be expected, the dependence of the critical rate with on the stationary variance is non-monotonic as well (see Fig. 25). Taking the derivative of B_c with respect to $\sigma^2_{0,*}$ and evaluated at the stationary state reads as

$$\frac{\partial B_c}{\partial \sigma^2_{0,*}} = \frac{1}{\sqrt{\ln\left[W^2_{max}\left(\frac{\omega^2}{\omega^2+\sigma^2_{0,*}}\right)\right]}} \frac{1}{2\left(\omega^2+\sigma^2_{0,*}\right)^{3/2}} \left\{\left(2\omega^2+\sigma^2_{0,*}\right)\ln\left[W^2_{max}\left(\frac{\omega^2}{\omega^2+\sigma^2_{0,*}}\right)\right] - \sigma^2_{0,*}\right\} \quad . \tag{5.52}$$

Equating to zero, it provides an implicit equation for which the value of sigma that maximizes B_c must be a solution,

$$0 = (2\omega^2+\sigma^2_{0,*})\ln\left[W^2_{max}\left(\frac{\omega^2}{\omega^2+\sigma^2_{0,*}}\right)\right] - \sigma^2_{0,*} \quad , \tag{5.53}$$

which depends on the maximum fitness. Despite the similarities, an important qualitative difference may be drawn in relation to the stationary mean fitness. An inspection of the domain of Eq. 5.51 reveals that there is a prohibitive region beyond the value of

$$\sigma^2_{0,*} = \omega^2(W^2_{max}-1) \quad , \tag{5.54}$$

i.e., a set of values of variance that leads to a negative growth rate given any rate of environmental change.

The restoration of positive growth rate results from the incapacity to adapt rapidly enough to an environmental change (SMITH, 1989), while the restoration of a positive growth rate through adaptation in the face of the new circumstances is a phenomenon known as evolutionary rescue (CARLSON; CUNNINGHAM; WESTLEY, 2014). The critical rate of environmental change is an important measure within the context of the evolutionary rescue issue which, in turn, belongs to the domain of conservation biology. In spite of extinction being an ubiquitous and constitutive occurrence of evolution, this discipline comes up in response to the contemporary depletion of biological diversity by anthropogenic action and, ironically, the demand for human intervention to maintain endangered species (FRANKHAM, 2014).

5.5 HERITABILITY

The heritability of a character, unlike mutation and selection, does not change the qualitative aspects of the dynamics of adaptation already discussed. The quantitative features involved, however, are always present and may be critical for species' fate. The addition of this mechanism updates the life cycle to

$$Z_{0,t+1} = M(H_t(S_t(Z_{0,t}))) \quad . \tag{5.55}$$

Heritability rules the efficacy of selection by determining how much of its outcome is inheritable. In the original formulation of the standard law of quantitative genetics (Eq. 5.10),

Figure 26 – Effective coefficient of selection $\sigma^2_{H,t}/\sigma^2_{0,t}$ versus variance of the zygotic stage $\sigma^2_{0,t}$ for different values of heritability h^2. Each asymptote in red is the constant curve $(1-h^2)^2$. In the limit case $h^2 = 1$, the variance of the inherited stage $\sigma^2_{H,*}$ equals the variance of the selection stage $\sigma^2_{S,*}$.

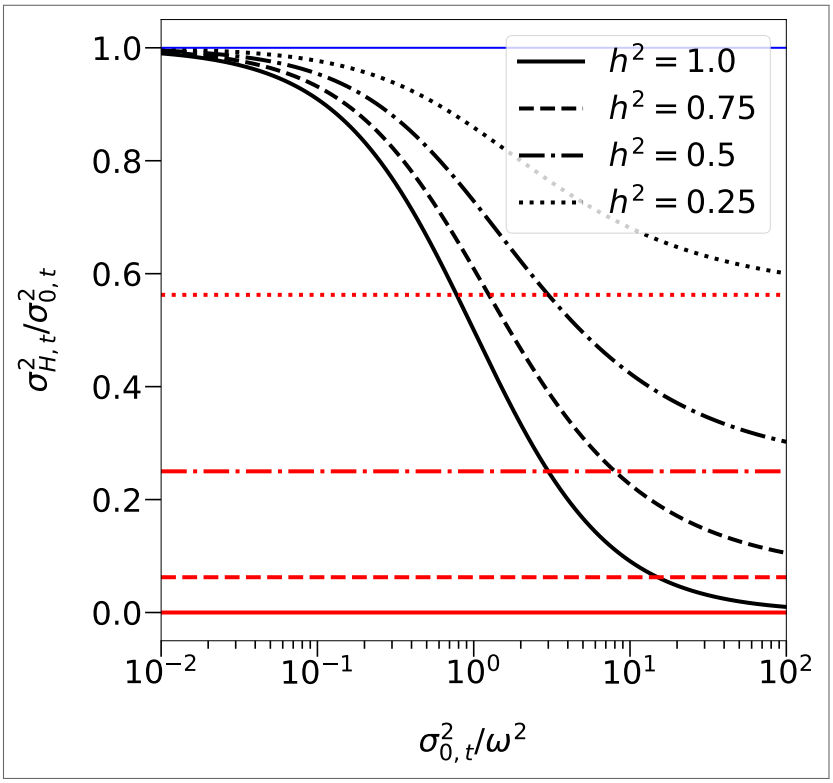

Source: Prepared by the author (2024)

this is established in terms of mean values,

$$\mu_{H,t} = h^2\mu_{S,t} + (1-h^2)\mu_{0,t} \quad , \tag{5.56}$$

according to Eq. 6.28. The novelty emerges in the expansion of this effect to the standard deviation (see Eqs. 6.25),

$$\sigma_{H,t} = h^2\sigma_{S,t} + (1-h^2)\sigma_{0,t} \quad . \tag{5.57}$$

This expression may be rearranged to provide the reduction of the intensity of selection upon the inherited character,

$$\frac{\sigma^2_{H,t}}{\sigma^2_{0,t}} = \left[1 - h^2\left(1 - \frac{\sigma_{S,t}}{\sigma_{0,t}}\right)\right]^2 \quad . \tag{5.58}$$

The variance of the inherited character, as well as that of the selected character, is always smaller than the variance of the parental generation and the supplying role of mutation is still indispensable. Moreover, the ratio above is higher than the coefficient of selection for a fixed and arbitrary value of variance of the zygotic stage and could be easily identified as the "effective coefficient of selection", as evinced by its inferior bound,

$$\lim_{\sigma_{0,t}\to\infty} \frac{\sigma^2_{H,t}}{\sigma^2_{0,t}} = (1-h^2)^2 \quad , \tag{5.59}$$

the coefficient of selection representing an ideal case (see Fig. 26).

The asymptote is just one of the several evidences of how the role of selection is mitigated as heritability diminishes. An alternative and convincing visualization of this feature and the quantitative role of the parameter h^2 involves the determination of the value required to make the standard deviation of the inherited character smaller than the width of selection in a single round of selection,

$$\omega < \sigma_{0,t} \quad \& \quad \sigma_{H,t} < \omega \quad \Rightarrow \quad h^2 > \left(1 - \frac{\omega}{\sigma_{0,t}}\right)\left(1 - \frac{\omega}{\sqrt{\omega^2 + \sigma_{0,t}^2}}\right)^{-1} \quad . \tag{5.60}$$

This limiting value of h^2 is an increasing function of the variance of the zygotic stage, always smaller than one, and approaches unity as $\sigma_{0,t}^2$ diverges. Only in a scenario of perfect heritability ($h^2 = 1$), the above condition is satisfied whatever the original variance.

Figure 27 – Stationary variance $\sigma_{0,*}$ versus scaled squared magnitude of the mutation effect δ^2 for different values of heritability h^2. Each asymptote in red is the linear function of slope $[1-(1-h^2)^2]^{-1}$. Each curve in purple corresponds to the function $\sigma_{0,t}^2 = \omega\delta/h$.

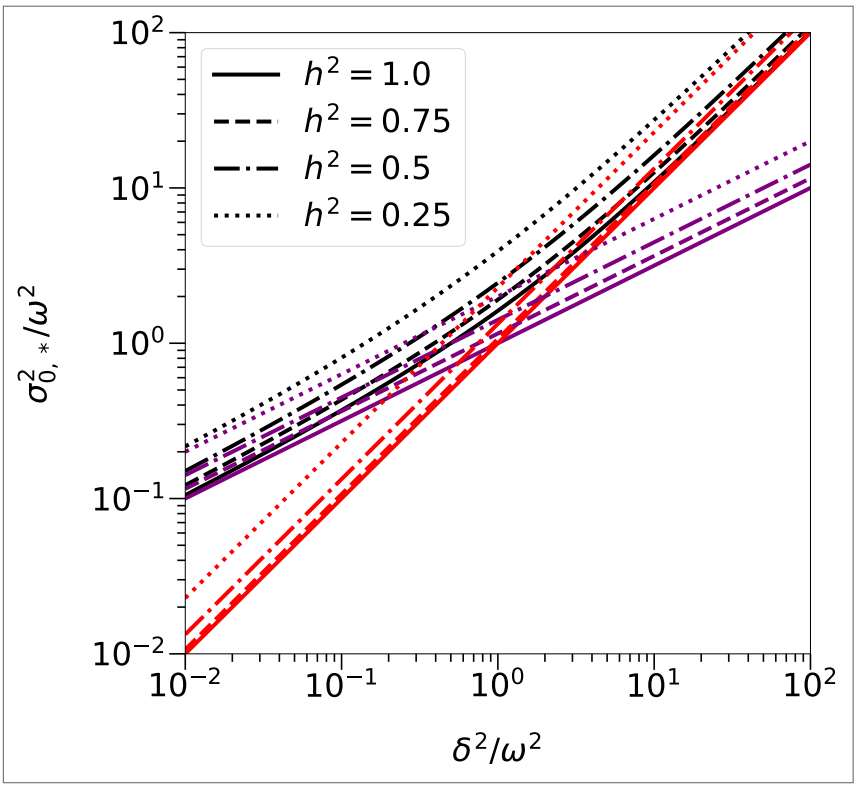

Source: Prepared by the author (2024)

The map for the variance of the zygotic stage is (see Eq. 6.27)

$$\sigma_{0,t+1}^2 = \sigma_{0,t}^2 \left[h^2 \frac{\omega}{\sqrt{\omega^2 + \sigma_{0,t}^2}} + (1 - h^2)\right]^2 + \delta^2 \quad , \tag{5.61}$$

whose stationary state can not be found analytically (see numerical solutions in Fig. 27). Notwithstanding, it is straightforward to see that the fixed point satisfies the following equality,

$$\sigma_{0,*}^2 \left\{ 1 - \left[h^2 \frac{\omega}{\sqrt{\omega^2 + \sigma_{0,*}^2}} + (1 - h^2) \right]^2 \right\} = \delta^2 \quad . \tag{5.62}$$

from which closed expressions for $\sigma_{0,*}^2$ can be easily obtained in the limit $\delta \to \infty$ and $\delta \to 0$, as follows,

$$\lim_{\delta \to \infty} \frac{\sigma_{0,*}^2}{\delta^2} = \frac{1}{1 - (1 - h^2)^2} \quad , \tag{5.63}$$

and

$$\lim_{\delta \to 0} \sigma_{0,*}^2 = \frac{\omega \delta}{h} \quad . \tag{5.64}$$

When it comes to the lag, the relation between inherited, selected and zygotic stages is identical to that of the mean as well as that of the variance,

$$\Delta_{H,t} = h^2 \Delta_{S,t} + (1 - h^2) \Delta_{0,t} \quad . \tag{5.65}$$

The resulting map is shown below (see Eq. 6.50),

$$\Delta_{0,t+1} = B + \left[\frac{\omega^2 + (1 - h^2)\sigma_{0,t}^2}{\omega^2 + \sigma_{0,t}^2} \right] \Delta_{0,t} \quad . \tag{5.66}$$

Similarly to the coefficient of selection, an analogue of the effective coefficient of selection had been defined earlier in association with the proportional return of the mean to the optimum,

$$\frac{\Delta_{H,t} - \Delta_{0,t}}{\Delta_{0,t}} = -h^2 \left(\frac{\sigma_{0,t}^2}{\omega^2 + \sigma_{0,t}^2} \right) \quad , \tag{5.67}$$

named the "homeostatic strength" by ROBERTSON (ROBERTSON, 1956).

The fixed point is

$$\Delta_{0,*} = \frac{B}{h^2} \left(\frac{\omega^2 + \sigma_{0,*}^2}{\sigma_{0,*}^2} \right) \quad , \tag{5.68}$$

and plotted in Fig. 28. Compared to the case of maximum heritability, an arbitrary value of h^2 induces larger lag. The overall capacity of pursuing the optimum is mitigated despite a greater value of variance, which can only be compensated by intensifying the magnitude of the mutation effect. The minimum achievable distance from the optimum is a monotonically decreasing function of h^2,

$$\lim_{\delta \to \infty} \Delta_{0,*} = \frac{B}{h^2} \quad . \tag{5.69}$$

Last but not least, the critical rate of environmental change becomes

$$B_c = \frac{h^2 \sigma_{0,*}^2}{\sqrt{\omega^2 + \sigma_{0,*}^2}} \sqrt{\ln \left[W_{max}^2 \left(\frac{\omega^2}{\omega^2 + \sigma_{0,*}^2} \right) \right]} \quad . \tag{5.70}$$

Figure 28 – Stationary lag $\Delta_{0,*}$ versus scaled squared magnitude of the mutation effect δ^2 for different values of heritability h^2. Each asymptote in red is the constant curve $1/h^2$.

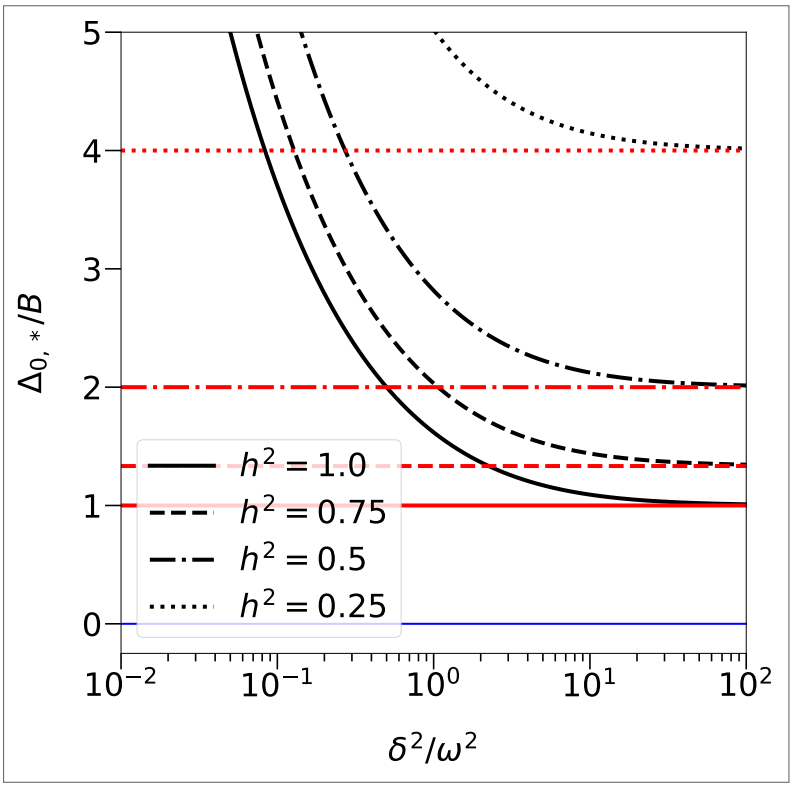

Source: Prepared by the author (2024)

In addition to the multiplicative explicit factor, the value of h^2 also influences B_c through $\sigma^2_{0,*}$. The dependence on h^2 is exposed in Fig. 29.

Now, the stability coefficients are investigated. The analysis follows the procedure applied for the mutation-selection balance and the unidimensional map for variance is considered first. With heritability included, the right-hand side of Eq. 5.36 becomes,

$$\frac{d\sigma^2_{H,t}}{d\sigma^2_{S,t}} = \left[h^2 + (1-h^2)\left(\frac{\sigma_{0,t}}{\sigma_{S,t}}\right)\right]\left[h^2 + (1-h^2)\left(\frac{\sigma_{0,t}}{\sigma_{S,t}}\right)^3\right] \quad , \tag{5.71}$$

The resulting eigenvalue is still below one for any set of parameters,

$$\frac{d\sigma^2_{0,t+1}}{d\sigma^2_{0,t}} = \left[h^2\left(\frac{\sigma_{S,t}}{\sigma_{0,t}}\right) + (1-h^2)\right]\left[h^2\left(\frac{\sigma_{S,t}}{\sigma_{0,t}}\right)^3 + (1-h^2)\right] \quad , \tag{5.72}$$

with the coefficient presenting a lower bound given by

$$\lim_{\delta\to\infty}\left|\frac{d\sigma^2_{0,t+1}}{d\sigma^2_{0,t}}\right|_{\sigma^2_{0,t}=\sigma^2_{0,*}} = (1-h^2)^2 \quad , \tag{5.73}$$

as shown in Fig. 30.

For the lag, the extra factor is

$$\frac{\partial\Delta_{H,t}}{\partial\Delta_{S,t}} = h^2 + (1-h^2)\frac{\sigma^2_{S,t}}{\sigma^2_{0,t}} \quad . \tag{5.74}$$

Figure 29 – Critical rate of environmental change B_c versus scaled squared magnitude of the mutation effect δ^2 for different values of heritability h^2 and maximum fitness set at $W_{max} = 2.0$.

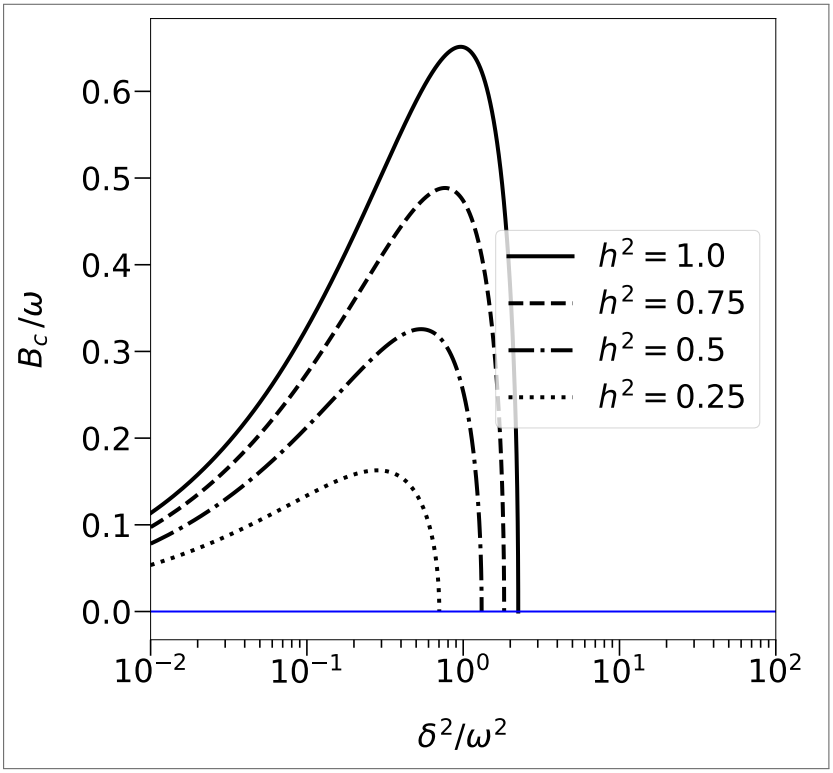

Source: Prepared by the author (2024)

Once again, the remaining factors are preserved and the outcome is below unity (see Fig. 31),

$$\frac{\partial \Delta_{0,t+1}}{\partial \Delta_{0,t}} = 1 - h^2 \left(1 - \frac{\sigma^2_{S,t}}{\sigma^2_{0,t}}\right) \quad . \tag{5.75}$$

The lower bound of the second coefficient is

$$\lim_{\delta \to \infty} \left| \frac{\partial \Delta_{0,t+1}}{\partial \Delta_{0,t}} \right|_{\left(\sigma^2_{0,t}, \Delta_{0,t}\right) = \left(\sigma^2_{0,*}, \Delta_{0,*}\right)} = 1 - h^2 \quad . \tag{5.76}$$

Both stability coefficients mimic the behavior of the effective coefficient of selection regarding all parameters (see Fig. 32 for a precise comparison with its stationary value). By reducing the efficacy of selection, decreasing heritability leads to the attenuation of the degree of stability.

Estimates of heritability are available everywhere and vary significantly from trait to trait as well as among species (VISSCHER; HILL; WRAY, 2008). As we have investigated a sustained environmental change and its consequences to extinction risk, however, the traits in focus are presumed to be of a very particular nature, those closely related to fitness. Several studies have reported that the heritability of these traits are severely biased to low values. This is the case for life history traits such as fecundity, viability and development, in contrast to morphological, behavioral and physiological ones (BARTON; TURELLI, 1989; ROFF; MOUSSEAU, 1987; MOUSSEAU; ROFF, 1987; VISSCHER; HILL; WRAY, 2008), as shown in Fig. 33.

Figure 30 – First coefficient of stability $|d\sigma^2_{0,t+1}/d\sigma^2_{0,t}|_{\sigma^2_{0,t}=\sigma^2_{0,*}}$ versus scaled squared magnitude of the mutation effect δ^2 for different values of heritability h^2. Each asymptote in red is the constant curve $(1-h^2)^2$.

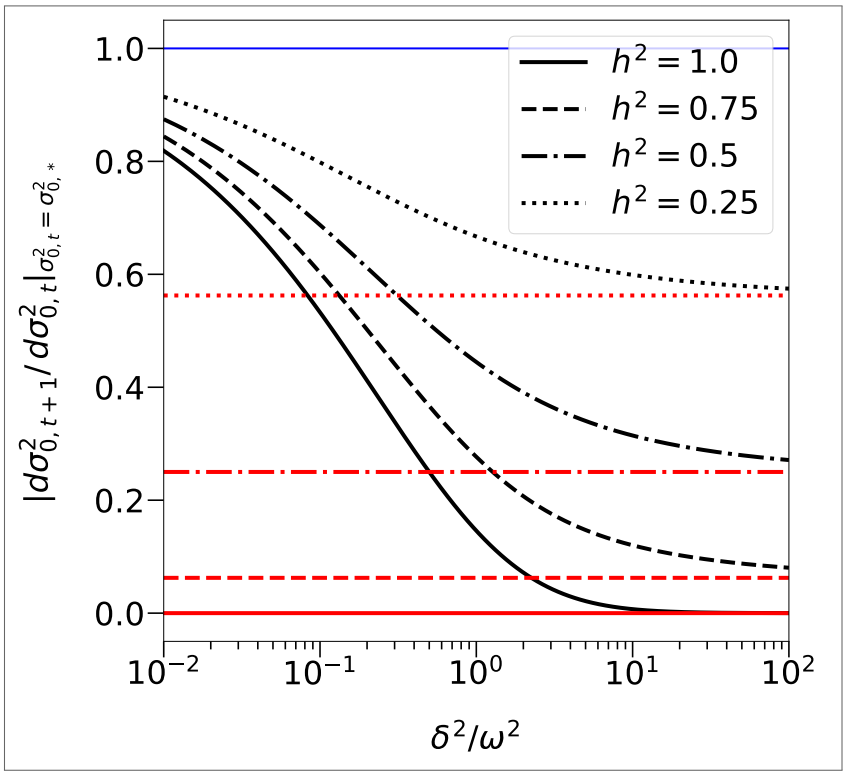

Source: Prepared by the author (2024)

Figure 31 – Second coefficient of stability $\left|d\Delta_{t+1}/d\Delta_t\right|_{(\sigma^2_{0,t},\Delta_{0,t})=(\sigma^2_{0,*},\Delta_{0,*})}$ versus scaled squared magnitude of the mutation effect δ^2 for different values of heritability h^2. Each asymptote in red is the constant curve $(1-h^2)$.

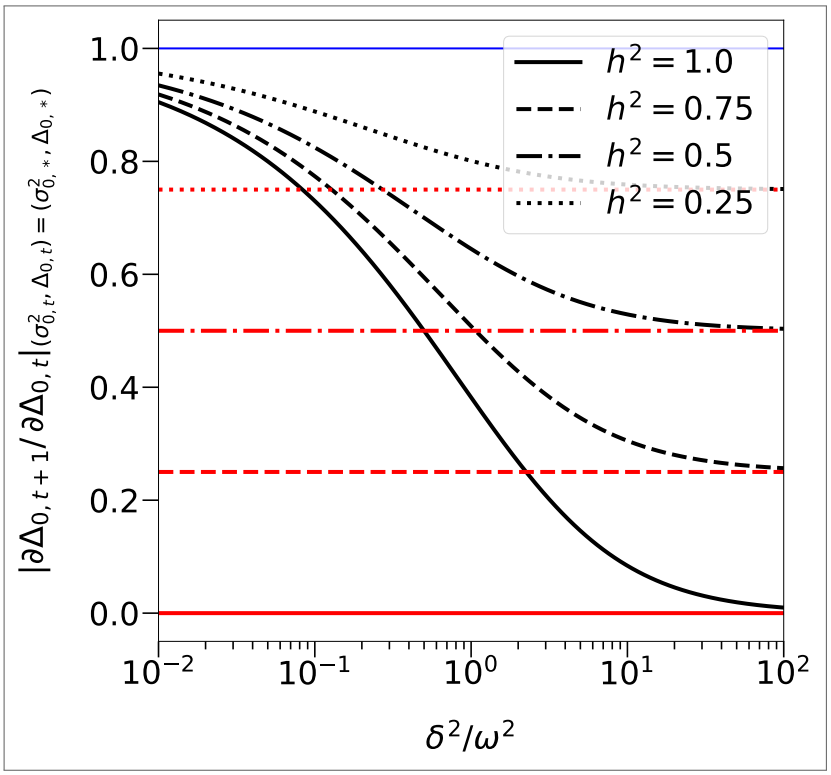

Source: Prepared by the author (2024)

Figure 32 – Stationary effective coefficient of selection $\sigma^2_{H,*}/\sigma^2_{0,*}$ versus scaled squared magnitude of the mutation effect δ^2 for different values of heritability h^2. Each asymptote in red is the constant curve $(1-h^2)^2$. In the limit case $h^2 = 1$, the stationary variance of the inherited stage $\sigma^2_{H,*}$ equals the stationary variance of the selection stage $\sigma^2_{S,*}$.

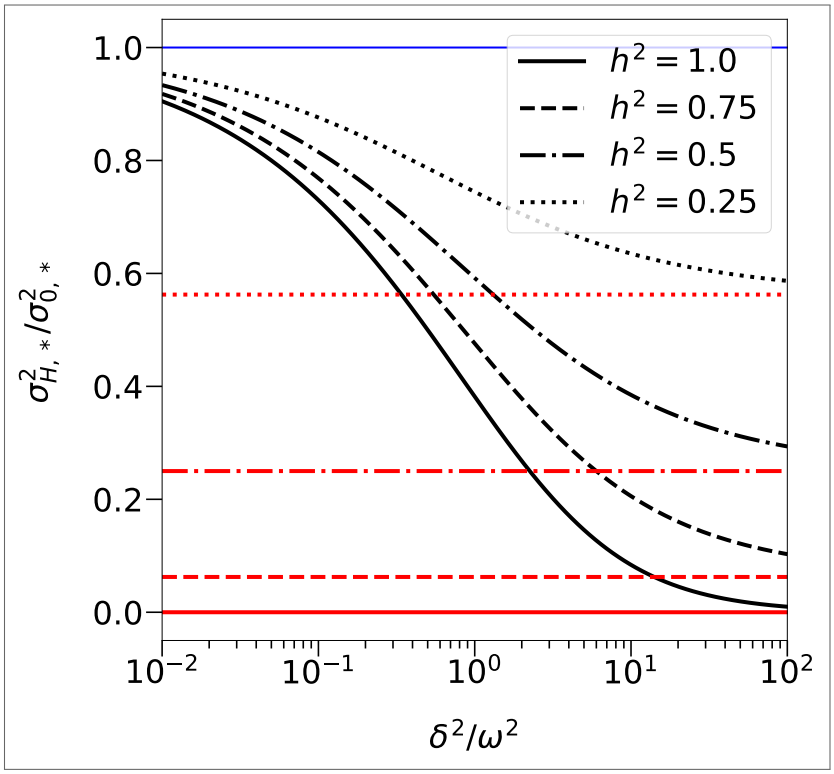

Source: Prepared by the author (2024)

Figure 33 – A set of heritability estimates across several studies has been assembled by VISSCHER; HILL; WRAY (VISSCHER; HILL; WRAY, 2008) and corroborates the tendency for traits associated with fitness to have lower heritability.

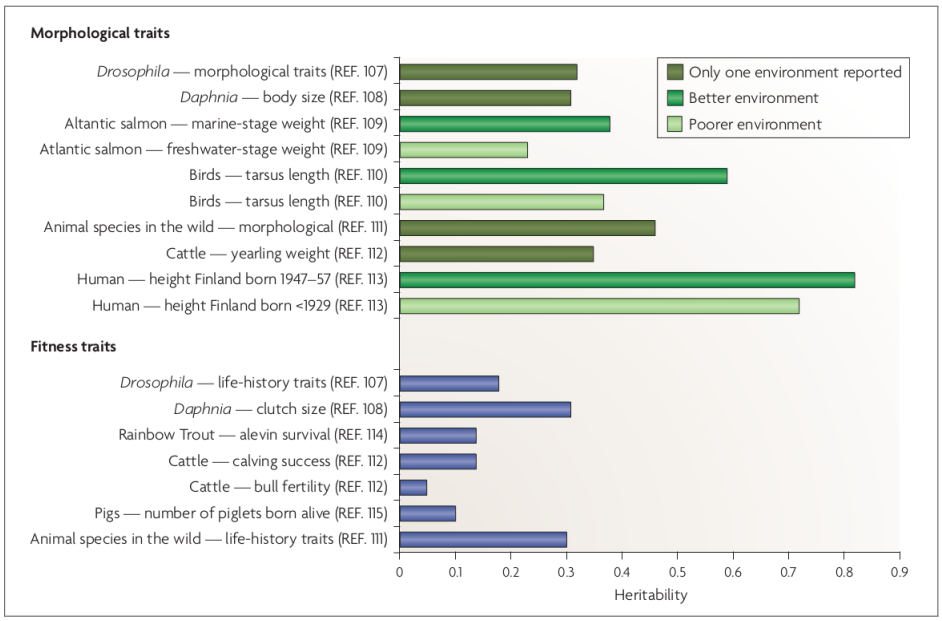

Source: VISSCHER; HILL; WRAY (2008)

5.6 PHENOTYPIC PLASTICITY

Lastly, The role of phenotypic plasticity is addressed. Heritability is taken out of the picture ($h^2 = 1$), for simplicity, and the life cycle is now represented by

$$Z_{0,t+1} = P_{t+1}(M(P_t^{-1}(S_t(Z_{0,t})))) \quad . \tag{5.77}$$

Concerning the two-dimensional map, the introduction of plasticity culminates in the rescaling of two fundamental parameters (see Eqs. 6.44 and 6.50),

$$\begin{cases} \delta \to (1-b)\delta \\ \\ B \to (1-b)B \end{cases} \quad . \tag{5.78}$$

Thus, the outcome of plasticity is mainly quantitative, in the very same fashion of heritability. The mechanisms by which this happens, however, are intricate and worth of elucidation.

By introducing plasticity we are dealing with adaptation by simultaneous genetic and plastic response to selection. The propensity for earlier egg laying in birds is thought to be an example of such instance. While substantial heritability for this trait is found among several populations, there is growing evidence of individual adjustment to local conditions by phenotypic plasticity (PULIDO; BERTHOLD, 2004). Similar interplay is found in the water flea *Daphnia magna* in reaction to increased fish predation (STOKS et al., 2016).

The primary consequence is the splinting of the phenotype into the genetic and non-genetic components. The phenotypic variance and its genetic component, here denoted by γ^2, are related by the same linear transformation whatever the stage of the life cycle (see Eqs. 6.9, 6.27 and 6.38),

$$\sigma_t^2 = (1-b)^2\gamma_t^2 \quad . \tag{5.79}$$

The variability of the genetic component is greater than that of the actual phenotype in any circumstances, as shown in Fig. 34. This is essentially due to the bias introduced by a plastic effect which is proportional to the lag: phenotypes further from the optimum develop more. More precisely, the genetic and non-genetic components present a negative covariance,

$$\langle\langle A_{0,t}, b(\theta_t - A_{0,t})\rangle\rangle = \langle A_{0,t}\,[b(\theta_t - A_{0,t})]\rangle - \langle A_{0,t}\rangle\langle b(\theta_t - A_{0,t})\rangle \tag{5.80}$$

$$= -b\langle\langle A_{0,t}\rangle\rangle \quad , \tag{5.81}$$

so that the variance of the actual phenotype is smaller than the sum of the variances of the complementary components,

$$\langle\langle P(A_{0,t})\rangle\rangle = \langle\langle A_{0,t}\rangle\rangle + \langle\langle b(\theta_t - A_{0,t})\rangle\rangle + 2\langle\langle A_{0,t},\, b(\theta_t - A_{0,t})\rangle\rangle \tag{5.82}$$

$$= \langle\langle A_{0,t}\rangle\rangle + b^2\langle\langle A_{0,t}\rangle\rangle - 2b\langle\langle A_{0,t}\rangle\rangle \tag{5.83}$$

$$= (1-b)^2\langle\langle A_{0,t}\rangle\rangle \quad . \tag{5.84}$$

Figure 34 – Stationary variance $\sigma^2_{0,*}$ (in black) along with its genetic component (in grey) versus magnitude of plasticity b for different magnitudes of mutation δ^2. Each asymptote in red is the constant curve of the value of phenotypic variance in the absence of plasticity, case in which it is equivalent to its genetic component.

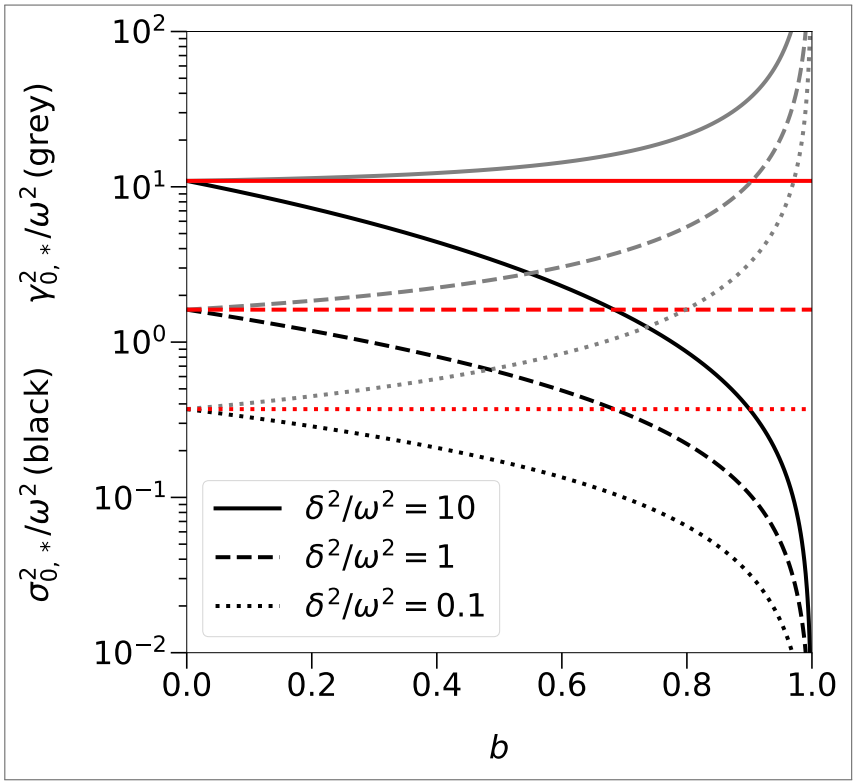

Source: Prepared by the author (2024)

When compared to the value expected in the absence of plasticity, the phenotypic variance is lower too. A comparison with the hypothetical case of a sub-population that develops plasticity "instantly" from a population that has attained the stationary state is very useful to understand the issue, explored in Fig. 35. Both populations share the genetic component of variance initially, so that the values after development differ exactly by a factor $(1-b)^2$. Selection, however, is not a linear operation like plasticity, such that the ratio between developed and non-developed instances above $(1-b)^2$ bout lower than 1, while the opposite happens to the genetic component of the selected character. An opposite situation stands for the mutated state. Mutation is not linear as well. Unlike selection, mutation is proportionally more noticeable on decreasing values of variance, and an opposite situation stands for the mutated state.

The influence of plasticity on the phenotypic variance is displayed in Fig 36. From Eq. 5.63 (applying $h^2 = 1$), it follows that the asymptotes to diverging values of the magnitude of the mutation effect have a slope of

$$\lim_{\delta\to\infty} \frac{\sigma^2_{0,*}}{\delta^2} = (1-b)^2 \quad . \tag{5.85}$$

In the limit of small delta, $\delta \to$, one has (see Eq. 5.64)

$$\lim_{\delta\to 0} \sigma^2_{0,*} = (1-b)\omega\delta \quad . \tag{5.86}$$

Figure 35 – Ratio between the variance of the character of a population "instantly" endowed with plasticity and that of the original population (not endowed) at consecutive stages of the life cycle (shown in the x-axis). The superior and inferior constant curves in red denote $(1-b)^{-2}$ and $(1-b)^2$, respectively.

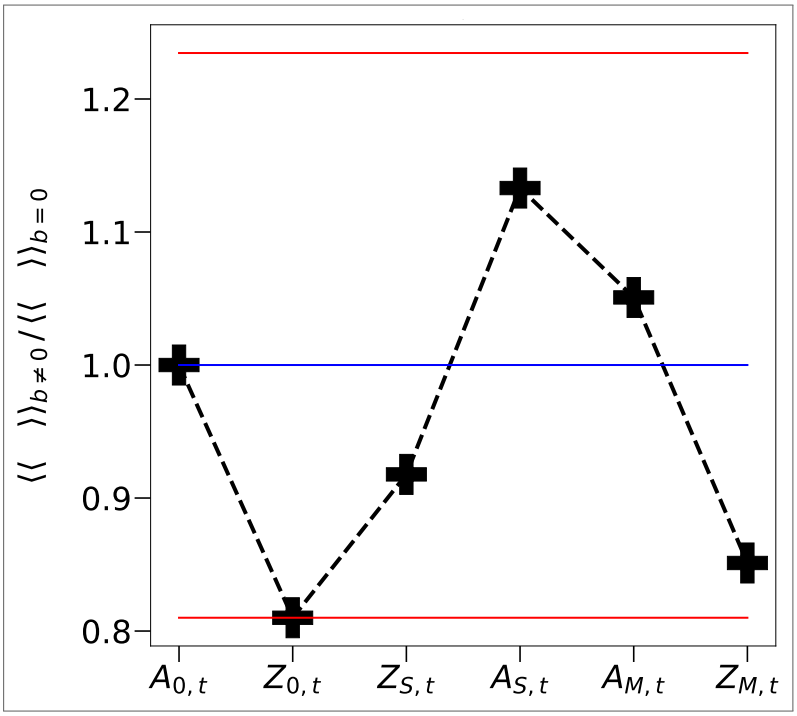

Source: Prepared by the author (2024)

In spite of causing the weakening of the coefficient of selection (see Fig. 37), the decrease of the stationary variance with the plasticity b originated on the rescaling of δ^2 (Eq. 5.78) does not convey enough information to determine the actual effect on the chance of survival as the critical rate is a non-monotonic function of this quantity.

From Fig. 38, we observe that phenotypic plastic allows the mean population phenotype to remain closer to the phenotypic optimum with a lag that is smaller than the rate of environmental change, as we can see from Eq. 5.69,

$$\lim_{\delta\to\infty}\frac{\Delta_{0,*}}{B}=(1-b)\quad . \tag{5.87}$$

Any individual in the next generation presents a larger plastic effect than its parent, i.e., of a fixed genetic component of the phenotype. The development of the offspring is always larger than that of the parent's generation for the same genetic component of the character. This is clearly inferred for the average value from

$$\mu_{0,t+1}=(1-b)\nu_{M,t}+b\theta_{t+1} \tag{5.88}$$

$$=\mu_{S,0}+b\left(\theta_{t+1}-\theta_t\right) \tag{5.89}$$

$$=\mu_{S,0}+bB\quad . \tag{5.90}$$

Conversely, it means that the cost of selection is larger on phenotypes that display larger

Figure 36 – Stationary variance $\sigma^2_{0,*}$ versus scaled squared magnitude of the mutation effect δ^2 for different magnitudes of plasticity b. Each asymptote in red is the linear function of slope $(1-b)^2$. Each curve in purple corresponds to the function $\sigma^2_{0,*} = (1-b)\omega\delta$.

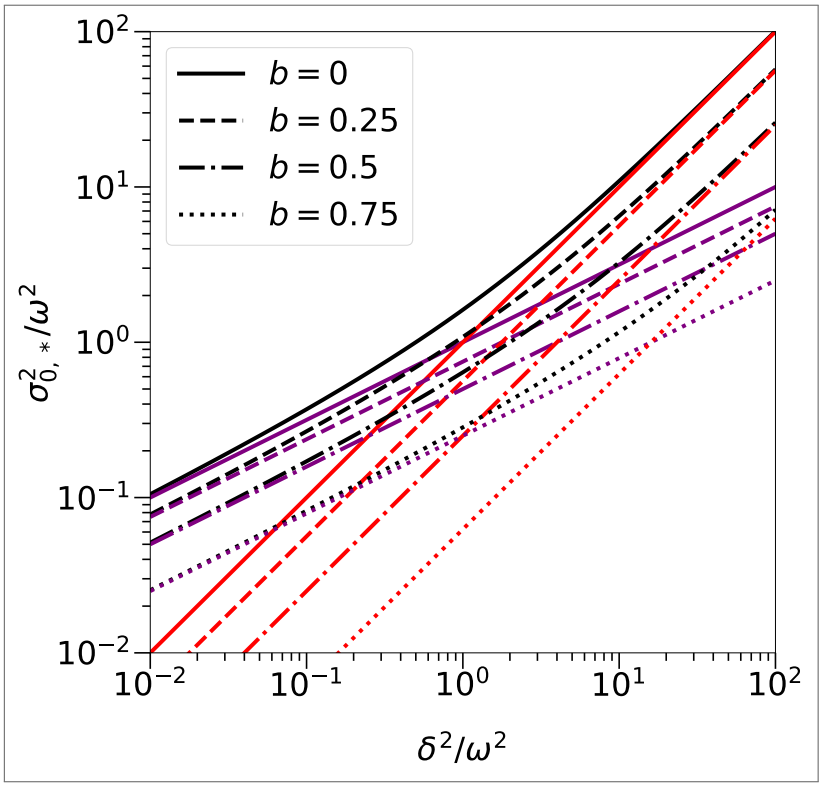

Source: Prepared by the author (2024)

genetic component for a fixed phenotype. The map for the lag follows directly,

$$\Delta_{0,t+1} = \theta_{t+1} - \mu_{0,t+1} \tag{5.91}$$

$$= (\theta_t + B) - (\mu_{S,0} + bB) \tag{5.92}$$

$$= (1-b)B + \Delta_{S,t} \quad . \tag{5.93}$$

The critical rate of environmental change then increases with plasticity, according to Fig. 39.

As phenotypic plasticity is thought to be an important mechanism of population's persistence in the face of environmental change, the developmental mechanisms and, more importantly, their potential forms of application to management and conservation practice have been in focus on the last decades (DONELSON et al., 2023). When it comes to the impacts of climate change on the taxa of mosquitoes, for instance, precise estimates of the role of phenotypic plasticity to thermal adaptation may be decisive to public health policies (COUPER et al., 2021). Moreover, current evidence indicates that directional selection is the most predictable scenario for adaptive plasticity, although it frequently originates from past selection events where it was previously non-adaptive (GHALAMBOR et al., 2007). The major limitation to the benefits of phenotypic plasticity under sustained environmental change seems to be the reliability of the environmental cues (DEWITT; SIH; WILSON, 1998). Different levels of cue reliability were investigated by (REED et al., 2010) REED et al. through a stochastic individual-based model.

Figure 37 – Stationary coefficient of selection $\sigma^2_{S,*}/\sigma^2_{0,*}$ versus scaled squared magnitude of the mutation effect δ^2 for different magnitudes of plasticity b and maximum reproductive rate set at $W_{max} = 2.0$.

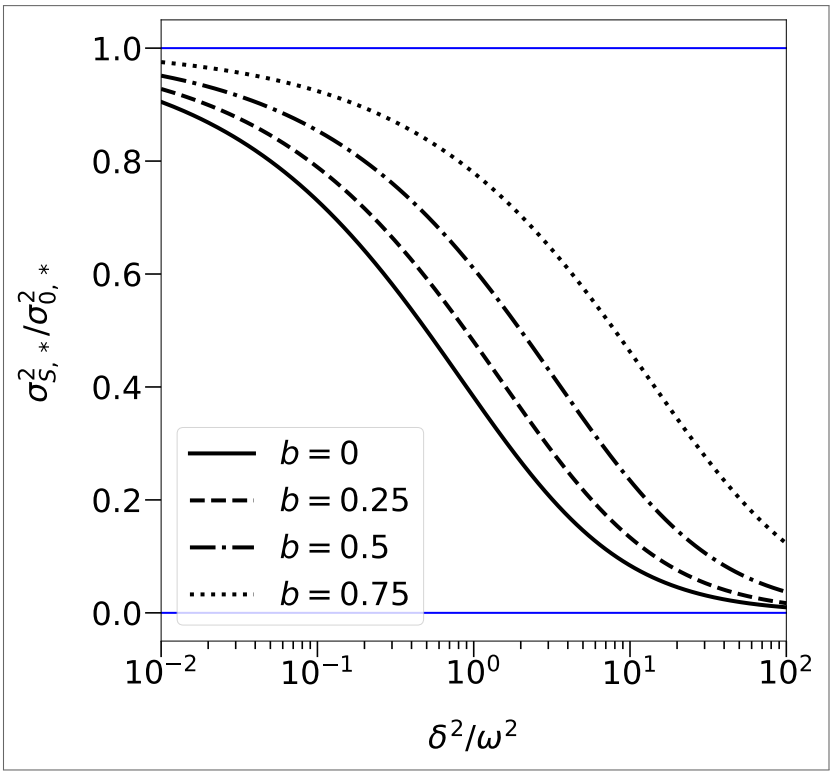

Source: Prepared by the author (2024)

While tightly correlated cue and optimum lead to high and invariant population sizes, plasticity may increase the chance of extinction under a small correlation.

Moreover, it may be useful to determine the selective advantage of plasticity. For a fixed genetic component of the character $A_{0,t}$, the selective advantage s_t of an individual endowed with plasticity relative to one deprived of it is here defined as

$$1 - s_t = \frac{W_t(A_{0,t})}{W_t(P_t(A_{0,t}))} \tag{5.94}$$

$$= \exp\left\{-\frac{1}{2}\left(\frac{\theta_t - A_{0,t}}{\omega}\right)^2 \left[1 - (1-b)^2\right]\right\} \quad , \tag{5.95}$$

and plotted in Fig. 40. The concept may be extended to the population level. Under stationarity, plasticity confers a selective advantage for the population given by

$$1 - \overline{s}_* = \frac{\overline{W}_*(b=0)}{\overline{W}_*} \tag{5.96}$$

$$= \sqrt{\frac{\omega^2 + \sigma^2_{0,*}}{\omega^2 + \sigma^2_{0,*}(b=0)}} \exp\left\{-\frac{1}{2}B^2\left[\left(\frac{\omega^2 + \sigma^2_{0,*}(b=0)}{\sigma^4_{0,*}(b=0)}\right) - (1-b)^2\left(\frac{\omega^2 + \sigma^2_{0,*}}{\sigma^4_{0,*}}\right)\right]\right\} \quad , \tag{5.97}$$

where $\sigma^2_{0,*}(b=0)$ denotes the stationary variance in the absence of plasticity.

Figure 38 – Stationary lag $\Delta_{0,*}$ versus scaled squared magnitude of the mutation effect δ^2 for different magnitudes of plasticity b. Each asymptote in red is the constant curve $(1-b)$.

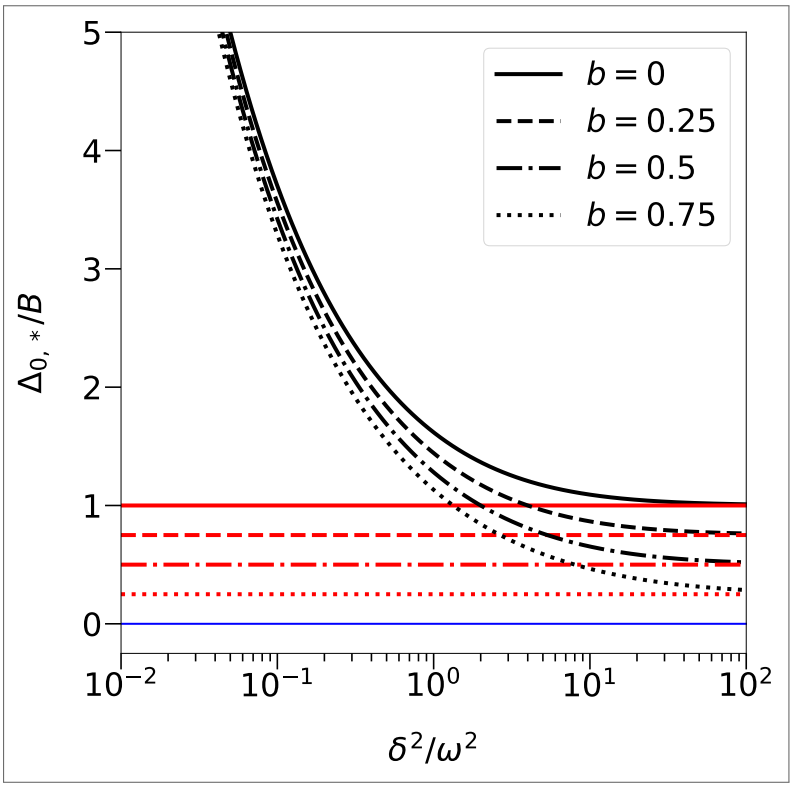

Source: Prepared by the author (2024)

The dependence of the selective advantage, s, on the scaled mutation effect is explored in Fig. 41. The differences brought by plasticity in load and capacity of pursuing the optimum are mitigated as δ^2 decreases,

$$\lim_{\delta \to 0} \overline{s}_* = 0 \quad , \tag{5.98}$$

severely attenuating the advantages of plasticity at the domain of small values. In the limit $\delta \to \infty$, although, the constriction of phenotypic variance caused by plasticity on variance is amplified, and so it does the differences in selective load too, resulting in a maximum possible ratio given by

$$\lim_{\delta \to \infty} \overline{s}_* = 1 - \lim_{\delta \to \infty} \left(\frac{\sigma_{0,*}(b=0)}{\sigma_{0,*}} \right) \tag{5.99}$$

$$= b \quad . \tag{5.100}$$

Now we prove that all phenotypic evolution is purely genetic in the stationary state. First, the difference between the genetic component of the mean of two arbitrary consecutive generations is

$$\nu_{0,t+1} - \nu_{0,t} = \frac{\mu_{0,t+1} - b\theta_{t+1}}{1-b} - \frac{\mu_{0,t} - b\theta_t}{1-b} \tag{5.101}$$

$$= B - (\Delta_{0,t+1} - \Delta_{0,t}) \quad . \tag{5.102}$$

Figure 39 – Critical rate of environmental change B_c versus scaled squared magnitude of the mutation effect δ^2 for different magnitudes of plasticity b.

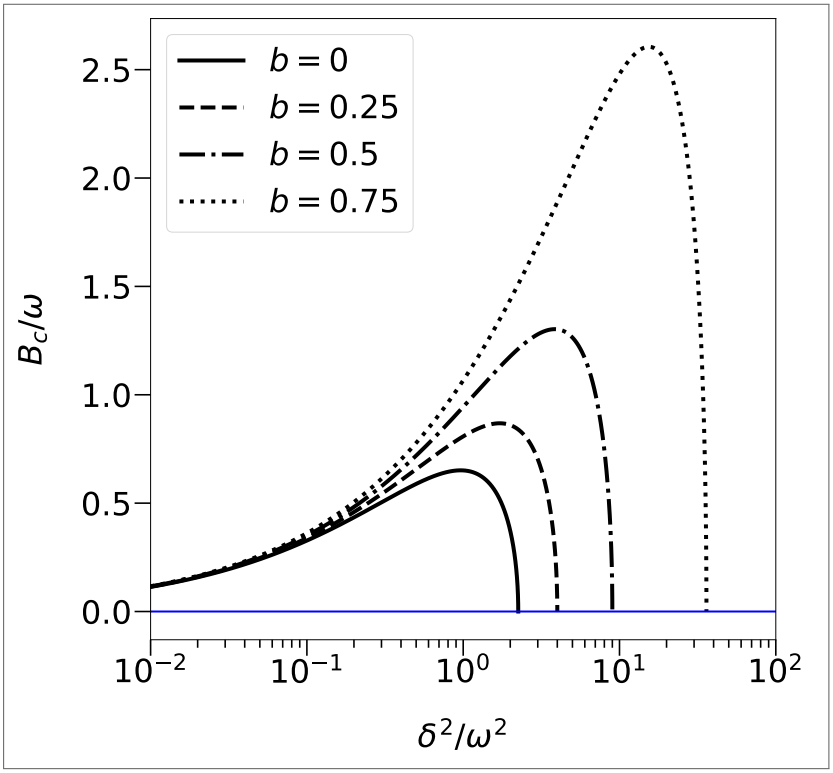

Source: Prepared by the author (2024)

Then it is straightforward to see that in the stationary state the value reads

$$(\nu_{0,t+1} - \nu_{0,t})_* = B \quad . \tag{5.103}$$

Finally, the repercussions on stability are scrutinized. As mentioned before, plasticity is associated with the mitigation of the coefficient of selection which is, in turn, a proxy of the stability coefficients (see Eqs. 5.38 and 5.41). From this link we can derive non beneficial consequences of the presence of plasticity to the population, but in terms of stability rather than fitness. Actually, the impact of the mechanism of plasticity in the propagation or mitigation of a disturbance is not direct but only indirect through the modification of the stationary variance. This is an outcome of linearity, as revealed by the chain rule in

$$\frac{d\sigma^2_{0,t+1}}{d\sigma^2_{0,t}} = \frac{d\sigma^2_{M,t}}{d\gamma^2_{M,t}} \frac{d\gamma^2_{M,t}}{d\gamma^2_{S,t}} \frac{d\gamma^2_{S,t}}{d\sigma^2_{S,t}} \frac{d\sigma^2_{S,t}}{d\sigma^2_{0,t}} \tag{5.104}$$

$$= (1-b)^2 \frac{d\gamma^2_{M,t}}{d\gamma^2_{S,t}} \frac{1}{(1-b)^2} \frac{d\sigma^2_{S,t}}{d\sigma^2_{0,t}} \tag{5.105}$$

$$= \frac{d\gamma^2_{M,t}}{d\gamma^2_{S,t}} \frac{d\sigma^2_{S,t}}{d\sigma^2_{0,t}} \tag{5.106}$$

$$= \frac{d\sigma^2_{S,t}}{d\sigma^2_{0,t}} \quad , \tag{5.107}$$

Figure 40 – Selective advantage of plasticity s_t versus difference of the genetic component of the character to the optimum phenotype $(\theta_t - A_{0,t})$ for different magnitudes of plasticity b.

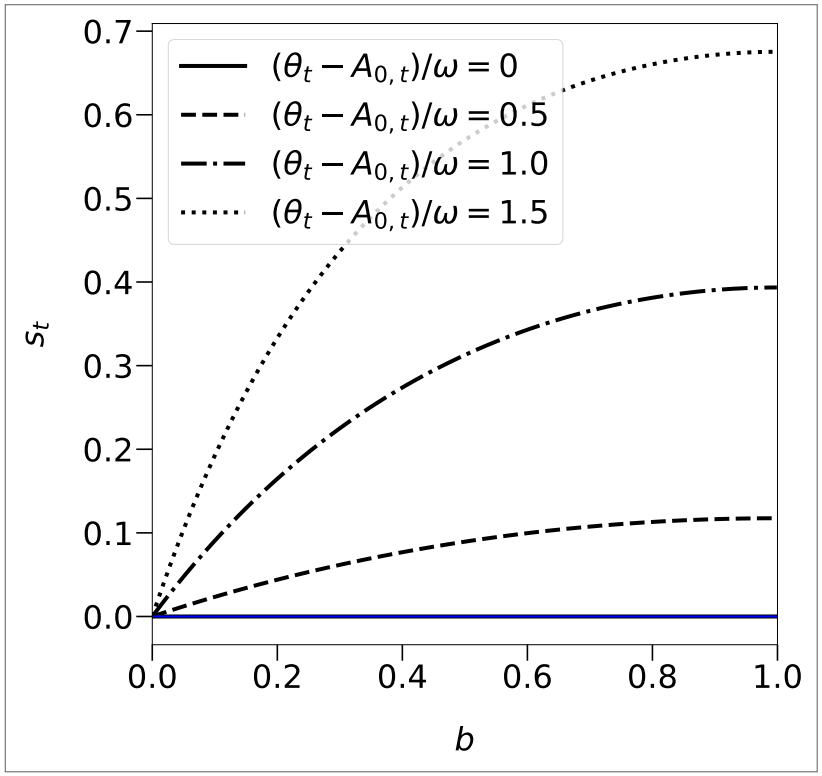

Source: Prepared by the author (2024)

and

$$\frac{d\Delta_{0,t+1}}{d\Delta_{0,t}} = \frac{d\Delta_{M,t}}{d\epsilon_{M,t}}\frac{d\epsilon_{M,t}}{d\epsilon_{S,t}}\frac{d\epsilon_{S,t}}{d\Delta_{S,t}}\frac{d\Delta_{S,t}}{d\Delta_{0,t}} \tag{5.108}$$

$$= (1-b)^2\frac{d\epsilon_{M,t}}{d\epsilon_{S,t}}\frac{1}{(1-b)^2}\frac{d\Delta_{S,t}}{d\Delta_{0,t}} \tag{5.109}$$

$$= \frac{d\epsilon_{M,t}}{d\epsilon_{S,t}}\frac{d\Delta_{S,t}}{d\Delta_{0,t}} \tag{5.110}$$

$$= \frac{d\Delta_{S,t}}{d\Delta_{0,t}} \quad , \tag{5.111}$$

where ϵ_t denotes the genetic component of the lag and relates to it by

$$\Delta_t = (1-b)\epsilon_t \quad , \tag{5.112}$$

and Eq. 5.79 has been applied. The inferior limits of the coefficients are not affected by plasticity as well (see Eqs. 5.73 and 5.76):

$$\lim_{\delta\to\infty}\left|\frac{d\sigma^2_{0,t+1}}{d\sigma^2_{0,t}}\right|_{\sigma^2_{0,t}=\sigma^2_{0,*}} = 0 \quad , \tag{5.113}$$

$$\lim_{\delta\to\infty}\left|\frac{d\Delta_{0,t+1}}{d\Delta_{0,t}}\right|_{\left(\sigma^2_{0,t},\Delta_{0,t}\right)=\left(\sigma^2_{0,*},\Delta_{0,*}\right)} = 0 \quad . \tag{5.114}$$

Figure 41 – Populational selective advantage of plasticity at the stationary state $\overline{s}_*$ versus scaled squared magnitude of the mutation effect δ^2 for different magnitudes of plasticity b and rate of environmental change set at $B = 0.5\omega$. Each asymptote in red is the constant curve b.

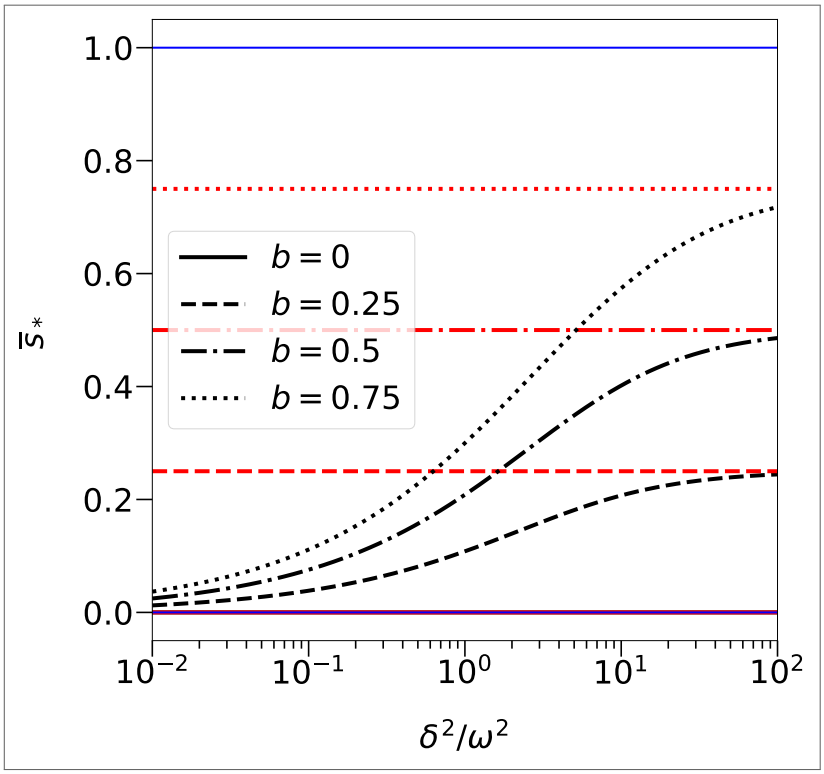

Source: Prepared by the author (2024)

This issue deserves further exploration. It is useful, for instance, to determine the cost to the population, in terms of time, to recover from a given amount of perturbation, for a given level of plasticity, assuming the normality of the distribution is preserved under this perturbation. A Taylor series expansion of the p-th composition of the variance map of first order in the perturbation $d\sigma^2$ provides the relation below,

$$\frac{\sigma^2_{0,t+p}(\sigma^2_{0,*} + d\sigma^2) - \sigma^2_{0,*}}{d\sigma^2} \approx \frac{d\sigma^2_{0,t+p}}{d\sigma^2_{0,t}}(\sigma^2_{0,*}) \tag{5.115}$$

$$= \prod_{l=0}^{p-1} \frac{d\sigma^2_{0,t+l+1}}{d\sigma^2_{0,t+l}}(\sigma^2_{0,t+l}(\sigma^2_{0,*})) \tag{5.116}$$

$$= \prod_{l=0}^{p-1} \frac{d\sigma^2_{0,t+1}}{d\sigma^2_{0,t}}(\sigma^2_{0,*}) \tag{5.117}$$

$$= \left[\frac{d\sigma^2_{0,t+1}}{d\sigma^2_{0,t}}(\sigma^2_{0,*})\right]^p \tag{5.118}$$

$$= \left(\frac{\sigma^2_{S,*}}{\sigma^2_{0,*}}\right)^{2p} \quad , \tag{5.119}$$

from which the minimum number of generations required to mitigate a deviation by half is

Figure 42 – Minimum number of generations required to mitigate a pertubation in the stationary phenotypic variance by half $p_{min,\sigma}$ versus scaled squared magnitude of the mutation effect δ^2 for different magnitudes of plasticity b. Each asymptote in red is the linear function of slope $(1-b)^2$. Each curve in red corresponds to the function $-(\ln 2)\,\sigma^2_{0,*}/(2\sigma^2_{0,*})$.

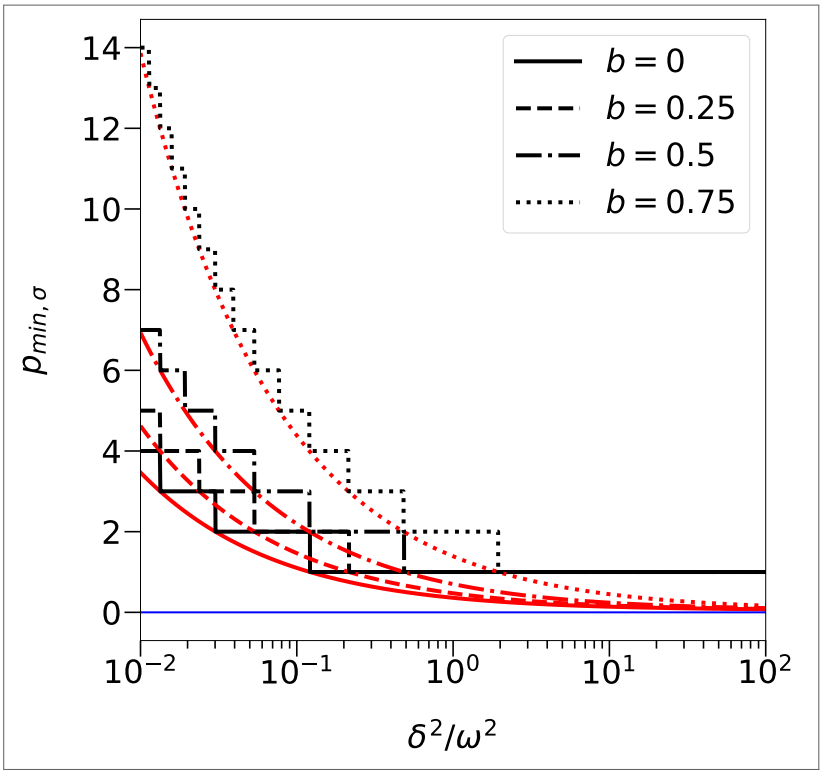

Source: Prepared by the author (2024)

easily obtained,

$$p_{min,\sigma} = \left\lceil -\frac{1}{2}\ln 2 \left(\frac{\sigma^2_{S,*}}{\sigma^2_{0,*}}\right)^{-1} \right\rceil \quad . \tag{5.120}$$

As shown in Fig. 42, such cost and the role of plasticity on it crucially depend on the mutation effect. While values of δ above the width of selection lead to a prompt mitigation of disturbance, regardless the intensity of plasticity, below this value the recovery demands several generations and becomes very sensitive to the plastic effect.

The recovery from deviations in the lag concerns a more tricky analysis as they can appear both spontaneously and induced by deviations in variance. The former situation is addressed

Figure 43 – Minimum number of generations required to mitigate a pertubation in the stationary phenotypic variance by half $p_{min,\Delta}$ versus scaled squared magnitude of the mutation effect δ^2 for different magnitudes of plasticity b. Each asymptote in red is the linear function of slope $(1-b)^2$. Each curve in red corresponds to the function $-(\ln 2)\,\sigma^2_{0,*}/(\sigma^2_{0,*})$.

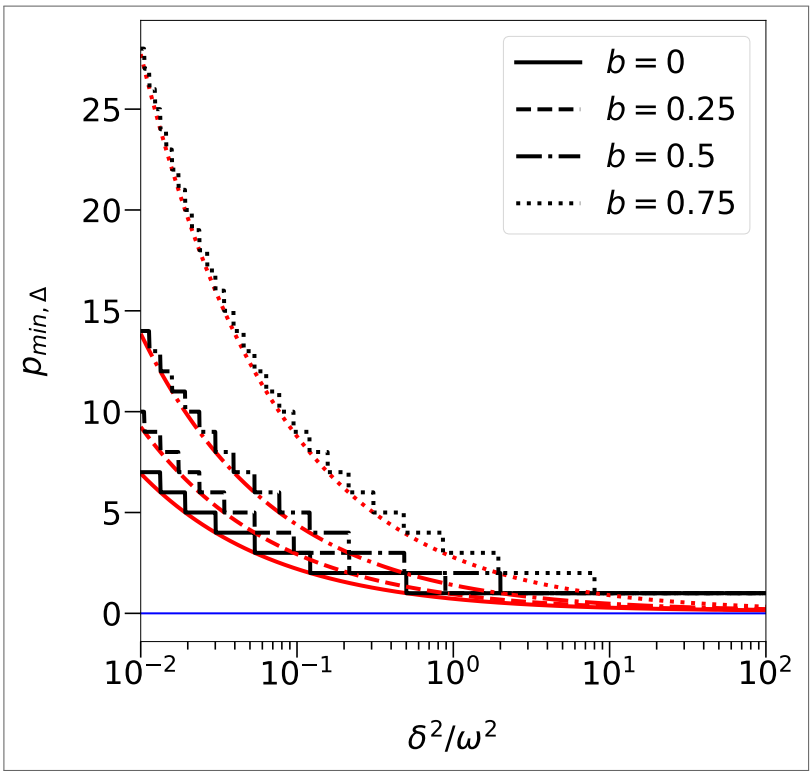

Source: Prepared by the author (2024)

first, and involves a calculation analogous to the one that originated Eq. 5.119,

$$\frac{\Delta_{0,t+p}(\sigma^2_{0,*},\Delta_{0,*}+d\Delta)-\Delta_{0,*}}{d\Delta} \approx \frac{\partial\Delta_{0,t+p}}{\partial\Delta_t}(\Delta_{0,*}) \tag{5.121}$$

$$= \prod_{l=0}^{p-1}\frac{\partial\Delta_{0,t+l+1}}{\partial\Delta_{0,t+l}}(\sigma^2_{0,t+l}(\sigma^2_{0,*}),\Delta_{0,t+l}(\sigma^2_{0,*},\Delta_{0,*})) \tag{5.122}$$

$$= \prod_{l=0}^{p-1}\frac{\partial\Delta_{0,t+1}}{\partial\Delta^2_{0,t}}(\sigma^2_{0,*},\Delta_{0,*}) \tag{5.123}$$

$$= \left[\frac{\partial\Delta_{0,t+1}}{\partial\Delta_{0,t}}(\sigma^2_{0,*},\Delta_{0,*})\right]^p \tag{5.124}$$

$$= \left(\frac{\sigma^2_{S,*}}{\sigma^2_{0,*}}\right)^p \quad . \tag{5.125}$$

The resulting minimum number of generations, in this case,

$$p_{min,\Delta} = \left\lceil -\ln 2\left(\frac{\sigma^2_{S,*}}{\sigma^2_{0,*}}\right)^{-1}\right\rceil \tag{5.126}$$

$$= 2\,p_{min,\sigma} \quad , \tag{5.127}$$

differs from the previous one by a factor of 2. Thus, the plot in Fig. 43 repeats the same

analysis of Fig. 42, and the same observations raised hold here. The only difference regards the doubling of the vertical scale.

Now we discuss the instance of a lag deviation induced by a perturbation on variance. A primary point is this discussion involves quantifying how much deviation on lag corresponds to a given deviation on variance in the next generation:

$$\left|\Delta_{0,t+1}(\sigma^2_{0,*}+d\sigma^2,\Delta_{0,*})-\Delta_{0,*}\right| = \left|\Delta_{0,t+1}(\sigma^2_{0,*},\Delta_{0,*}+d\Delta)-\Delta_{0,*}\right| \tag{5.128}$$

$$\left|d\sigma^2\right|\left|\frac{\partial\Delta_{0,t+1}}{\partial\sigma^2_{0,t}}(\sigma^2_{0,*},\Delta_{0,*})\right| \approx \left|d\Delta\right|\left|\frac{\partial\Delta_{0,t+1}}{\partial\Delta_{0,t}}(\sigma^2_{0,*},\Delta_{0,*})\right| \tag{5.129}$$

$$\frac{\left|d\sigma^2\right|}{\sigma^2_{0,*}} = \frac{\left|d\Delta\right|}{B} \quad . \tag{5.130}$$

According to the last expression, the stationary variance and the rate of environmental change are the natural units for the comparison between distinct origins of lag deviation. There may be then two possible situations: first, the deviation in variance is negligible compared to an spontaneous deviation in the lag and Eq. 5.127 provides a precise measure of the recovery time; or the deviation in variance is of an order equal or greater than an spontaneous deviation in the lag and so Eq. 5.127 only gives a lower limit for the recovery time, since it sums up with the spontaneous deviation and continues to provoke new deviations during the time scale of restoration of the stationary variance.

At last, the range of values for the plastic effect b is discussed. As a matter of fact, a closer look at any expression in this section confirms that any value of the parameter b leads to physically possible systems. Although the range $0 \leq b < 1$ has been introduced along with the operational definition of plasticity in Eq. 5.8 because, in practice, that range satisfactorily synthesizes the role played by an adaptive plasticity. While the interval $1 < b < 2$, associated with a plastic effect that overcomes the optimum, is equivalent to the interval $0 \leq b < 1$, except for the change of sign of the lag, values outside these ranges are harmful (non-adaptive).

5.6.1 Alternative case I: linear on the optimum

To thoroughly justify the features assigned to the particular case of plasticity linear with the lag, the other two possibilities are investigated now. What changes occur if the plastic effect is proportional to the optimum value instead of the distance to it? The instance mentioned is defined by

$$Z_t = A_t + b\theta_t \quad . \tag{5.131}$$

A primary property is the equivalence between the phenotypic variance and its genetic component. The random variable associated to the first differs from the later by a constant (see Eq. 5.131), and the variance of a normal variable is unaltered by such transformation.

With no correlation between the genetic and non-genetic components of the phenotype, this form of plasticity has no effect in terms of variance,

$$\sigma_t^2 = \gamma_t^2 \quad . \tag{5.132}$$

The equation of motion of the mean value, although, is preserved,

$$\mu_{0,t+1} = \nu_{M,t} + b\theta_{t+1} \tag{5.133}$$

$$= \mu_{S,0} + b\left(\theta_{t+1} - \theta_t\right) \tag{5.134}$$

$$= \mu_{S,0} + bB \quad , \tag{5.135}$$

as well as the lag map. The conclusion is that this form of plasticity brings about the rescaling of the rate of environmental change.

Figure 44 – Selective advantage of plasticity (linear to the optimum) s_t versus difference of the genetic component of the character to the optimum phenotype $(\theta_t - A_{0,t})$ for different magnitudes of plasticity b and optimum phenotype set at $\theta_t = \omega$.

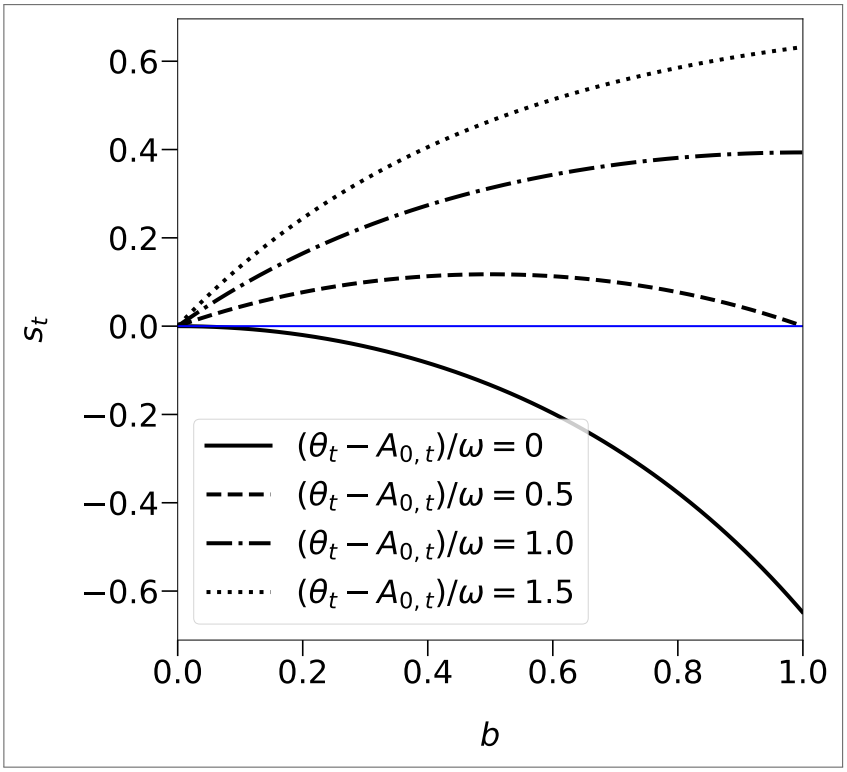

Source: Prepared by the author (2024)

It is essential to highlight that the plastic effect b has a similar meaning yet not completely equivalent to the previous one. Unlike the main case, pushing the current parameter b beyond 1 should be considered unfeasible as it does not lead to a symmetrical but an even stranger situation of a genetic evolution opposed to the direction of the environmental change. Values below 0, on the other hand, are still associated with a counterproductive development and decreasing chances of survival. Furthermore, the value of b that causes the overcoming of the

optimum (formerly 1) depends on the actual value of the optimum itself as well as on the genetic component of the phenotype:

$$Z_{0,t} < \theta_t \quad \Rightarrow \quad b < \frac{\theta_t - A_{0,t}}{\theta_t} \quad . \tag{5.136}$$

Beyond this value, the selective advantage of plasticity,

$$1 - s_t = \exp\left\{-\frac{1}{2}\frac{b\theta_t}{\omega^2}\left[2\left(\theta_t - A_{0,t}\right) - b\theta_t\right]\right\} \quad , \tag{5.137}$$

starts to decrease, as demonstrated in Fig. 44.

Figure 45 – Populational selective advantage of plasticity (linear to the optimum) at the stationary state $\overline{s}_*$ versus scaled squared magnitude of the mutation effect δ^2 for different magnitudes of plasticity b and rate of environmental change set at $B = 0.5\omega$.

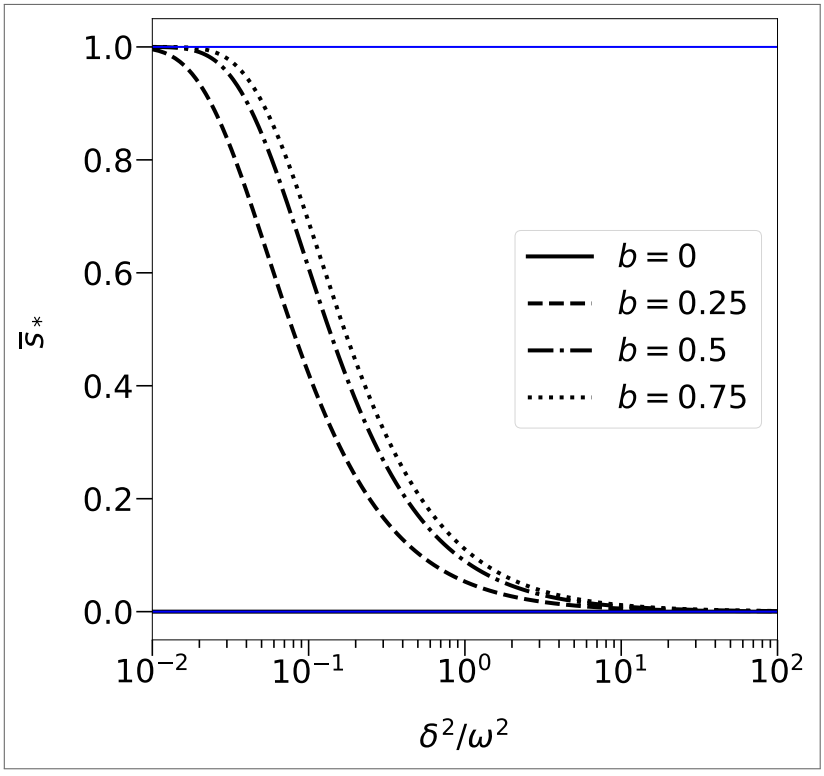

Source: Prepared by the author (2024)

The population selective advantage, on the other hand, is obtained by equating the phenotypic variance under plasticity $\sigma^2_{0,*}$ to that in its absence $\sigma^2_{0,*}(b = 0)$ in Eq. 5.97, which simplifies to

$$1 - \overline{s}_* = \exp\left\{-\frac{1}{2}B^2\left(\frac{\omega^2 + \sigma^2_{0,*}}{\sigma^4_{0,*}}\right)\left[1 - (1-b)^2\right]\right\} \quad . \tag{5.138}$$

As opposed to the main case, there are no differences in variance and, therefore, in load. The improvement of the capacity of pursuing the optimum dominates the dependence on the mutation effect all over the domain. These are maximal at small values of δ^2,

$$\lim_{\delta \to 0} \overline{s}_* = 1 \quad , \tag{5.139}$$

when the ability to seek the optimum is most intensely impaired, amplifying the advantages of plasticity in this case, as shown in Fig. 45. By the same reasoning, any advantage vanishes at high values of δ^2,

$$\lim_{\delta \to 0} \overline{s}_* = 0 \quad . \tag{5.140}$$

The overall result is precisely the opposite of that observed in a plasticity linear to the lag: the dependence is monotonically decreasing instead of increasing.

The amount of genetic evolution of the mean value per generation is calculated,

$$\begin{aligned} \nu_{0,t+1} - \nu_{0,t} &= (\mu_{0,t+1} - b\theta_{t+1}) - (\mu_{0,t} - b\theta_t) && (5.141) \\ &= (1-b)B - (\Delta_{0,t+1} - \Delta_{0,t}) \quad , && (5.142) \end{aligned}$$

which in the stationary state constitutes only a fraction of the phenotypic evolution,

$$(\nu_{0,t+1} - \nu_{0,t})_* = (1-b)B \quad . \tag{5.143}$$

The remainder comes from the non-genetic component,

$$\begin{aligned} (\mu_{0,t+1} - \nu_{0,t+1}) - (\mu_{0,t} - \nu_{0,t}) &= (\Delta_{0,t+1} + b\theta_{t+1}) - (\Delta_{0,t} - b\theta_t) && (5.144) \\ &= bB + (\Delta_{0,t+1} - \Delta_{0,t}) && (5.145) \\ [(\mu_{0,t+1} - \nu_{0,t+1}) - (\mu_{0,t} - \nu_{0,t})]_* &= bB \quad . && (5.146) \end{aligned}$$

This means development accumulates at a rate of exactly bB per generation, increasing indefinitely as the optimum moves forward, while the genetic component of the mean becomes more and more distant from the optimum as time goes by,

$$\begin{aligned} \lim_{t \to \infty} \frac{\epsilon_t}{\theta_t} &= \Delta_{0,*} \lim_{t \to \infty} \left(\frac{1}{\theta_t} \right) + b && (5.147) \\ &= b \quad . && (5.148) \end{aligned}$$

The new relation between the lag and its genetic component,

$$\Delta_t = \epsilon_t - b\theta_t \quad , \tag{5.149}$$

has been applied in the previous calculation.

The lack of rescaling on the mutation effect leads to a major difference concerning stability. The mechanism of plasticity in focus has no direct influence on the eigenvalues of the Jacobian matrix,

$$\begin{aligned} \frac{d\sigma^2_{M,0}}{d\gamma^2_{M,0}} &= 1 && (5.150) \\ &= \left(\frac{d\gamma^2_{S,0}}{d\sigma^2_{S,0}} \right)^{-1} \quad , && (5.151) \end{aligned}$$

and

$$\frac{d\Delta_{M,0}}{d\epsilon_{M,0}} = 1 \tag{5.152}$$

$$= \left(\frac{d\epsilon_{S,0}}{d\Delta_{S,0}}\right)^{-1} \quad , \tag{5.153}$$

as before. The total derivatives are then kept. The coefficients, however, no longer depend on the magnitude of plasticity, since the stationary variance does not as well, and plasticity has no impact on the degree of stability.

This specific form of plasticity has been implemented by CHEVIN; LANDE; MACE (CHEVIN; LANDE; MACE, 2010) under the same circumstances that we have explored, with exception of the extension of the standard law of quantitative genetics (Eq. 5.11), which is irrelevant to the conclusions drawn about plasticity. A stability analysis has not been performed, however. This is understandable as long as the system is stable and, even if done, it could not unveil a decrease of the degree of stability as consequence of plasticity, as seen above. Naturally, the authors imposed a fitness cost explicitly, so that the resulting critical rate of environmental change is a non-monotonic function of the plastic effect, with the analysis focused on the role of the different parameters on the persistence of the population.

5.6.2 Alternative case II: constant plasticity

One more case is addressed, which happens to be the most simple one, that of a fixed amount of plasticity regardless the genetic component of the phenotype,

$$Z_t = A_t + b \quad . \tag{5.154}$$

The parameter b is no longer dimensionless but defines the exact measure of development in phenotypic units. Similarly to the first alternative case, this kind of transformation is unable to alter the variance of a normal variable,

$$\sigma_t^2 = \gamma_t^2 \quad , \tag{5.155}$$

thus no rescaling of mutation effects is needed, while it makes the mean phenotypic value to differ from its genetic component by the additive constant b,

$$\mu_t = \nu_t + b \quad , \tag{5.156}$$

Notwithstanding, no consequences are observed in the equation of motion for the mean value,

$$\mu_{0,t+1} = \nu_{M,t} + b \tag{5.157}$$

$$= \nu_{S,0} + b \tag{5.158}$$

$$= \mu_{S,0} \quad , \tag{5.159}$$

as well as on the lag,

$$\Delta_{0,t+1} = \theta_{t+1} - \mu_{0,t+1} \tag{5.160}$$
$$= (\theta_t + B) - \mu_{S,0} \tag{5.161}$$
$$= B + \Delta_{S,t} \quad . \tag{5.162}$$

The conclusion is that the rescaling of the rate of environmental change is also lost and the effects of a fixed amount of plasticity in viability are proven to be completely unnoticed, at least under sustained environmental change.

This feature is specially interesting as one notices that the individual advantages of plasticity are solid for an arbitrary generation. The expression of the individual selective advantage is totally equivalent to that of the previous case of plasticity linear to the optimum with the exception that the parameter b occupies the role of $b\theta_t$ (see Eq. 5.137),

$$1 - s_t = \exp\left\{-\frac{1}{2}\frac{b}{\omega^2}\left[2\left(\theta_t - A_{0,t}\right) - b\right]\right\} \quad , \tag{5.163}$$

and, accordingly, it confers benefits as long as the distance from the genetic component of the phenotype to the optimum does not exceed $b/2$. Notice that the selective advantage given above would result in exactly the same plot of Fig. 44, once θ_t measured in units of the width of selection, making the equivalence absolute. Given this identity, added to the fact that the unidirectional dynamics of the optimum should favor, in principle, a unidirectional development, we would expect an advantage for plasticity, but

$$\overline{s}_* = 0 \quad . \tag{5.164}$$

Once the stationary state has been achieved, parents and offspring are always subject to the same environmental stress at the selection stage while displaying the same development as usual. All phenotypic evolution comes from the genes,

$$\nu_{0,t+1} - \nu_{0,t} = (\mu_{0,t+1} - b) - (\mu_{0,t} - b) \tag{5.165}$$
$$= B - (\Delta_{0,t+1} - \Delta_{0,t}) \tag{5.166}$$
$$(\nu_{0,t+1} - \nu_{0,t})_* = B \quad . \tag{5.167}$$

The only difference relative to a scenario without plasticity is observed on the genetic component of the mean, which stands b phenotypic units behind the value expected in the absence of plastic effects.

$$\epsilon_{0,t} = \Delta_{0,t} + b \tag{5.168}$$
$$\epsilon_{0,*} = \Delta_{0,*} + b \quad . \tag{5.169}$$

Furthermore, stability is not affected by the addition of a fixed amount of plasticity, either directly,

$$\frac{d\sigma^2_{M,0}}{d\gamma^2_{M,0}} = 1 \tag{5.170}$$

$$= \left(\frac{d\gamma^2_{S,0}}{d\sigma^2_{S,0}}\right)^{-1} \quad , \tag{5.171}$$

$$\frac{d\Delta_{M,0}}{d\epsilon_{M,0}} = 1 \tag{5.172}$$

$$= \left(\frac{d\epsilon_{S,0}}{d\Delta_{S,0}}\right)^{-1} \quad , \tag{5.173}$$

or indirectly (no rescaling of the mutation effect).

5.7 OTHER FIXED POINTS OR ORBITS?

Figure 46 – p-th composition of the phenotypic variance map σ^2_{t+p} for different periods p and scaled squared magnitude of the mutation effect set at $\delta^2 = 0.1\omega^2$. The map corresponds to the most simple form of the life-cycle (Eq. 5.23) for simplicity, since the qualitative behavior is preserved for arbitrary values of heritability h^2 and magnitude of plasticity b.

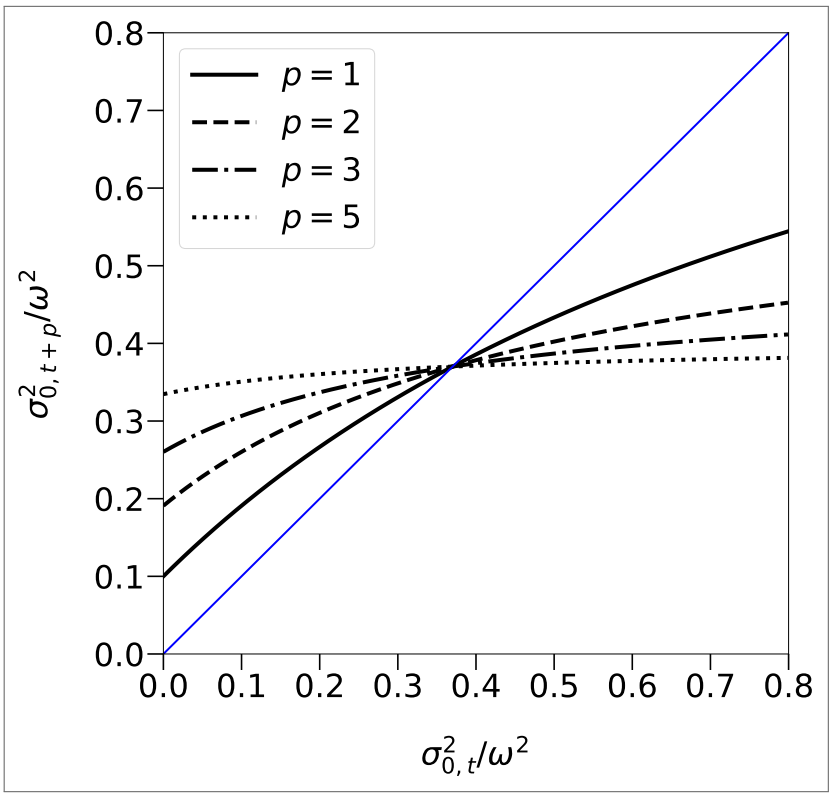

Source: Prepared by the author (2024)

This section is devoted to the proofs of two important properties on the two-dimensional map of phenotypic cumulants (Eqs. 6.44 and 6.50) derived from the most general form of the life cycle defined in Eq. 5.21. These are:

1. The fixed point established in Eqs. 5.62 and 5.68 is unique.

2. There are no superior orbits.

The first statement follows directly from Eq. 5.72: given that the value of the derivative of the variance map (Eq. 5.61) belongs to the interval

$$0 < \frac{d\sigma^2_{0,t+1}}{d\sigma^2_{0,t}} < 1, \quad \sigma^2_{0,t} \in [0, \infty) \quad , \tag{5.174}$$

in the entire domain, the map must cross the bisector axis exactly once (see Fig. 46). For a given value of the stationary variance, in turn, there is always a unique value of stationary lag.

Figure 47 – p-th composition of the lag map for different periods p and stationary variance of $\sigma^2_{0,*} = 0.5\omega^2$. The map corresponds to the most simple form of the life-cycle (Eq. 5.23) for simplicity, since the qualitative behavior is preserved for arbitrary values of heritability h^2 and magnitude of plasticity b.

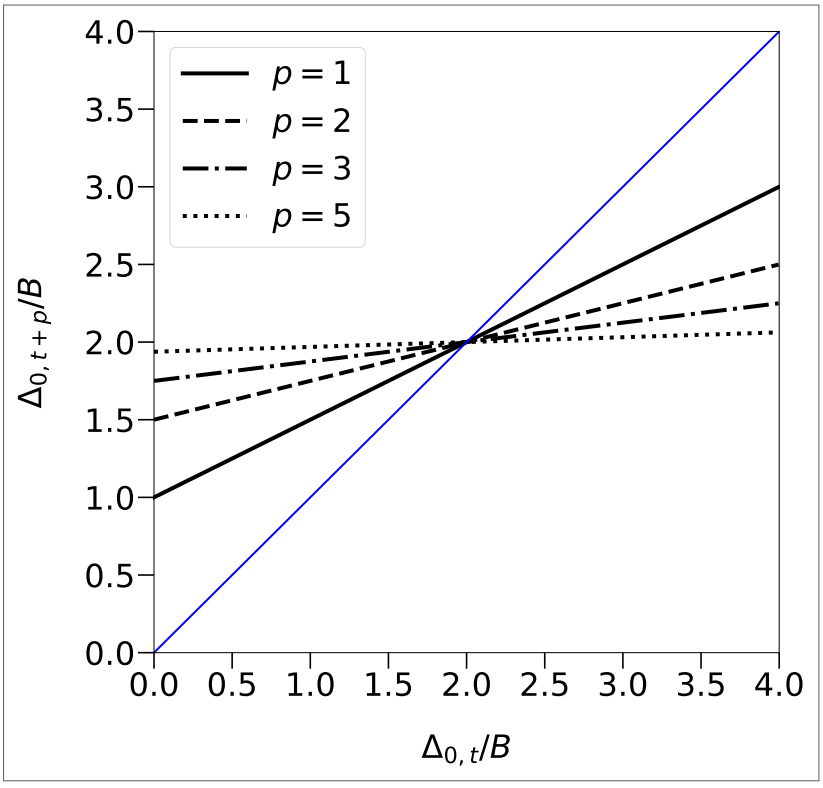

Source: Prepared by the author (2024)

Regarding the second statement, the approach is virtually the same: non-trivial superior orbits of period p exist if and only if the fixed point of the p-th composition of the map is not unique. Being a product of the derivative of the variance map evaluated at distinct points of

the same domain,

$$\frac{d\sigma^2_{0,t+p}}{d\sigma^2_{0,t}} = \prod_{l=0}^{p-1} \frac{d\sigma^2_{0,t+1}}{d\sigma^2_{0,t}} \left(\sigma^2_{0,t+l}\right) \quad , \tag{5.175}$$

the derivative of the p-th composition is clearly constrained to the interval

$$0 < \frac{d\sigma^2_{0,t+p}}{d\sigma^2_{0,t}} < 1, \quad \sigma^2_{0,t} \in [0, \infty) \quad , \tag{5.176}$$

as well, and the previous reasoning applies promptly The extension to the two-dimensional map is trivial since the lag map and any composition of it are linear (see Fig. 47). An alternative analytical confirmation is also possible as an explicit expression of the p-th composition of the lag map is obtained by induction,

$$\Delta_{0,t+p} = B \sum_{t=0}^{p-1} \prod_{l=t}^{p-1} \left(\frac{\omega^2}{\omega^2 + \sigma^2_{t+l}} \right) + \Delta_{0,t} \prod_{l=0}^{p-1} \left(\frac{\omega^2}{\omega^2 + \sigma^2_{t+l}} \right) \quad , \tag{5.177}$$

from which the uniqueness of the fixed point of Eq. 5.68 can be readily verified. Notice that the rescalings owe to plasticity can not affect these proofs and this is the reason why the formulas relative to the form of the life cycle in Eq. 5.55 have been correctly used for the general case.

6 APPENDIX

6.1 GENERAL PROCESS

The general case of the random variable mapping of Eq. 5.21 defining a complete species life cycle is thoroughly developed in this appendix. As mentioned in Sec. 5.2.5, departing from a normally distributed zygotic character, each consecutive stage of this process represents a normal random variable as well, conferring to Eq. 5.22 the status of *ansatz* rather than hypothesis. Hereafter, the stage are addressed in their order of occurrence and 4 informations are provided for each:

1. Why this transformation results in a Gaussian variable.
2. Phenotypic variance σ^2 (denoted by γ^2 when associated to the genetic component).
3. Phenotypic mean μ (denoted by ν when associated to the genetic component).
4. Phenotypic lag Δ (denoted by ϵ when associated to the genetic component).

6.2 SELECTED PHENOTYPE: $Z_{S,t} = S_t(Z_{0,t})$

A normally distributed character subjected to Gaussian selection (Eq. 5.1) results in a distribution of the selected character (Eq. 5.3) which is proportional to

$$p_{0,t}(z)W_t(z) = \frac{W_{max}}{\sigma_{0,t}\sqrt{2\pi}} \exp\left\{-\frac{1}{2}\left[\left(\frac{z-\mu_{0,t}}{\sigma_{0,t}}\right)^2 + \left(\frac{z-\theta_t}{\omega}\right)^2\right]\right\} \quad , \tag{6.1}$$

where the mean fitness (Eq. 5.4) fits the role of the normalizing constant. The convolution of two normal distributions must be a normal distribution as well. Through the completing the square method, the exponent may be shown to satisfy

$$\left(\frac{z-\mu_{0,t}}{\sigma_{0,t}}\right)^2 + \left(\frac{z-\theta_t}{\omega}\right)^2 = \left(\frac{\omega^2\sigma_{0,t}^2}{\omega^2+\sigma_{0,t}^2}\right)^{-1}\left[z - \left(\frac{\omega^2\mu_{0,t}+\sigma_{0,t}^2\theta_t}{\omega^2+\sigma_{0,t}^2}\right)\right]^2 \tag{6.2}$$

$$+ \frac{(\theta-\mu_{0,t})^2}{\omega^2+\sigma_{0,t}^2} \quad , \tag{6.3}$$

from which variance and mean stand out as,

$$\sigma_{S,t}^2 = \frac{\omega^2\sigma_{0,t}^2}{\omega^2+\sigma_{0,t}^2} \quad , \tag{6.4}$$

and

$$\mu_{S,t} = \frac{\omega^2\mu_{0,t}+\sigma_{0,t}^2\,\theta_t}{\omega^2+\sigma_{0,t}^2} \quad , \tag{6.5}$$

respectively. Lag follows directly,

$$\Delta_{S,t} = \theta_t - \mu_{S,t} \tag{6.6}$$

$$= \left(\frac{\omega^2}{\omega^2 + \sigma_{0,t}^2}\right) \Delta_{0,t} \quad . \tag{6.7}$$

6.3 GENETIC COMPONENT OF THE SELECTED PHENOTYPE: $A_{S,t} = P_t^{-1}(Z_{S,t})$

The plasticity function (Eq. 5.7), as its inverse (Eq. 5.9), are linear operations. Maintaining normality is an immediate property of linearity. The rescaling involved becomes obvious by appropriately introducing and rearranging mean and variance of the original variable as to convert it to the standard normal distribution:

$$\frac{Z_{S,t} - \mu_{S,t}}{\sigma_{S,t}} = \left(\frac{\sigma_{S,t}}{1-b}\right)^{-1} \left[A_{S,t} - \left(\frac{\mu_{S,t} - b\theta_t}{1-b}\right)\right] \quad . \tag{6.8}$$

Variance and mean are clearly given by

$$\gamma_{S,t}^2 = \frac{\sigma_{S,t}^2}{(1-b)^2} \tag{6.9}$$

$$= \frac{\omega^2 \sigma_{0,t}^2}{(1-b)^2(\omega^2 + \sigma_{0,t}^2)} \quad , \tag{6.10}$$

and

$$\nu_{S,t} = \frac{\mu_{S,t} - b\theta_t}{1-b} \tag{6.11}$$

$$= \frac{\omega^2 \mu_{0,t} + \left[-b\omega^2 + (1-b)\sigma_{0,t}^2\right] \theta_t}{(1-b)(\omega^2 + \sigma_{0,t}^2)} \quad , \tag{6.12}$$

while lag reads

$$\epsilon_{S,t} = \theta_t - \nu_{S,t} \tag{6.13}$$

$$= \frac{1}{1-b} \left(\frac{\omega^2}{\omega^2 + \sigma_{0,t}^2}\right) \Delta_{0,t} \quad . \tag{6.14}$$

6.4 GENETIC COMPONENT OF THE INHERITED PHENOTYPE: $A_{H,t} = H_t(A_{S,t})$

The heritability function (Eq. 5.12) is also an affine transformation. Notice that the convolution associating $Z_{S,t}$ and $Z_{0,t}$ (Eq. 5.3) constitutes a linear operation as well, a property

which extends to their genetic components $A_{S,t}$ and $A_{0,t}$ due to the linearity of plasticity:

$$\frac{Z_{0,t}-\mu_{0,t}}{\sigma_{0,t}} = \frac{Z_{S,t}-\mu_{S,t}}{\sigma_{S,t}} \tag{6.15}$$

$$\frac{[(1-b)A_{0,t}+b\theta_t]-\mu_{0,t}}{\sigma_{0,t}} = \frac{[(1-b)A_{S,t}+b\theta_t]-\mu_{S,t}}{\sigma_{S,t}} \tag{6.16}$$

$$\sigma_{0,t}^{-1}\left[A_{0,t}-\left(\frac{\mu_{0,t}-b\theta_t}{1-b}\right)\right] = \sigma_{S,t}^{-1}\left[A_{S,t}-\left(\frac{\mu_{S,t}-b\theta_t}{1-b}\right)\right] \tag{6.17}$$

$$\frac{A_{0,t}-\nu_{0,t}}{\gamma_{0,t}} = \frac{A_{S,t}-\nu_{S,t}}{\gamma_{S,t}} \quad . \tag{6.18}$$

This time, the suitable rescaling comes from

$$A_{H,t}-A_{0,t} = h^2(A_{S,t}-A_{0,t}) \tag{6.19}$$

$$A_{H,t} = h^2 A_{S,t}+(1-h^2)A_{0,t} \tag{6.20}$$

$$= h^2\left[\nu_{S,t}+\frac{\gamma_{S,t}}{\gamma_{0,t}}(A_{0,t}-\nu_{0,t})\right]+(1-h^2)A_{0,t} \tag{6.21}$$

$$= h^2\left(\nu_{S,t}+\frac{\gamma_{S,t}}{\gamma_{0,t}}\nu_{0,t}\right)+\left[1-h^2\left(1-\frac{\gamma_{S,t}}{\gamma_{0,t}}\right)\right]A_{0,t} \tag{6.22}$$

$$A_{0,t} = \frac{1}{1-h^2\left(1-\frac{\gamma_{S,t}}{\gamma_{0,t}}\right)}\left[A_{H,t}-h^2\left(\nu_{S,t}-\frac{\gamma_{S,t}}{\gamma_{0,t}}\nu_{0,t}\right)\right] \tag{6.23}$$

$$\frac{A_{0,t}-\nu_{0,t}}{\gamma_{0,t}} = \frac{1}{h^2\gamma_{S,t}+(1-h^2)\gamma_{0,t}}\{A_{H,t}-[h^2\nu_{S,t}+(1-h^2)\nu_{0,t}]\} \quad . \tag{6.24}$$

The relationship between variances is most simply expressed in terms of the standard deviations at this stage,

$$\gamma_{H,t} = h^2\gamma_{S,t}+(1-h^2)\gamma_{0,t} \tag{6.25}$$

$$= \frac{h^2\omega\sigma_{0,t}}{(1-b)\sqrt{\omega^2+(\sigma_{0,t})^2}}+\frac{(1-h^2)\sigma_{0,t}}{1-b} \tag{6.26}$$

$$= \frac{\sigma_{0,t}}{1-b}\left[\frac{h^2\omega}{\sqrt{\omega^2+\sigma_{0,t}^2}}+(1-h^2)\right] \quad . \tag{6.27}$$

Mean and lag worth

$$\nu_{H,t} = h^2\nu_{S,t}+(1-h^2)\nu_{0,t} \tag{6.28}$$

$$= \frac{h^2\left\{\omega^2\mu_{0,t}+\left[-b\omega^2+(1-b)\sigma_{0,t}^2\right]\theta_t\right\}}{(1-b)(\omega^2+\sigma_{0,t}^2)}+\frac{(1-h^2)(\mu_{0,t}-b\theta_t)}{1-b} \tag{6.29}$$

$$= \frac{\left[\omega^2+(1-h^2)\sigma_{0,t}^2\right]\mu_{0,t}+\left[-b\omega^2+(h^2-b)\sigma_{0,t}^2\right]\theta_t}{(1-b)(\omega^2+\sigma_{0,t}^2)} \quad , \tag{6.30}$$

and

$$\epsilon_{H,t} = \theta_t-\nu_{H,t} \tag{6.31}$$

$$= \frac{1}{1-b}\left[\frac{\omega^2+(1-h^2)\sigma_{0,t}^2}{\omega^2+\sigma_{0,t}^2}\right]\Delta_{0,t} \quad , \tag{6.32}$$

respectively.

6.5 GENETIC COMPONENT OF THE MUTATED PHENOTYPE: $A_{M,t} = M(A_{H,t})$

When applied to a normal distribution,

$$p_{M,t}(a) = \int_{-\infty}^{\infty} da' \left\{ \frac{1}{\gamma_{H,t}\sqrt{2\pi}} \exp\left[-\frac{1}{2} \left(\frac{a' - \nu_{H,t}}{\gamma_{H,t}} \right)^2 \right] \right\} \left\{ \frac{1}{\delta\sqrt{2\pi}} \exp\left[-\frac{1}{2} \left(\frac{a - a'}{\delta} \right)^2 \right] \right\} \tag{6.33}$$

$$= \int_{-\infty}^{\infty} da' \, \frac{1}{\gamma_{H,t}\sqrt{2\pi}} \exp\left[-\frac{1}{2} \left(\frac{a' - \nu_{H,t}}{\gamma_{H,t}} \right)^2 \right] \int_{-\infty}^{\infty} da'' \, \frac{1}{\delta\sqrt{2\pi}} \exp\left[-\frac{1}{2} \left(\frac{a''}{\delta} \right)^2 \right] \tag{6.34}$$

$$\delta(a - a' - a'') \quad , \tag{6.35}$$

(notice that the last δ corresponds to the Dirac delta function and not to the magnitude of the mutation effect) the Gaussian mutation procedure defined in Eq. 5.14 is equivalent to the addition of an independent normally distributed random variable of null mean and variance of δ^2,

$$A_{M,t} = A_{H,t} + \mathcal{N}(0, \delta) \quad , \tag{6.36}$$

also resulting in an normal variable whose variance is increased by an amount of δ^2,

$$\gamma_{M,t}^2 = \gamma_{H,t}^2 + \delta^2 \tag{6.37}$$

$$= \frac{\sigma_{0,t}^2}{(1-b)^2} \left[\frac{h^2\omega}{\sqrt{\omega^2 + \sigma_{0,t}^2}} + (1 - h^2) \right]^2 + \delta^2 \quad , \tag{6.38}$$

same mean value,

$$\nu_{M,t} = \nu_{H,t} \quad . \tag{6.39}$$

and same lag,

$$\epsilon_{M,t} = \theta_t - \nu_{M,t} \tag{6.40}$$

$$= \epsilon_{H,t} \quad , \tag{6.41}$$

evidently.

6.6 OFFSPRING PHENOTYPE: $Z_{0,t+1} = P_{t+1}(A_{M,t})$

The pertinent rescaling in the case of the direct plasticity function is

$$\frac{A_{M,t} - \nu_{M,t}}{\gamma_{M,t}} = \frac{Z_{0,t+1} - [(1-b)\nu_{M,t} + b\theta_{t+1}]}{(1-b)\gamma_{M,t}} \quad . \tag{6.42}$$

Variance:

$$\sigma_{0,t+1}^2 = (1-b)^2\gamma_{M,t}^2 \tag{6.43}$$

$$= \sigma_{0,t}^2 \left[\frac{h^2\omega}{\sqrt{\omega^2+\sigma_{0,t}^2}} + (1-h^2)\right]^2 + (1-b)^2\delta^2 \quad . \tag{6.44}$$

Mean:

$$\mu_{0,t+1} = (1-b)\nu_{M,t} + b\theta_{t+1} \tag{6.45}$$

$$= \frac{\left[\omega^2 + (1-h^2)\sigma_{0,t}^2\right]\mu_{0,t} + \left[-b\omega^2 + (h^2-b)\sigma_{0,t}^2\right]\theta_t}{\omega^2+\sigma_{0,t}^2} + b(\theta_t + B) \tag{6.46}$$

$$= \frac{\left[\omega^2 + (1-h^2)\sigma_{0,t}^2\right]\mu_{0,t} + h^2\sigma_{0,t}^2\theta_t}{\omega^2+\sigma_{0,t}^2} + bB \quad . \tag{6.47}$$

Lag:

$$\Delta_{0,t+1} = \theta_{t+1} - \mu_{0,t+1} \tag{6.48}$$

$$= B + \theta_t - \frac{\left[\omega^2 + (1-h^2)\sigma_{0,t}^2\right]\mu_{0,t} + h^2\sigma_{0,t}^2\theta_t}{\omega^2+\sigma_{0,t}^2} - bB \tag{6.49}$$

$$= (1-b)B + \left[\frac{\omega^2 + (1-h^2)\sigma_{0,t}^2}{\omega^2+\sigma_{0,t}^2}\right]\Delta_{0,t} \quad . \tag{6.50}$$

7 CONCLUSIONS

In the last years, we have considerably enhanced our understanding of adaptation in constant and stable environments, both theoretically and empirically (BLEUVEN; LANDRY, 2016; GOOD et al., 2017; COOPER, 2018). However, an understanding of how environmental changes can affect adaptation remains challenging. Environmental variation triggers organisms' responses, which may improve their fitness by modifying their traits. Phenotypic plasticity, the ability of an organism to express different phenotypes from the same genome in response to stimuli or inputs from the environment, is an important mechanism of adaptation, being ubiquitous (AGRAWAL, 2001; OOSTRA et al., 2018). Alternatively, evolutionary adaptation shaped by natural selection acting on genetic variation can also account for such responses (SHIMADA; ISHII; SHIBAO, 2010; BOYER; HÉRISSANT; SHERLOCK, 2021).

Our present study aimed a better characterization of the dynamics of the evolution of populations under a scenario of environmental variation. It is important to emphasize that as opposed to the environmental dynamics used in the work of BOYER; HÉRISSANT; SHERLOCK, in our formulation of Chapter 3, the switching between the two ecological conditions ensues from a series of short-lived states. In particular, we look for quantification of the adaptive process itself by measuring not only the degree of repeatability of outcomes but also evolutionary trajectories. Using an adaptive walk approximation, expected to hold in a scenario of strong-selection weak-mutation, we have shown that the rate of environmental variation influences the number of substitutions that occur during adaptive walks to a locally optimal genotype. In general, slowly changing environments lead to a greater number of substitutions.

According to our simulation results, abrupt environmental variations lead to more unpredictable outcomes. The increase of the predictability with the transient time τ can be understood as a drastic reduction of accessibility of some of the locally optimal genotypes. The rise of predictability with τ is notably steeper when the timescale of ecological variation surpasses that of the timescale of adaptation. The results reveal the role of the dynamics of environmental changes in shaping the attraction basin of the locally optimal genotypes. This occurs concomitantly with the constraint of the evolutionary paths towards those local optima of the fitness landscape, as clearly established by measures of the predictability with respect to the evolutionary pathways and mean path divergence.

In Chapter 4, the two main premises of our modeling are the existence of an underlying mechanism of gene regulation that allows the population to promptly respond to environmental variation and the occurrence of epistatic interactions among genes. As different sets of genes are directly selected at each phase, gene regulation naturally leads to some degree of neutrality, causing the fitness landscape to be smoother. The degree of neutrality depends on the amount of epistasis; the larger the K, the smaller the correlation among one-mutant neighbors. In the absence of epistasis, the gene subsets not directly under selection will solely be driven by genetic drift. The misalignment of the subsets over the periods at which they are not directly

selected explains the abrupt drops in fitness when a phase switch takes place.

As observed by (TRUBENOVA et al., 2019), the amplitude of the oscillations gets larger when the length of the seasons is extended. This result is independent of the topography of the fitness landscape. Another interesting feature, not previously shown, but made possible in our finite population approach, is that the demography plays a role in oscillation. We show that larger populations result in larger fluctuations. The effect of population size is twofold: first, larger populations allow them to reach higher fitness peaks but at the same time lead to more profound valleys of the fitness landscape at the moment a phase switch occurs. In principle, larger populations get more easily trapped in local optima of the fitness landscape as evolution is expected to be more deterministic, but at the same time, they generate more beneficial mutations per generation, while smaller populations follow more erratic evolutionary paths, thus increasing their potential to reach higher fitness peaks HANDEL; ROZEN. The latter effect seems to be the dominating mechanism, mainly because the population suddenly becomes maladapted at the phase change. The abundant supply of beneficial mutations at the earlier stages of each phase creates a favorable scenario and provides alternative routes to find higher fitness peaks. This observation becomes even more pronounced with the amount of epistasis K, especially as the number of distinct phases increases.

We observe a strong influence of the oscillations on the amount of epistasis K and the number of phases N_P. The rise of both quantities results in more significant oscillations. While the change of N_P does not affect the efficacy of the search for fitness peaks, it has a profound effect on the fitness drop at the phase change. For fixed genome size N, by making N_P greater, we increase the influence of loci outside a given subset $\Gamma(P)$ on fitness. So when the subset $\Gamma(P)$ is not being directly selected, the likelihood that those loci find themselves in a less favorable configuration grows. In turn, the rise of K has a more profound effect on the evolutionary dynamics, as it lowers both the maximum and the minimum fitness levels achieved by the population. The epistasis has a critical role in the dynamics as its enhancement constrains the population to even smaller domains of the fitness landscape. This outcome is clearly shown in Fig. 18, where we see that $h_{amp}(G_{MA,\Gamma}, G_{GO,\Gamma})$, the variation of the Hamming distance to the suboptimal configuration of each subset $\Gamma(P)$, narrows with K, i.e., a large amount of the loci freeze out the genotype. Despite small changes at the genotypic level, the increase of K precipitates bigger fitness gaps as the phase change occurs. This can be explained in part because the larger the K, the smaller the correlation of fitness effects among first mutant neighbors. As shown in Fig 17, in which for $K = 8$ the minimum fitness approaches 0.5, corresponding to the average fitness value. At the same time, the population seems to evolve to increase its evolvability at the phase changes despite little genetic variation, thus mitigating the effect of frustration inflicted by epistasis. The evidence that larger K entails the exploration of a smaller domain of the fitness landscape is reflected in the drop of the entropy S_{path} with K, as exhibited in Fig. 20-B.

Our analysis of entropy is concerned with the distribution of ending points at the end of

each phase, i.e., it is closely related to the distribution of fitness peaks found by the population at a genotypic level. The entropy is influenced by both dynamics of environmental changes and demography. Looking at the distribution of ending points within a given evolutionary path, the entropy analysis reveals that N_P and K display opposite effects. While S_{path} grows with N_P, mainly because of increased levels of neutrality that allow the population to more likely drift over the landscape, the epistasis K confines the population to smaller domains increasing the repeatability of the ending points.

Finally, we discuss the findings and perspectives of Chapter 5. The hypotheses on the agents of selection and mutation are quite conservative. Eqs. 5.3, 5.1 and 5.14 define what is known as Gaussian selection and mutation and have been widely explored in the investigation of the mutation-selection balance. In the particular case of non-overlapping generations and a single trait, LYNCH; GABRIEL set the formulas for the change of the phenotypic mean and variance, Eqs. 5.25 and 5.24, between parents and prole for a maladapted population, as well as the mean population fitness, Eq. 5.45. Since the change in the variance does not depend on the value of the optimum phenotype but only on the strength of selection and its value, LYNCH; GABRIEL were also able to determine the stationary variance (Eq. 5.26) achieved after repeated rounds of selection, regardless the trajectory of the optimal phenotype during this period.

Development has already been explored by CHEVIN; LANDE; MACE in the context of sustained environmental change. Departing from the same stationary lag of Eq. 5.31 and assuming a fitness cost due to plasticity in the form of a multiplicative factor that increases with the plasticity b, they have found an optimal magnitude for the plasticity that maximizes the critical rate of environmental change tolerated by a population. Without any fitness cost associated with plasticity, the critical rate of environmental change would grow indefinitely with the amount of plasticity allowed. A stability analysis, on the other hand, was not carried out by CHEVIN; LANDE; MACE, which is understandable given it could not unveil the inherent harmful effect of plasticity to stability as long as the phenotypic variance was taken as a constant. From Eqs. 5.72 and 5.75, it is clear that the dependence of the stability coefficients on b is wholly confined to that present in the stationary standard deviation $\sigma_{0,*}$. Furthermore, the type of plasticity investigated by CHEVIN; LANDE; MACE is linear in the absolute value of the optimum (see Eq. 5.131) and not in the lag as we propose (see Eq. 5.7). In their scenario, only one of the rescalings, Eq. 5.78, namely $B \to (1-b)B$, comes up. In the absence of the rescaling of the mutation rate, the stability coefficients do not depend on the plastic effect. Such difference in the type of plasticity assumed also hides the effect of plasticity on stability and makes their case more stable. When confronting the validity of each hypothesis, there is a crucial difference. A plastic effect proportional to the optimum, as in CHEVIN; LANDE; MACE (CHEVIN; LANDE; MACE, 2010), incurs an endless accumulation of the plastic effect, given by $b\theta_t$ at generation t, which sounds especially inconsistent in the case of sustained environmental change. Our choice, plasticity linear in the lag, seems far more reasonable as the phenotypic

evolution per generation is completely genetic in the stationary state, equaling the rate of environmental change B.

Rather than a pure mathematical feature, the direct relation between the stability and the time to recover from a disturbance has profound biological consequences in this context. Mathematically, our model of the infinite-size population directly addresses one of the two paradigms of the conservation problem, the declining population (CAUGHLEY, 1994). The small population paradigm, on the other hand, is indirectly connected with the stability issue. Disturbances in real populations induce demographic costs (bottlenecks) and, in particular, depletion of genetic variation, which enhances genetic drift as an evolutionary driving force compared to natural selection. In sum, the selective benefits of an increasing magnitude of plasticity are opposed by the amplification of the stochastic forces threatening the population's viability (LANDE; BARROWCLOUGH, 1987; LANDE, 1995; LACY, 1997; BOOY et al., 2000; FLATHER et al., 2011).

Concerning its generality and perspective, as already mentioned, proposing a map between random variables constitutes a technical innovation. Nonetheless, as carried out here, the development through cumulants is not characteristic of the technique. The analytical formulation developed here was possible only due to our particular choices for each operation in the life cycle. We have dealt with a two-dimensional map, and this is so only because the first two cumulants can perfectly describe the normal distribution. The normal distribution occurs, in turn, because this is the unique distribution that could fit the stationary state of the operational life cycle in Eq. 5.21, i.e., proposition 5.22 represents an ansatz rather than an assumption. In sum, the analytical approach presented here depends first on the recognition of the distribution of the stationary state and, secondly, the possibility of describing it in a finite number of moments. Since these conditions are not expected to hold commonly, exploring new forms for the operations represents a current limitation of the model. Overcoming such restrictions would allow questions of impressive generality to be pursued, especially concerning the identification of features common to stable systems. Identifying systems with superior orbits and even chaos would be equally enjoyable, while in the present one, it may be proved that the period one orbit is unique (SMART, 1980).

REFERENCES

ACASUSO-RIVERO, C.; MURREN, C. J.; SCHLICHTING, C. D.; STEINER, U. K. Adaptive phenotypic plasticity for life-history and less fitness-related traits. *Proceedings of the Royal Society B*, The Royal Society, v. 286, n. 1904, p. 20190653, 2019.

AGRAWAL, A. A. Phenotypic plasticity in the interactions and evolution of species. *Science*, American Association for the Advancement of Science, v. 294, n. 5541, p. 321–326, 2001.

AGUIRRE, J.; CATALÁN, P.; CUESTA, J. A.; MANRUBIA, S. On the networked architecture of genotype spaces and its critical effects on molecular evolution. *Open biology*, The Royal Society, v. 8, n. 7, p. 180069, 2018.

AMICONE, M.; GORDO, I. Molecular signatures of resource competition: Clonal interference favors ecological diversification and can lead to incipient speciation. *Evolution*, Wiley Online Library, v. 75, n. 11, p. 2641–2657, 2021.

BARRETT, R.; SCHLUTER, D. Adaptation from standing genetic variation. *Trends in ecology & evolution*, Elsevier, v. 23, n. 1, p. 38–44, 2008. Https://doi.org/10.1016/j.tree.2007.09.008.

BARTON, N.; TURELLI, M. Evolutionary quantitative genetics: how little do we know? *Annual review of genetics*, Annual Reviews 4139 El Camino Way, PO Box 10139, Palo Alto, CA 94303-0139, USA, v. 23, n. 1, p. 337–370, 1989. Https://doi.org/10.1146/annurev.ge.23.120189.002005.

BENNETT, K. D. Milankovitch cycles and their effects on species in ecological and evolutionary time. *Paleobiology*, Cambridge University Press, v. 16, n. 1, p. 11–21, 1990.

BERGER, A. The milankovitch astronomical theory of paleoclimates: a modern review. *Vistas in Astronomy*, Elsevier, v. 24, p. 103–122, 1980.

BITTER, M.; KAPSENBERG, L.; GATTUSO, J.-P.; PFISTER, C. Standing genetic variation fuels rapid adaptation to ocean acidification. *Nature communications*, Nature Publishing Group UK London, v. 10, n. 1, p. 5821, 2019. Https://doi.org/10.1038/s41467-019-13767-1.

BLANQUART, F.; ACHAZ, G.; BATAILLON, T.; TENAILLON, O. Properties of selected mutations and genotypic landscapes under fisher's geometric model. *Evolution*, Wiley Online Library, v. 68, n. 12, p. 3537–3554, 2014.

BLEUVEN, C.; LANDRY, C. R. Molecular and cellular bases of adaptation to a changing environment in microorganisms. *Proceedings of the Royal Society B: Biological Sciences*, The Royal Society, v. 283, n. 1841, p. 20161458, 2016.

BOOY, G.; HENDRIKS, R.; SMULDERS, M.; GROENENDAEL, J. V.; VOSMAN, B. Genetic diversity and the survival of populations. *Plant biology*, Georg Thieme Verlag Stuttgart, v. 2, n. 4, p. 379–395, 2000. Https://doi.org/10.1055/s-2000-5958.

BOTTA, F.; DAHL-JENSEN, D.; RAHBEK, C.; SVENSSON, A.; NOGUÉS-BRAVO, D. Abrupt change in climate and biotic systems. *Current Biology*, Elsevier, v. 29, n. 19, p. R1045–R1054, 2019.

BOYER, S.; HÉRISSANT, L.; SHERLOCK, G. Adaptation is influenced by the complexity of environmental change during evolution in a dynamic environment. *PLoS Genetics*, Public Library of Science San Francisco, CA USA, v. 17, n. 1, p. e1009314, 2021.

BRADSHAW, A. The croonian lecture, 1991. genostasis and the limits to evolution. *Philosophical transactions of the royal society B: biological sciences*, The Royal Society London, v. 333, n. 1267, p. 289–305, 1991. Https://doi.org/10.1098/rstb.1991.0079.

BÜRGER, R.; LYNCH, M. Evolution and extinction in a changing environment: a quantitative-genetic analysis. *Evolution*, Wiley Online Library, v. 49, n. 1, p. 151–163, 1995.

CABALLERO, A.; TORO, M.; LOPEZ-FANJUL, C. The response to artificial selection from new mutations in drosophila melanogaster. *Genetics*, Oxford University Press, v. 128, n. 1, p. 89–102, 1991. Https://doi.org/10.1093/genetics/128.1.89.

CAMPOS, P. R.; ADAMI, C.; WILKE, C. O. Optimal adaptive performance and delocalization in nk fitness landscapes. *Physica A: Statistical Mechanics and its Applications*, Elsevier, v. 304, n. 3-4, p. 495–506, 2002.

CAMPOS, P. R.; MOREIRA, F. B. Adaptive walk on complex networks. *Physical Review E—Statistical, Nonlinear, and Soft Matter Physics*, APS, v. 71, n. 6, p. 061921, 2005.

CARLSON, S.; CUNNINGHAM, C.; WESTLEY, P. Evolutionary rescue in a changing world. *Trends in ecology & evolution*, Elsevier, v. 29, n. 9, p. 521–530, 2014. Https://doi.org/10.1016/j.tree.2014.06.005.

CAUGHLEY, G. Directions in conservation biology. *Journal of animal ecology*, JSTOR, p. 215–244, 1994.

CHABOYER, B. The age of the universe. *Physics reports*, Elsevier, v. 307, n. 1-4, p. 23–30, 1998. Https://doi.org/10.1016/S0370-1573(98)00054-4.

CHARLESWORTH, B. Directional selection and the evolution of sex and recombination. *Genetics research*, Cambridge University Press, v. 61, n. 3, p. 205–224, 1993. Https://doi.org/10.1017/S0016672300031372.

CHATTERJEE, K.; PAVLOGIANNIS, A.; ADLAM, B.; NOWAK, M. A. The time scale of evolutionary innovation. *PLoS computational biology*, Public Library of Science San Francisco, USA, v. 10, n. 9, p. e1003818, 2014.

CHEVIN, L.-M.; DECORZENT, G.; LENORMAND, T. Niche dimensionality and the genetics of ecological speciation. *Evolution*, Wiley Online Library, v. 68, n. 5, p. 1244–1256, 2014.

CHEVIN, L.-M.; LANDE, R.; MACE, G. Adaptation, plasticity, and extinction in a changing environment: towards a predictive theory. *PLoS biology*, Public Library of Science San Francisco, USA, v. 8, n. 4, p. e1000357, 2010. Https://doi.org/10.1371/journal.pbio.1000357.

CHU, X.; WANG, M.; FAN, Z.; LI, J.; YIN, H. Molecular mechanisms of seasonal gene expression in trees. *International Journal of Molecular Sciences*, MDPI, v. 25, n. 3, p. 1666, 2024.

CIRNE, D.; CAMPOS, P. R. Rate of environmental variation impacts the predictability in evolution. *Physical Review E*, APS, v. 106, n. 6, p. 064408, 2022.

CIRNE, D.; CAMPOS, P. R. A study about the evolutionary dynamics and repeatability in time-varying fitness landscapes. *Physica A: Statistical Mechanics and its Applications*, Elsevier, v. 585, p. 126453, 2022.

CIRNE, D.; CAMPOS, P. R. A discrete-time model of phenotypic evolution. *Applied Mathematics and Computation*, Elsevier, v. 476, p. 128781, 2024.

COLEGRAVE, N.; BUCKLING, A. Microbial experiments on adaptive landscapes. *Bioessays*, Wiley Online Library, v. 27, n. 11, p. 1167–1173, 2005.

COOPER, V. S. Experimental evolution as a high-throughput screen for genetic adaptations. *MSphere*, Am Soc Microbiol, v. 3, n. 3, p. e00121–18, 2018.

COUPER, L. I.; FARNER, J. E.; CALDWELL, J. M.; CHILDS, M. L.; HARRIS, M. J.; KIRK, D. G.; NOVA, N.; SHOCKET, M.; SKINNER, E. B.; URICCHIO, L. H. et al. How will mosquitoes adapt to climate warming? *Elife*, eLife Sciences Publications, Ltd, v. 10, p. e69630, 2021.

CRESSWELL, J. Stabilizing selection and the structural variability of flowers within species. *Annals of Botany*, Elsevier, v. 81, n. 4, p. 463–473, 1998.

CRONIN, T.; SCHNEIDER, C. Climatic influences on species: evidence from the fossil record. *Trends in ecology & evolution*, Elsevier, v. 5, n. 9, p. 275–279, 1990. Https://doi.org/10.1016/0169-5347(90)90080-W.

CROZIER, L.; HUTCHINGS, J. Plastic and evolutionary responses to climate change in fish. *Evolutionary applications*, Wiley Online Library, v. 7, n. 1, p. 68–87, 2014. Https://doi.org/10.1111/eva.12135.

DALRYMPLE, G. The age of the earth in the twentieth century: a problem (mostly) solved. *Geological society, London, special publications*, The Geological Society of London, v. 190, n. 1, p. 205–221, 2001. Https://doi.org/10.1144/GSL.SP.2001.190.01.1.

DEWITT, T.; SIH, A.; WILSON, D. Costs and limits of phenotypic plasticity. *Trends in ecology & evolution*, Elsevier, v. 13, n. 2, p. 77–81, 1998. Https://doi.org/10.1016/S0169-5347(97)01274-3.

DOBRETSOV, N.; KOLCHANOV, N.; SUSLOV, V. On important stages of geosphere and biosphere evolution. In: DOBRETSOV, N.; KOLCHANOV, N.; ROZANOV, A.; SUSLOV, V. (Ed.). *Biosphere origin and evolution*. [S.l.]: Springer, 2008. p. 3–23.

DOMINGO, E.; SCHUSTER, P. What is a quasispecies? historical origins and current scope. In: *Quasispecies: From Theory to Experimental Systems*. [S.l.]: Springer, 2015. p. 1–22.

DONELSON, J.; GAITAN-ESPITIA, J.; HOBDAY, A.; MOKANY, K.; ANDREW, S.; BOULTER, S.; COOK, C.; DICKSON, F.; MACGREGOR, N.; MITCHELL, N. et al. Putting plasticity into practice for effective conservation actions under climate change. *Nature Climate Change*, Nature Publishing Group UK London, v. 13, n. 7, p. 632–647, 2023.

DOPICO, X. C.; EVANGELOU, M.; FERREIRA, R. C.; GUO, H.; PEKALSKI, M. L.; SMYTH, D. J.; COOPER, N.; BURREN, O. S.; FULFORD, A. J.; HENNIG, B. J. et al. Widespread seasonal gene expression reveals annual differences in human immunity and physiology. *Nature communications*, Nature Publishing Group UK London, v. 6, n. 1, p. 7000, 2015.

DORN, L. A.; PYLE, E. H.; SCHMITT, J. Plasticity to light cues and resources in arabidopsis thaliana: testing for adaptive value and costs. *Evolution*, Wiley Online Library, v. 54, n. 6, p. 1982–1994, 2000.

DURRETT, R.; LIMIC, V. Rigorous results for the nk model. *Annals of probability*, JSTOR, p. 1713–1753, 2003.

DYKHUIZEN, D. E. Experimental evolution: replicating history. *Trends in ecology & evolution*, Elsevier Current Trends, v. 7, n. 8, p. 250–252, 1992.

EIGEN, M.; MCCASKILL, J.; SCHUSTER, P. The molecular quasi-species. *Advances in chemical physics*, v. 75, p. 149–263, 1989.

EISEN, E. Conclusions from long-term selection experiments with mice. *Zeitschrift fur tierzuchtung und zuchtungsbiologie*, v. 97, n. 4, p. 305–319, 1980. Https://doi.org/10.1111/j.1439-0388.1980.tb00937.x.

FALCONER, D. *Introduction to quantitative genetics*. New York: Longman, 1989.

FILHO, J. de L.; MOREIRA, F.; CAMPOS, P.; OLIVEIRA, V. M. D. Adaptive walks on correlated fitness landscapes with heterogeneous connectivities. *Journal of Statistical Mechanics: Theory and Experiment*, IOP Publishing, v. 2012, n. 02, p. P02014, 2012.

FISHER, R. The genetical theory of natural selection. 1958.

FLATHER, C.; HAYWARD, G.; BEISSINGER, S.; STEPHENS, P. Minimum viable populations: is there a 'magic number' for conservation practitioners? *Trends in ecology & evolution*, Elsevier, v. 26, n. 6, p. 307–316, 2011. Https://doi.org/10.1016/j.tree.2011.03.001.

FRAGATA, I.; BLANCKAERT, A.; LOURO, M. A. D.; LIBERLES, D. A.; BANK, C. Evolution in the light of fitness landscape theory. *Trends in ecology & evolution*, Elsevier, v. 34, n. 1, p. 69–82, 2019.

FRANKHAM, R. Genetics and extinction. *Biological conservation*, Elsevier, v. 126, n. 2, p. 131–140, 2005. Https://doi.org/10.1016/j.biocon.2005.05.002.

FRANKHAM, R. Conservation genetics. *Encyclopedia of Genetics*, Routledge, p. 910–914, 2014.

FREITAS, O.; ARAUJO, S. B.; CAMPOS, P. R. Speciation in a metapopulation model upon environmental changes. *Ecological Modelling*, Elsevier, v. 468, p. 109958, 2022.

FUDICKAR, A. M.; PETERSON, M. P.; GREIVES, T. J.; ATWELL, J. W.; BRIDGE, E. S.; KETTERSON, E. D. Differential gene expression in seasonal sympatry: mechanisms involved in diverging life histories. *Biology Letters*, The Royal Society, v. 12, n. 3, p. 20160069, 2016.

GANCO, M. Nk model as a representation of innovative search. *Research Policy*, Elsevier, v. 46, n. 10, p. 1783–1800, 2017.

GHALAMBOR, C. K.; MCKAY, J. K.; CARROLL, S. P.; REZNICK, D. N. Adaptive versus non-adaptive phenotypic plasticity and the potential for contemporary adaptation in new environments. *Functional ecology*, Wiley Online Library, v. 21, n. 3, p. 394–407, 2007.

GILMAN, R. T.; NUISMER, S. L.; JHWUENG, D.-C. Coevolution in multidimensional trait space favours escape from parasites and pathogens. *Nature*, Nature Publishing Group UK London, v. 483, n. 7389, p. 328–330, 2012.

GOLDINGER, A.; SHAKHBAZOV, K.; HENDERS, A. K.; MCRAE, A. F.; MONTGOMERY, G. W.; POWELL, J. E. Seasonal effects on gene expression. *PloS one*, Public Library of Science San Francisco, CA USA, v. 10, n. 5, p. e0126995, 2015.

GOMULKIEWICZ, R.; HOULE, D. Demographic and genetic constraints on evolution. *The american naturalist*, The University of Chicago Press, v. 174, n. 6, p. 218–229, 2009. Https://doi.org/10.1086/645086.

GOOD, B. H.; MCDONALD, M. J.; BARRICK, J. E.; LENSKI, R. E.; DESAI, M. M. The dynamics of molecular evolution over 60,000 generations. *Nature*, Nature Publishing Group, v. 551, n. 7678, p. 45–50, 2017.

GORDO, I.; CAMPOS, P. R. Evolution of clonal populations approaching a fitness peak. *Biology Letters*, The Royal Society, v. 9, n. 1, p. 20120239, 2013.

GOULD, S. J. *Wonderful Life: The Burgess Shale and the Nature of History*. [S.l.]: WW Norton & Company, 1989.

GRADSTEIN, F.; OGG, J.; SCHMITZ, M.; OGG, G. *The geologic time scale 2012*. [S.l.]: Elsevier, 2012.

GREENBURY, S. F.; LOUIS, A. A.; AHNERT, S. E. The structure of genotype-phenotype maps makes fitness landscapes navigable. *Nature Ecology & Evolution*, Nature Publishing Group UK London, v. 6, n. 11, p. 1742–1752, 2022.

GUO, W.; LAMPOUDI, S.; SHEA, J.-E. Temperature dependence of the free energy landscape of the src-sh3 protein domain. *Proteins: Structure, Function, and Bioinformatics*, Wiley Online Library, v. 55, n. 2, p. 395–406, 2004.

HALL, A. E.; KARKARE, K.; COOPER, V. S.; BANK, C.; COOPER, T. F.; MOORE, F. B.-G. Environment changes epistasis to alter trade-offs along alternative evolutionary paths. *Evolution*, Blackwell Publishing Inc Malden, USA, v. 73, n. 10, p. 2094–2105, 2019.

HANDEL, A.; ROZEN, D. E. The impact of population size on the evolution of asexual microbes on smooth versus rugged fitness landscapes. *BMC Evolutionary Biology*, BioMed Central, v. 9, n. 1, p. 1–10, 2009.

HARTL, D. L.; TAUBES, C. H. Compensatory nearly neutral mutations: selection without adaptation. *Journal of Theoretical Biology*, Elsevier, v. 182, n. 3, p. 303–309, 1996.

HAYS, J.; IMBRIE, J.; SHACKLETON, N. Variations in the earth's orbit: pacemaker of the ice ages: for 500,000 years, major climatic changes have followed variations in obliquity and precession. *Science*, American Association for the Advancement of Science, v. 194, n. 4270, p. 1121–1132, 1976. Https://doi.org/10.1126/science.194.4270.1121.

HIDE, R.; DICKEY, J. Earth's variable rotation. *Science*, American Association for the Advancement of Science, v. 253, n. 5020, p. 629–637, 1991. Https://doi.org/10.1126/science.253.5020.629.

HILL, W. G. Predictions of response to artificial selection from new mutations. *Genetics Research*, Cambridge University Press, v. 40, n. 3, p. 255–278, 1982.

HOLT, R. The microevolutionary consequences of climate change. *Trends in ecology & evolution*, Elsevier, v. 5, n. 9, p. 311–315, 1990. Https://doi.org/10.1016/0169-5347(90)90088-U.

HÖRING, F.; BISCONTIN, A.; HARMS, L.; SALES, G.; REISS, C. S.; PITTÀ, C. D.; MEYER, B. Seasonal gene expression profiling of antarctic krill in three different latitudinal regions. *Marine genomics*, Elsevier, v. 56, p. 100806, 2021.

HWANG, S.; PARK, S.-C.; KRUG, J. Genotypic complexity of fisher's geometric model. *Genetics*, Oxford University Press, v. 206, n. 2, p. 1049–1079, 2017.

JOHNSTON, R. A.; PAXTON, K. L.; MOORE, F. R.; WAYNE, R. K.; SMITH, T. B. Seasonal gene expression in a migratory songbird. *Molecular Ecology*, Wiley Online Library, v. 25, n. 22, p. 5680–5691, 2016.

JONG, S. D.; NEELEMAN, M.; LUYKX, J. J.; BERG, M. J. T.; STRENGMAN, E.; BREEIJEN, H. H. D.; STIJVERS, L. C.; BUIZER-VOSKAMP, J. E.; BAKKER, S. C.; KAHN, R. S. et al. Seasonal changes in gene expression represent cell-type composition in whole blood. *Human molecular genetics*, Oxford University Press, v. 23, n. 10, p. 2721–2728, 2014.

JR, J. J. S. Periodicity in extinction and the problem of catastrophism in the history of life. *Journal of the Geological Society*, The Geological Society of London, v. 146, n. 1, p. 7–19, 1989.

KASHTAN, N.; NOOR, E.; ALON, U. Varying environments can speed up evolution. *Proceedings of the National Academy of Sciences*, National Acad Sciences, v. 104, n. 34, p. 13711–13716, 2007.

KAUFFMAN, S.; LEVIN, S. Towards a general theory of adaptive walks on rugged landscapes. *Journal of theoretical Biology*, Elsevier, v. 128, n. 1, p. 11–45, 1987.

KAUFFMAN, S. A. et al. *The origins of order: Self-organization and selection in evolution*. [S.l.]: Oxford University Press, USA, 1993.

KAUFFMAN, S. A.; WEINBERGER, E. D. The nk model of rugged fitness landscapes and its application to maturation of the immune response. *Journal of theoretical biology*, Elsevier, v. 141, n. 2, p. 211–245, 1989.

KEIGHTLEY, P.; HILL, W. Estimating new mutational variation in growth rate of mice. In: *Proceedings of the 4th world congress of genetics applied and livestock production*. [S.l.: s.n.], 1990. v. 13, p. 325–328.

KIBOTA, T. T.; LYNCH, M. Estimate of the genomic mutation rate deleterious to overall fitness in e. coll. *Nature*, Nature Publishing Group UK London, v. 381, n. 6584, p. 694–696, 1996.

KINGSOLVER, J. G.; DIAMOND, S. E. Phenotypic selection in natural populations: what limits directional selection? *The American Naturalist*, University of Chicago Press Chicago, IL, v. 177, n. 3, p. 346–357, 2011.

KLEKOWSKI, E. Genetic load and its causes in long-lived plants. *Trees*, Springer, v. 2, p. 195–203, 1988. Https://doi.org/10.1007/BF00202374.

KORONA, R.; NAKATSU, C. H.; FORNEY, L. J.; LENSKI, R. E. Evidence for multiple adaptive peaks from populations of bacteria evolving in a structured habitat. *Proceedings of the National Academy of Sciences*, National Acad Sciences, v. 91, n. 19, p. 9037–9041, 1994.

KREMER, A.; HIPP, A. L. Oaks: an evolutionary success story. *New Phytologist*, Wiley Online Library, v. 226, n. 4, p. 987–1011, 2020.

LACY, R. Importance of genetic variation to the viability of mammalian populations. *Journal of mammalogy*, American Society of Mammalogists, v. 78, n. 2, p. 320–335, 1997. Https://doi.org/10.2307/1382885.

LANDE, R. The maintenance of genetic variability by mutation in a polygenic character with linked loci. *Genetics research*, Cambridge University Press, v. 26, n. 3, p. 221–235, 1976. Https://doi.org/10.1017/S0016672300016037.

LANDE, R. Natural selection and random genetic drift in phenotypic evolution. *Evolution*, JSTOR, v. 30, n. 2, p. 314–334, 1976. Https://doi.org/10.2307/2407703.

LANDE, R. The influence of the mating system on the maintenance of genetic variability in polygenic characters. *Genetics*, Oxford University Press, v. 86, n. 2, p. 485–498, 1977.

LANDE, R. Mutation and conservation. *Conservation biology*, Wiley Online Library, v. 9, n. 4, p. 782–791, 1995. Https://doi.org/10.1046/j.1523-1739.1995.09040782.x.

LANDE, R.; BARROWCLOUGH, G. Effective population size, genetic variation, and their use in population management. In: SOULé, M. (Ed.). *Viable populations for conservation*. [S.l.]: Cambridge University Press, 1987. p. 87–124.

LATTER, B. Natural selection for an intermediate optimum. *Australian Journal of Biological Sciences*, CSIRO Publishing, v. 13, n. 1, p. 30–35, 1960.

LATTER, B. Selection in finite populations with multiple alleles. ii. centripetal selection, mutation, and isoallelic variation. *Genetics*, Oxford University Press, v. 66, n. 1, p. 165, 1970.

LAUGHLIN, D. C.; MESSIER, J. Fitness of multidimensional phenotypes in dynamic adaptive landscapes. *Trends in Ecology & Evolution*, Elsevier, v. 30, n. 8, p. 487–496, 2015.

LENORMAND, T.; ROZE, D.; ROUSSET, F. Stochasticity in evolution. *Trends in ecology & evolution*, Elsevier, v. 24, n. 3, p. 157–165, 2009.

LENSKI, R. E.; ROSE, M. R.; SIMPSON, S. C.; TADLER, S. C. Long-term experimental evolution in escherichia coli. i. adaptation and divergence during 2,000 generations. *The American Naturalist*, University of Chicago Press, v. 138, n. 6, p. 1315–1341, 1991.

LEVIN, S. A. The problem of pattern and scale in ecology: the robert h. macarthur award lecture. *Ecology*, Wiley Online Library, v. 73, n. 6, p. 1943–1967, 1992.

LEWONTIN, R. C. *The genetic basis of evolutionary change*. [S.l.: s.n.], 1974.

LI, C.; ZHANG, J. Multi-environment fitness landscapes of a trna gene. *Nature ecology & evolution*, Nature Publishing Group UK London, v. 2, n. 6, p. 1025–1032, 2018.

LIU, C.; FAN, Y. Emergent fractal energy landscape as the origin of stress-accelerated dynamics in amorphous solids. *Physical Review Letters*, APS, v. 127, n. 21, p. 215502, 2021.

LOBKOVSKY, A. E.; KOONIN, E. V. Replaying the tape of life: quantification of the predictability of evolution. *Frontiers in genetics*, Frontiers Media SA, v. 3, p. 246, 2012.

LOBKOVSKY, A. E.; WOLF, Y. I.; KOONIN, E. V. Predictability of evolutionary trajectories in fitness landscapes. *PLoS computational biology*, Public Library of Science San Francisco, USA, v. 7, n. 12, p. e1002302, 2011.

LÓPEZ-MAURY, L.; MARGUERAT, S.; BÄHLER, J. Tuning gene expression to changing environments: from rapid responses to evolutionary adaptation. *Nature Reviews Genetics*, Nature Publishing Group UK London, v. 9, n. 8, p. 583–593, 2008.

LYNCH, M. The rate of polygenic mutation. *Genetics research*, Cambridge University Press, v. 51, n. 2, p. 137–148, 1988. Https://doi.org/10.1017/S0016672300024150.

LYNCH, M.; GABRIEL, W. Phenotypic evolution and parthenogenesis. *The american naturalist*, University of Chicago Press, v. 122, n. 6, p. 745–764, 1983. Https://doi.org/10.1086/284169.

LYNCH, M.; GABRIEL, W.; WOOD, A. Adaptive and demographic responses of plankton populations to environmental change. *Limnology and oceanography*, Wiley Online Library, v. 36, n. 7, p. 1301–1312, 1991. Https://doi.org/10.4319/lo.1991.36.7.1301.

LYNCH, M.; LANDE, R. Evolution and extinction in response to environmental change. In: KAREIVA, P.; KINGSOLVER, J.; HUEY, R. (Ed.). *Biotic interactions and global change*. [S.l.]: Sinauer Associates Incorporated, 1993. p. 234–250.

MACKEN, C. A.; PERELSON, A. S. Protein evolution on rugged landscapes. *Proceedings of the National Academy of Sciences*, National Acad Sciences, v. 86, n. 16, p. 6191–6195, 1989.

MANHART, M.; MOROZOV, A. V. Statistical physics of evolutionary trajectories on fitness landscapes. In: *First-passage phenomena and their applications*. [S.l.]: World Scientific, 2014. p. 416–446.

MARTIN, G.; LENORMAND, T. The fitness effect of mutations across environments: a survey in light of fitness landscape models. *Evolution*, Blackwell Publishing Ltd Oxford, UK, v. 60, n. 12, p. 2413–2427, 2006.

MATHER, K. Polygenic inheritance and natural selection. *Biological reviews*, Wiley Online Library, v. 18, n. 1, p. 32–64, 1943. Https://doi.org/10.1111/j.1469-185X.1943.tb00287.x.

MATUSZEWSKI, S.; HERMISSON, J.; KOPP, M. Fisher's geometric model with a moving optimum. *Evolution*, Wiley Online Library, v. 68, n. 9, p. 2571–2588, 2014.

MCELWAIN, J.; PUNYASENA, S. Mass extinction events and the plant fossil record. *Trends in ecology & evolution*, Elsevier, v. 22, n. 10, p. 548–557, 2007. Https://doi.org/10.1016/j.tree.2007.09.003.

MERILÄ, J.; HENDRY, A. Climate change, adaptation, and phenotypic plasticity: the problem and the evidence. *Evolutionary applications*, Wiley Online Library, v. 7, n. 1, p. 1–14, 2014. Https://doi.org/10.1111/eva.12137.

MORRIS, S. C. The predictability of evolution: glimpses into a post-darwinian world. *Naturwissenschaften*, Springer, v. 96, n. 11, p. 1313–1337, 2009.

MORRIS, S. C. Evolution: like any other science it is predictable. *Philosophical Transactions of the Royal Society B: Biological Sciences*, The Royal Society, v. 365, n. 1537, p. 133–145, 2010.

MOUSSEAU, T. A.; ROFF, D. A. Natural selection and the heritability of fitness components. *Heredity*, Nature Publishing Group, v. 59, n. 2, p. 181–197, 1987.

MUELLER, U.; MAZUR, A. Evidence of unconstrained directional selection for male tallness. *Behavioral Ecology and Sociobiology*, Springer, v. 50, p. 302–311, 2001.

NICOGLOU, A. The evolution of phenotypic plasticity: genealogy of a debate in genetics. *Studies in History and Philosophy of Science Part C: Studies in History and Philosophy of Biological and Biomedical Sciences*, Elsevier, v. 50, p. 67–76, 2015.

NOTTER, D. The importance of genetic diversity in livestock populations of the future. *Journal of animal science*, Oxford University Press, v. 77, n. 1, p. 61–69, 1999. Https://doi.org/10.2527/1999.77161x.

NOWAK, M. A. What is a quasispecies? *Trends in ecology & evolution*, Elsevier, v. 7, n. 4, p. 118–121, 1992.

NOWAK, M. A. *Evolutionary dynamics: exploring the equations of life*. [S.l.]: Harvard University Press, 2006.

NOWAK, S.; KRUG, J. Analysis of adaptive walks on nk fitness landscapes with different interaction schemes. *Journal of Statistical Mechanics: Theory and Experiment*, IOP Publishing, v. 2015, n. 6, p. P06014, 2015.

OOSTRA, V.; SAASTAMOINEN, M.; ZWAAN, B. J.; WHEAT, C. W. Strong phenotypic plasticity limits potential for evolutionary responses to climate change. *Nature communications*, Nature Publishing Group, v. 9, n. 1, p. 1–11, 2018.

ORR, H. A. A minimum on the mean number of steps taken in adaptive walks. *Journal of Theoretical Biology*, Elsevier, v. 220, n. 2, p. 241–247, 2003.

ORR, H. A. The probability of parallel evolution. *Evolution*, Wiley Online Library, v. 59, n. 1, p. 216–220, 2005.

ORR, H. A. The distribution of fitness effects among beneficial mutations in fisher's geometric model of adaptation. *Journal of theoretical biology*, Elsevier, v. 238, n. 2, p. 279–285, 2006.

OTT, E. *Chaos in dynamical systems*. [S.l.]: Cambridge university press, 2002.

PAIXÃO, T.; HEREDIA, J. P.; SUDHOLT, D.; TRUBENOVÁ, B. Towards a runtime comparison of natural and artificial evolution. *Algorithmica*, Springer, v. 78, p. 681–713, 2017.

PARSONS, P. Evolutionary rates under environmental stress. In: HECHT, M.; WALLACE, B.; PRANCE, G. (Ed.). *Evolutionary biology*. [S.l.]: Springer, 1987. v. 21, p. 311–347.

PERFEITO, L.; SOUSA, A.; BATAILLON, T.; GORDO, I. Rates of fitness decline and rebound suggest pervasive epistasis. *Evolution*, Wiley Online Library, v. 68, n. 1, p. 150–162, 2014.

POELWIJK, F. J.; TĂNASE-NICOLA, S.; KIVIET, D. J.; TANS, S. J. Reciprocal sign epistasis is a necessary condition for multi-peaked fitness landscapes. *Journal of theoretical biology*, Elsevier, v. 272, n. 1, p. 141–144, 2011.

PULIDO, F.; BERTHOLD, P. Microevolutionary response to climatic change. *Advances in ecological research*, Elsevier, v. 35, p. 151–183, 2004. Https://doi.org/10.1016/S0065-2504(04)35008-7.

RAM, Y.; HADANY, L. The probability of improvement in fisher's geometric model: A probabilistic approach. *Theoretical population biology*, Elsevier, v. 99, p. 1–6, 2015.

RAMPINO, M.; CALDEIRA, K. Major episodes of geologic change: correlations, time structure and possible causes. *Earth and planetary science letters*, Elsevier, v. 114, n. 2-3, p. 215–227, 1993. Https://doi.org/10.1016/0012-821X(93)90026-6.

RAMPINO, M. R.; CALDEIRA, K. Episodes of terrestrial geologic activity during the past 260 million years: A quantitative approach. *Celestial Mechanics and Dynamical Astronomy*, Springer, v. 54, p. 143–159, 1992.

RAMPINO, M. R.; CALDEIRA, K.; ZHU, Y. A pulse of the earth: A 27.5-myr underlying cycle in coordinated geological events over the last 260 myr. *Geoscience Frontiers*, Elsevier, v. 12, n. 6, p. 101245, 2021.

REED, T. E.; WAPLES, R. S.; SCHINDLER, D. E.; HARD, J. J.; KINNISON, M. T. Phenotypic plasticity and population viability: the importance of environmental predictability. *Proceedings of the Royal Society B: Biological Sciences*, The Royal Society, v. 277, n. 1699, p. 3391–3400, 2010.

REIA, S. M.; CAMPOS, P. R. Analysis of statistical correlations between properties of adaptive walks in fitness landscapes. *Royal Society Open Science*, The Royal Society, v. 7, n. 1, p. 192118, 2020.

REZNICK, D. N.; SHAW, F. H.; RODD, F. H.; SHAW, R. G. Evaluation of the rate of evolution in natural populations of guppies (poecilia reticulata). *Science*, American Association for the Advancement of Science, v. 275, n. 5308, p. 1934–1937, 1997.

RICH, J. E.; JOHNSON, G. L.; JONES, J. E.; CAMPSIE, J. A significant correlation between fluctuations in seafloor spreading rates and evolutionary pulsations. *Paleoceanography*, Wiley Online Library, v. 1, n. 1, p. 85–95, 1986.

ROBERTSON, A. The effect of selection against extreme deviants based on deviation or on homozygosis: With two text-figures. *Journal of Genetics*, Springer, v. 54, p. 236–248, 1956.

ROCHA, F.; MEDEIROS, H.; KLACZKO, L. The reaction norm for abdominal pigmentation and its curve in drosophila mediopunctata depend on the mean phenotypic value. *Evolution*, Blackwell Publishing Inc Malden, USA, v. 63, n. 1, p. 280–287, 2009. Https://doi.org/10.1111/j.1558-5646.2008.00503.x.

ROFF, D. A.; MOUSSEAU, T. A. Quantitative genetics and fitness: lessons from drosophila. *Heredity*, Nature Publishing Group, v. 58, n. 1, p. 103–118, 1987.

ROWE, W.; PLATT, M.; WEDGE, D. C.; DAY, P. J.; KELL, D. B.; KNOWLES, J. Analysis of a complete dna–protein affinity landscape. *Journal of The Royal Society Interface*, The Royal Society, v. 7, n. 44, p. 397–408, 2010.

RUDMAN, S.; GREENBLUM, S.; RAJPUROHIT, S.; BETANCOURT, N.; HANNA, J.; TILK, S.; YOKOYAMA, T.; PETROV, D.; SCHMIDT, P. Direct observation of adaptive tracking on ecological time scales in drosophila. *Science*, American Association for the Advancement of Science, v. 375, n. 6586, p. eabj7484, 2022. Https://doi.org/10.1126/science.abj7484.

SALISBURY, F. B. Natural selection and the complexity of the gene. *Nature*, Springer, v. 224, n. 5217, p. 342–343, 1969.

SALVERDA, M. L.; DELLUS, E.; GORTER, F. A.; DEBETS, A. J.; OOST, J. V. D.; HOEKSTRA, R. F.; TAWFIK, D. S.; VISSER, J. A. G. de. Initial mutations direct alternative pathways of protein evolution. *PLoS genetics*, Public Library of Science San Francisco, USA, v. 7, n. 3, p. e1001321, 2011.

SANJAK, J. S.; SIDORENKO, J.; ROBINSON, M. R.; THORNTON, K. R.; VISSCHER, P. M. Evidence of directional and stabilizing selection in contemporary humans. *Proceedings of the National Academy of Sciences*, National Acad Sciences, v. 115, n. 1, p. 151–156, 2018.

SCHEINER, S. Genetics and evolution of phenotypic plasticity. *Annual review of ecology, evolution and systematics*, Annual Reviews 4139 El Camino Way, PO Box 10139, Palo Alto, CA 94303-0139, USA, v. 24, p. 35–68, 1993. Https://doi.org/10.1146/annurev.es.24.110193.000343.

SCHEINER, S. M.; LYMAN, R. F. The genetics of phenotypic plasticity. ii. response to selection. *Journal of evolutionary Biology*, Wiley Online Library, v. 4, n. 1, p. 23–50, 1991.

SCHLICHTING, C. D.; PIGLIUCCI, M. Control of phenotypic plasticity via regulatory genes. *The American Naturalist*, University of Chicago Press, v. 142, n. 2, p. 366–370, 1993.

SCHWARTZ, C.; ANDREWS, M. T. Circannual transitions in gene expression: lessons from seasonal adaptations. *Current topics in developmental biology*, Elsevier, v. 105, p. 247–273, 2013.

SEELEY, R. H. Intense natural selection caused a rapid morphological transition in a living marine snail. *Proceedings of the National Academy of Sciences*, National Acad Sciences, v. 83, n. 18, p. 6897–6901, 1986.

SESSIONS, A.; DOUGHTY, D.; WELANDER, P.; SUMMONS, R.; NEWMAN, D. The continuing puzzle of the great oxidation event. *Current biology*, Elsevier, v. 19, n. 14, p. R567–R574, 2009. Https://doi.org/10.1016/j.cub.2009.05.054.

SHAH, P.; GILCHRIST, M. A. Is thermosensing property of rna thermometers unique? *PLoS One*, Public Library of Science San Francisco, USA, v. 5, n. 7, p. e11308, 2010.

SHIMADA, M.; ISHII, Y.; SHIBAO, H. Rapid adaptation: a new dimension for evolutionary perspectives in ecology. *Population ecology*, Springer, v. 52, n. 1, p. 5–14, 2010.

SHIRES, B. W.; PICKARD, C. J. Visualizing energy landscapes through manifold learning. *Physical Review X*, APS, v. 11, n. 4, p. 041026, 2021.

SLATKIN, M. Heritable variation and heterozygosity under a balance between mutations and stabilizing selection. *Genetics research*, Cambridge University Press, v. 50, n. 1, p. 53–62, 1987. Https://doi.org/10.1017/S0016672300023338.

SMART, D. *Fixed point theorems*. [S.l.]: Cambridge University Press, 1980.

SMITH, J. The causes of extinction. *Philosophical transactions of the royal society B: biological sciences*, The Royal Society London, v. 325, n. 1228, p. 241–252, 1989. Https://doi.org/10.1098/rstb.1989.0086.

SMITH, J. M. Natural selection and the concept of a protein space. *Nature*, Nature Publishing Group, v. 225, n. 5232, p. 563–564, 1970.

SRIVASTAVA, M.; PAYNE, J. L. On the incongruence of genotype-phenotype and fitness landscapes. *PLOS Computational Biology*, Public Library of Science San Francisco, CA USA, v. 18, n. 9, p. e1010524, 2022.

STADLER, P. F. Fitness landscapes. In: *Biological evolution and statistical physics*. [S.l.]: Springer, 2002. p. 183–204.

STADLER, P. F.; STADLER, B. M. Genotype-phenotype maps. *Biological Theory*, Springer, v. 1, p. 268–279, 2006.

STERN, R. The evolution of plate tectonics. *Philosophical transactions of the royal society A: mathematical, physical and engineering sciences*, The Royal Society Publishing, v. 376, n. 2132, p. 20170406, 2018. Https://doi.org/10.1098/rsta.2017.0406.

STOKS, R.; GOVAERT, L.; PAUWELS, K.; JANSEN, B.; MEESTER, L. D. Resurrecting complexity: the interplay of plasticity and rapid evolution in the multiple trait response to strong changes in predation pressure in the water flea daphnia magna. *Ecology letters*, Wiley Online Library, v. 19, n. 2, p. 180–190, 2016.

SZENDRO, I. G.; FRANKE, J.; VISSER, J. A. G. de; KRUG, J. Predictability of evolution depends nonmonotonically on population size. *Proceedings of the National Academy of Sciences*, National Acad Sciences, v. 110, n. 2, p. 571–576, 2013.

SZENDRO, I. G.; SCHENK, M. F.; FRANKE, J.; KRUG, J.; VISSER, J. A. G. D. Quantitative analyses of empirical fitness landscapes. *Journal of Statistical Mechanics: Theory and Experiment*, IOP Publishing, v. 2013, n. 01, p. P01005, 2013.

TANG, X.; KRAUSFELDT, L. E.; SHAO, K.; LECLEIR, G. R.; STOUGH, J. M.; GAO, G.; BOYER, G. L.; ZHANG, Y.; PAERL, H. W.; QIN, B. et al. Seasonal gene expression and the ecophysiological implications of toxic microcystis aeruginosa blooms in lake taihu. *Environmental science & technology*, ACS Publications, v. 52, n. 19, p. 11049–11059, 2018.

TENAILLON, O. The utility of fisher's geometric model in evolutionary genetics. *Annual review of ecology, evolution, and systematics*, Annual Reviews, v. 45, n. 1, p. 179–201, 2014.

TEOTÓNIO, H.; ROSE, M. R. Perspective: reverse evolution. *Evolution*, Wiley Online Library, v. 55, n. 4, p. 653–660, 2001.

THOMPSON, J. N. Rapid evolution as an ecological process. *Trends in ecology & evolution*, Elsevier, v. 13, n. 8, p. 329–332, 1998.

THOMPSON, N. F.; ANDERSON, E. C.; CLEMENTO, A. J.; CAMPBELL, M. A.; PEARSE, D. E.; HEARSEY, J. W.; KINZIGER, A. P.; GARZA, J. C. A complex phenotype in salmon controlled by a simple change in migratory timing. *Science*, American Association for the Advancement of Science, v. 370, n. 6516, p. 609–613, 2020.

TRUBENOVA, B.; KREJCA, M. S.; LEHRE, P. K.; KÖTZING, T. Surfing on the seascape: Adaptation in a changing environment. *Evolution*, Blackwell Publishing Inc Malden, USA, v. 73, n. 7, p. 1356–1374, 2019.

TURELLI, M. Heritable genetic variation via mutation-selection balance: Lerch's zeta meets the abdominal bristle. *Theoretical population biology*, Elsevier, v. 25, n. 2, p. 138–193, 1984. Https://doi.org/10.1016/0040-5809(84)90017-0.

TYLIANAKIS, J. M.; DIDHAM, R. K.; BASCOMPTE, J.; WARDLE, D. A. Global change and species interactions in terrestrial ecosystems. *Ecology letters*, Wiley Online Library, v. 11, n. 12, p. 1351–1363, 2008.

VALCIN, D.; BERNAL, J.; JIMENEZ, R.; VERDE, L.; WANDELT, B. Inferring the age of the universe with globular clusters. *Journal of cosmology and astroparticle physics*, IOP Publishing, v. 2020, n. 12, p. 002, 2020. Https://doi.org/10.1088/1475-7516/2020/12/002.

VERD, B.; MONK, N. A.; JAEGER, J. Modularity, criticality, and evolvability of a developmental gene regulatory network. *Elife*, eLife Sciences Publications, Ltd, v. 8, p. e42832, 2019.

VIA, S. Adaptive phenotypic plasticity: target or by-product of selection in a variable environment? *The American Naturalist*, University of Chicago Press, v. 142, n. 2, p. 352–365, 1993.

VIA, S.; GOMULKIEWICZ, R.; JONG, G. D.; SCHEINER, S. M.; SCHLICHTING, C. D.; TIENDEREN, P. H. V. Adaptive phenotypic plasticity: consensus and controversy. *Trends in ecology & evolution*, Elsevier, v. 10, n. 5, p. 212–217, 1995.

VIA, S.; LANDE, R. Genotype-environment interaction and the evolution of phenotypic plasticity. *Evolution*, Blackwell Publishing Inc Malden, USA, v. 39, n. 3, p. 505–522, 1985.

VISSCHER, P. M.; HILL, W. G.; WRAY, N. R. Heritability in the genomics era—concepts and misconceptions. *Nature reviews genetics*, Nature Publishing Group UK London, v. 9, n. 4, p. 255–266, 2008.

VISSER, J. A. G. D.; KRUG, J. Empirical fitness landscapes and the predictability of evolution. *Nature Reviews Genetics*, Nature Publishing Group UK London, v. 15, n. 7, p. 480–490, 2014.

VISSER, J. A. G. de; ELENA, S. F.; FRAGATA, I.; MATUSZEWSKI, S. The utility of fitness landscapes and big data for predicting evolution. *Heredity*, Springer International Publishing Cham, v. 121, n. 5, p. 401–405, 2018.

VOS, M. G. de; SCHOUSTRA, S. E.; VISSER, J. A. G. de. Ecology dictates evolution? about the importance of genetic and ecological constraints in adaptation (a). *Europhysics Letters*, IOP Publishing, v. 122, n. 5, p. 58002, 2018.

WANG, S.; DAI, L. Evolving generalists in switching rugged landscapes. *PLoS computational biology*, Public Library of Science San Francisco, CA USA, v. 15, n. 10, p. e1007320, 2019.

WEBER, K.; DIGGINS, L. Increased selection response in larger populations. ii. selection for ethanol vapor resistance in drosophila melanogaster at two population sizes. *Genetics*, Oxford University Press, v. 125, n. 3, p. 585–597, 1990. Https://doi.org/10.1093

WEINBERGER, E. D. Local properties of kauffman's n-k model: A tunably rugged energy landscape. *Physical review A*, APS, v. 44, n. 10, p. 6399, 1991.

WEINBERGER, E. D. et al. Np completeness of kauffman's nk model, a tuneably rugged fitness landscape. *Santa Fe Institute Technical Reports*, 1996.

WEINREICH, D. M.; DELANEY, N. F.; DEPRISTO, M. A.; HARTL, D. L. Darwinian evolution can follow only very few mutational paths to fitter proteins. *Science*, American Association for the Advancement of Science, v. 312, n. 5770, p. 111–114, 2006.

WEINREICH, D. M.; WATSON, R. A.; CHAO, L. Perspective: sign epistasis and genetic costraint on evolutionary trajectories. *Evolution*, Wiley Online Library, v. 59, n. 6, p. 1165–1174, 2005.

WHITMAN, D. W.; AGRAWAL, A. A. et al. What is phenotypic plasticity and why is it important. *Phenotypic plasticity of insects: Mechanisms and consequences*, p. 1–63, 2009.

WILKE, C. O.; MARTINETZ, T. Adaptive walks on time-dependent fitness landscapes. *Physical Review E*, APS, v. 60, n. 2, p. 2154, 1999.

WILLIAMS, M.; ZALASIEWICZ, J.; HAFF, P.; SCHWÄGERL, C.; BARNOSKY, A.; ELLIS, E. The anthropocene biosphere. *The anthropocene review*, SAGE Publications Sage UK: London, England, v. 2, n. 3, p. 196–219, 2015. Https://doi.org/10.1177/2053019615591020.

WRIGHT, S. Evolution in mendelian populations. *Genetics*, Oxford University Press, v. 16, n. 2, p. 97, 1931.

WRIGHT, S. The roles of mutation, inbreeding, crossbreeding, and selection in evolution. In: *Genetics: Proceedings of the Sixth International Congress on*. [S.l.: s.n.], 1932. p. 355–366.

WUCHER, V.; SODAEI, R.; AMADOR, R.; IRIMIA, M.; GUIGÓ, R. Day-night and seasonal variation of human gene expression across tissues. *Plos Biology*, Public Library of Science San Francisco, CA USA, v. 21, n. 2, p. e3001986, 2023.